UNIVERSITY OF CALIFORNIA SAN DIEGO

Stochastic electron acceleration in laser-plasma interactions

A dissertation submitted in partial satisfaction of the
requirements for the degree
Doctor of Philosophy

in

Engineering Sciences (Engineering Physics)

by

Yanzeng Zhang

Committee in charge:

Professor Sergei I. Krasheninnikov, Chair
Professor Alexey Arefiev
Professor Farhat Beg
Professor Patrick H. Diamond
Professor Antonio L. Sánchez

2020

The dissertation of Yanzeng Zhang is approved, and it is acceptable in quality and form for publication on microfilm and electronically:

_____

_____

_____

_____

Chair

University of California San Diego

2020

DEDICATION

To my family.

EPIGRAPH

"The beginning is the most important part of the work."

—Plato

TABLE OF CONTENTS

LIST OF FIGURES

ACKNOWLEDGEMENTS

I am deeply indebted to my adviser Prof. Sergei I. Krasheninnikov for his continuous support of my Ph.D. study. He provided me with every bit of guidance, assistance, and expertise that I needed for my research. Working with such a remarkable theorist as Sergei contributed greatly to my aspiration in plasma physics. He is the funniest advisor and one of the smartest people I know. His hardworking and passionate attitude not only influence me on my research but also my life. I quite simply cannot imagine a better adviser.

I would also like to thank the rest of my dissertation committee members: Prof. Arefiev, Prof. Beg, Prof. Diamond, and Prof. Sánchez for their great support and invaluable advice on a preliminary version of this thesis and the substantial influence that their courses have had on my research. I would particularly like to acknowledge Prof. Diamond, who has long been an inspiring figure for me. I appreciate all his scientific suggestions, insightful discussions, and helpful career advice.

I am also grateful to all the present members of Sergei's group for their continued support. They are friendly and considerate. I am thankful to Alexey Knyazev for his collaboration and contribution related to this dissertation. I would also like to thank the past members of Sergei's group, Justin Angus and Jerome Guterl, for their helpful career suggestions. Moreover, I extend great gratitude to my collaborators, Andrei Smolyakov and Mikhail Dorf, for their great support on the projects outside this dissertation.

Last but not least, I would like to express my deepest gratitude to my family for their love, support, and sacrifices. Without them, this thesis would never have been written. I am also thankful to all my friends for their support. The last word of acknowledgment I have saved for my dear wife Hanyu Xiao for enlightening and supporting me spiritually throughout writing this thesis and my life in general. She has made my Ph.D. time the best years of my life.

Chapter 2, in part, is a reprint of the material as it appears in *Novel approach to stochastic acceleration of electrons in colliding laser fields* in Physics of Plasmas 26, 050702, by Y. Zhang

and S. Krasheninnikov, 2019. The dissertation author was the primary investigator and author of this paper.

Chapter 3, in full, is a reprint of the material as it appears in *Stochastic electron acceleration in relativistic laser pulse and quasi-static periodic electric and magnetic fields* in Physics of Plasmas 26, 113112, by Y. Zhang and S. Krasheninnikov, 2019. The dissertation author was the primary investigator and author of this paper.

Chapter 4, in full, is a reprint of the materials as they appear in *Stochastic electron heating in the laser and quasi-static electric and magnetic fields* in Physics of Plasmas 25, 123110, by Y. Zhang, S. Krasheninnikov, and A. Knyazev, 2018; and in *Electron dynamics in laser and quasi-static transverse electric and longitudinal magnetic fields* in Plasma Physics and Controlled Fusion 61, 074008, by Y. Zhang and S. Krasheninnikov, 2019. The dissertation author was the primary investigator and author of this paper.

VITA

2015	B.S. in Applied Physics University of Science and Technology of China, China
2015-2016	MAE Department Fellowship University of California, San Diego
2016	M.S. in Engineering Sciences (Engineering Physics) University of California, San Diego
2016-2020	Graduate Research Assistant Sergei Krasheninnikov's group Department of Mechanical and Aerospace Engineering University of California, San Diego
2017	Teaching Assistant MAE210a: Fluid Mechanics I Department of Mechanical and Aerospace Engineering University of California, San Diego
2017, 2018	Teaching Assistant MAE118: Introduction to Energy and Environment Department of Mechanical and Aerospace Engineering University of California, San Diego
2020	Ph. D. in Engineering Sciences (Engineering Physics) University of California, San Diego

PUBLICATIONS

"Blobs in the framework of drift wave dynamics", Y. Zhang and S. I. Krasheninnikov, Phys. of Plasmas, 23, 124501 (2016).

"Blobs and drift wave dynamics", Y. Zhang and S. I. Krasheninnikov, Phys. of Plasmas, 24, 092313 (2017).

"Electron heating in the laser and static electric and magnetic fields", Y. Zhang and S. I. Krasheninnikov, Phys. of Plasmas, 25, 013120 (2018).

"Electron dynamics in the laser and static electric and magnetic fields", Y. Zhang and S. I. Krasheninnikov, Phys. Lett. A, 27, 1801 (2018).

"Stochastic electron heating in the laser and quasi-static electric and magnetic fields", Y. Zhang, S. I. Krasheninnikov and A. Knyazev, Phys. of Plasmas, 25, 123110 (2018).

"Radiation friction force effects on electron dynamics in ultra-intensity laser pulse", Y. Zhang and S. I. Krasheninnikov, Phys. of Plasmas, 26, 010702 (2019).

"Novel approach to stochastic acceleration of electrons in colliding laser fields", Y. Zhang and S. I. Krasheninnikov, Phys. of Plasmas, 26, 050702 (2019).

"Electron dynamics in laser and quasi-static transverse electric and longitudinal magnetic fields", Y. Zhang and S. I. Krasheninnikov, Plasma Phys. Control. Fusion, 61, 074008 (2019).

"Stochastic electron acceleration in relativistic laser pulse and stationary periodic electric and magnetic fields", Y. Zhang and S. I. Krasheninnikov, Phys. of Plasmas, 26, 113112 (2019).

"Influence of flow shear on localized Rayleigh–Taylor and resistive drift wave instabilities", Y. Zhang, S. I. Krasheninnikov, and A. I. Smolyakov, Contrib. Plasma Phys., e201900098 (2019)

"Velocity shear effects on localized Rayleigh-Taylor, interchange, and resistive drift wave instabilities", Y. Zhang, S. I. Krasheninnikov, and A. I. Smolyakov, Phys. of Plasmas, 27, 020701 (2020).

"Edge and divertor plasma: detachment, stability, and plasma-wall interactions", S. I. Krasheninnikov, A. Kukushkin, Wonjae Lee, A. A. Phsenov, R. Smirnov, A. I. Smolyakov, A. A. Stepanenko, and Y. Zhang, Nuclear Fusion, 57, 102010 (2017).

"Stability of divertor detachment", S. I. Krasheninnikov, A. S. Kukushkin, A. A. Pshenov, A. I. Smolyakov, Y. Zhang, Nuclear Materials and Energy, 12, 1061 (2017).

ABSTRACT OF THE DISSERTATION

Stochastic electron acceleration in laser-plasma interactions

by

Yanzeng Zhang

Doctor of Philosophy in Engineering Sciences (Engineering Physics)

University of California San Diego, 2020

Professor Sergei I. Krasheninnikov, Chair

The ability of the interaction of intense laser radiation with plasma to generate highly energetic electrons is one of the most interesting features in laser-plasma physics that has great potentials for many applications (including ion acceleration, X-ray generation, and positron production). Different mechanisms of electron acceleration including the direct laser acceleration (DLA) have been proposed and studied analytically, numerically, and experimentally over many years. Many of these works reveal that the presence of self-generated or externally applied quasi-static electric and magnetic (QEM) fields or a counter-propagating laser wave could significantly increase the electron energy gained from the laser well beyond the ponderomotive energy scaling. However, due to the multidimensional spatiotemporal characteristics of the electromagnetic

fields and strong nonlinearity of relativistic electron dynamics, the analytic investigations of the mechanism of electron acceleration in the earlier studies of DLA are quite limited and complicated.

This dissertation is devoted to examining the electron acceleration in the laser waves and QEM fields by employing the Hamiltonian approach. By using proper canonical variables, we find a new Hamiltonian, which is time-independent when an appropriately selected perturbation is absent. Such characteristic of the new Hamiltonian can significantly simplify the analysis of the electron dynamics. Three different configurations of laser waves and QEM fields will be considered: the counter-propagating laser waves, single laser and QEM fields that can confine the electron motions (e.g., QEM fields in the ion channels), and single laser and spatially periodic QEM fields (e.g., QEM fields in the electric and magnetic undulators). The Hamiltonians, canonical variables, effective time, and thus the physics underlying the electron acceleration are different for these cases, where we pay particular attention to the stochastic acceleration of electrons. By deriving the Chirikov-like mappings, we obtain the stochastic conditions and thus the upper limits of the electron energy depending on the parameters of the laser waves, QEM fields, and the electron initial conditions. The universal characteristics of our approach make it easy to be applied to many other situations and thus paves the way for notable progress in the theoretical analysis of the laser-plasma interaction.

Chapter 1

Introduction

1.1 Electron acceleration in laser-plasma interaction

Recent progress in laser technology has led to a dramatic increase of laser power and intensity [1], which naturally open up new physics regimes for fundamental research. At relativistic intensity, $I = 1.37 \times 10^{18}(1\mu m/\lambda)^2 W/cm^2$, the laser pulses readily ionize matter into a plasma that the plasma electrons is the primary species for the energy transfer from the laser pulse, provided that it is more responsive to the laser field than other species. As a result, the generation of high-energy electron beams in the course of laser-plasma interaction has attracted a great deal of attention (e.g., see Refs. [2, 3, 4, 5, 6, 7, 8, 9, 10, 11, 12, 13, 14, 15, 16, 17, 18, 19, 20, 21, 22, 23, 24, 25, 26, 27, 28, 29, 30] and references therein) for many different applications (e.g., ion acceleration, X-ray generation, positron production, etc.).

The acceleration of electrons via the laser-plasma interaction strongly depends on the density of the target, where the laser beam is able to go through the target plasma only if the density is sub-critical (e.g., see Refs. [31, 32, 33, 34]). Such low-density targets enable a higher energy gain by the electrons compared with that from the over-density target. The sub-critical plasma layer can also naturally occur in experiments with solid-density targets where

a significant pre-pulse is present (e.g., see Refs. [35, 36, 37, 38, 39]). On the other hand, the electron acceleration mechanism in the laser interaction with the sub-critical plasma depends significantly on the laser pulse duration. Given that the ponderomotive force of the propagating laser beam pushes electrons forward and radially outwards, it will cause cavitation of the electron density. Then if the duration of the laser pulse is much shorter than the characteristic electron response time (plasma wave period), the laser pulse can generate a plasma structure that is moving together with the pulse. Such the so-called wakefield can accelerate the electrons through the longitudinal electric field (e.g., see [40, 41, 42]). However, if the duration of the laser pulse is much longer than the characteristic electron response time, the laser pulse can create a quasi-static channel in the electron density that slowly evolves on an ion time-scale (e.g., see [43]). This would be the case for typical pulse duration used in experiments on fast proton generation. The electron acceleration in the latter case is identified as direct laser acceleration (DLA), which is usually assisted with different configurations of quasi-static electric and magnetic (QEM) fields (e.g., see [5, 8, 15, 16, 18, 20, 21, 22]).

Different mechanisms of DLA of electrons with these QEM fields have been proposed, including the betatron resonance [21], parametric amplification [22], stochastic heating [25, 26, 27, 44] and other resonant heating [11, 29], where the electron is confined and thus oscillates in these QEM fields while moving along with the beam. The stochastic heating of electrons can also result from the counter-propagating laser beams [45, 46, 47] or adding the stochastic fields in the transverse direction [48]. Other collisionless heating of electrons by the laser radiation can also take place via resonance heating [30, 49], vacuum heating (Brunel absorption) [50], anomalous skin effect [51], sheath inverse-bremsstrahlung absorption [52], relativistic $J \times B$ heating [53]. Recent simulation results have also demonstrated that the DLAcan also be important in the context of the laser wakefield acceleration [54, 55]. Therefore, understanding the details of the DLA process is crucial in learning the core laser-plasma interactions processes, which requires us to at least understand single electron dynamics in configurations that include the majority of the

realistic features of these interactions. However, the presence of the QEM fields and multiple laser pulses leads to a rather complicated dynamical system, which is difficult to fully understand.

1.1.1 Overview of electron interaction with laser in vacuum

Before we jump into such complicated dynamical system, we give a brief overview of the physics of a free electron interaction with laser in vacuum, which is characterized by the normalized laser amplitude

$$a_0 = \frac{eE_0}{m\omega c} \tag{1.1}$$

where E_0 is the amplitude of the electric field of the laser wave, ω is the wave frequency, e is the elementary charge, m is the electron mass and c is the speed of light in vacuum (when the normalized amplitude is equal to unity, the intensity of a linearly polarized laser wave is $I = 1.37 \times 10^{18}(1\mu m/\lambda)^2 W/cm^2$, where the quiver electron motion becomes relativistic). The conventional wisdom to describe such an interaction is a Hamiltonian equivalent to the kinetic energy of the electron. For a linearly polarized plane wave (e.g., a plane wave polarized in x-direction which propagates along z-direction), it shows that the electron dynamics has two constants of motion (e.g., see Ref. [10]), i.e., $c_x = p_x/mc - a$ and $R = \gamma - p_z/mc$, where a is the normalized vector potential describing the laser field, p_i is the i-component of the momentum and $\gamma^2 = 1 + p^2/(mc)^2$. As a result, for an initially rest electron, the maximum electron energy gained from the interaction with the laser wave (the so-called ponderomotive scaling energy) is $\gamma_{pond} = 1 + a_0^2/2$.

1.2 Stochastic motion

On aspect of the difficulty in understanding the electron dynamics in the configurations of multiple lasers and QEM fields is the strong nonlinearity of the relativistic electron dynamics. One direct result of such strong nonlinearity is that there exist regimes of the parameters, where, when

the stochastic condition is satisfied, the local instability can lead to mixing in the configuration space and thus the electron can undergo stochastic motion [56, 57]. Unlike the acceleration of electrons via regular resonance, the stochastic mechanism usually leads to a slower energy growth through diffusion of electrons in energy space described by a Fokker-Planck-Kolmogorov equation [56, 58].

The Lyapunov exponent, characterizing the rate of separation of infinitesimally close trajectories, can be used to distinguish a stochastic motion from the regular one. However, more conveniently, we use Chirikov mapping to study the mixing of phase space [58]. It is characterized by a stochastic parameter K, where $K \tilde{>} 1$ denotes the stochastic regime. It was shown that $\ln K$ is inversely proportional to the time for the decoupling of correlations or the time for the loss of memory of the original conditions so that for $K \gg 1$, the electron trajectory in phase space behaves like undergoing a series of "kicks", occurring in an extremely short time period (on the remaining part of the trajectory the motion is adiabatic) [56]. However, for K being order of unity, the fraction of stable components of the motion plays an important role. Stochastic trajectories form in this region an extraordinarily complicated structured set, the so-called fat fractals [59], where the particle trajectories can stick for a long time in this region.

1.3 Dissertation Outline

The stochastic electron acceleration in the laser-plasma interaction has been revealed in several cases, including in an additive small transverse stochastic field [48], in the multiple laser waves [24, 47, 60], and in the laser radiation and an attractive longitudinal electrostatic potential well [15]. However, due to the multidimensional spatio-temporal characteristics of the laser pulses and QEM fields, and the strong nonlinearity of the dynamics of relativistic electrons, the analytic investigations of the stochastic electron acceleration in the previous study are rather limited and complicated. For example, the analysis of the electron dynamics in multiple lasers in earlier

studies has been limited to either non-relativistic case [4, 61], or the stochastic instability near the separatrices using quite complicated multidimensional Hamiltonian approach [24, 46, 62], whereas, for electrons in the longitudinal electric field, the analysis was only given in a simplified V-shape electrostatic potential [25, 26], $U = E_0 z$. Even though the numerical simulations can shed some light on the stochastic electron acceleration (e.g., see Refs. [15, 46, 47, 60, 63]), they are only valid within the simulated parameter range. Therefore, some scenarios where the electron can be stochastically accelerated, and the physics underlying the stochastic motion are still missing.

This work is devoted to investigating the electron dynamics, especially paying attention to the stochastic electron acceleration, in different configurations of laser beams and QEM fields. A novel approach is proposed, the main idea of which is to find proper canonical variables so that the new Hamiltonian describing the electron dynamics is time-independent without the appreciated perturbation. Such a approach can significantly simplify the analysis of the electron dynamics and allow us to utilize the fundamental results of previous studies on regular and stochastic motion in Hamiltonian systems (e.g., see Refs. [56, 57] and the references therein). However, the perturbation, Hamiltonian, and the canonical variables are different for the electron in different configurations of lasers and QEM fields. Three main scenarios will be considered: the counter-propagating laser beams, single laser wave and QEM fields that can confine the electron motions (e.g., QEM fields in the ion channels), and single laser wave and spatially periodic QEM fields (e.g., QEM fields in electric and magnetic undulators). They will be studied in separate chapters and outlined below.

1.3.1 Ch 2: Stochastic electron acceleration in colliding laser beams

There is a long-lasting interest to the stochastic electron acceleration in the colliding laser beams provided that it is insensitive to the frequency differences of the two laser pulses [47] and can work without a self-focusing ion channel that it is easier to be achieved. Underlying physics

of such stochastic motion are poorly understood and, therefore, further theoretical studies are necessary. In this chapter, we will examine the electron dynamics in the colliding laser beams by employing the new approach. The threshold for the onset of stochastic motion is founded by using the Chirikov-like mapping, which agrees with the previous results that the stochasticity occurs when the amplitudes of lasers exceed some thresholds [46, 47]. The maximum electron energy gained from the stochastic motion is obtained, corresponding to the boundaries of the stochastic region in the Hamiltonian space. It is shown that the stochastic region can be separated from the regular motion region only in the Hamiltonian space rather than the energy space. Numerical simulations solving the Hamiltonian equations are performed, which have confirmed the very good agreement of numerical and analytical results.

1.3.2 Ch 3: Stochastic electron acceleration in laser and quasi-static periodic electric and magnetic fields

In this chapter, we will investigate the stochastic electron acceleration in the laser radiation with the presence of a periodic quasi-static longitudinal electric or transverse magnetic field. Such periodic electric and magnetic fields has been widely used in studies of electron dynamics, including electric and magnetic undulators [64, 65, 66, 67] and wiggler magnetic field [68, 69]. Moreover, it was shown that the plasma wave can also be taken as a periodic electrostatic field [7, 70, 71, 72], where electrons in laser and the plasma wave can be stochastically accelerated.

The new Hamiltonian equations have been derived, where the periodic QEM fields are taken as the perturbations and the new Hamiltonian is the same with that of the electron in the colliding lasers. The physics underlying the stochastic electron motion is revealed and the stochastic condition is obtained. The maximum electron energy is estimated well beyond the ponderomotive scaling energy, which is mainly determined by the normalized laser amplitude and the frequency of the periodic QEM fields. The numerical simulations confirm all the analytical results.

1.3.3 Ch 4: Stochastic electron acceleration in laser and confining quasi-static electric and magnetic fields

This chapter studies the electron dynamics in the laser radiation with the presence of QEM fields like in the ion channels, which can confine the electron motion within the potential wells (thus we call them as confining QEM fields). For relativistic electrons, the laser radiation will be taken as the perturbation and thus the expected Hamiltonian is the total electron energy in the quasi-static fields. The role of these quasi-static fields is to reduce the longitudinal dephasing rate between the electron and laser beam instead of directly transferring substantial energy to the electron.

Three different configurations of QEM fields will be considered: QEM fields both across to the laser propagation direction, a transverse magnetic field but a longitudinal electric field, and a transverse electric field but a homogeneous longitudinal magnetic field. In each case, both the electric and magnetic fields depend only on the transverse or longitudinal coordinate (determined by the electric field). The Chirikov-like mappings are derived for each case, from which we find the upper limits of the electron energy from the stochastic motion. All the analyses are checked by the numerical simulations.

Chapter 2

Stochastic electron acceleration in colliding laser beams

Electron in multiple laser pulses is an interesting topic in the course of laser-plasma interactions and has been considerably studied (e.g., see Refs. [6, 19, 24, 45, 46, 47, 60, 63, 73]). It was shown that a counter-propagating lasers can be slightly detuned by the electron plasma frequency and thus drive the coherent motion of electrons [73, 74]. More importantly, it was shown that the electrons in the multiple laser waves can be accelerated resulting from the stochastic motion of electrons [24, 46, 47, 60, 63], which occurs when the amplitudes of lasers exceed some thresholds (numerical simulations show that thresholds in counter-propagating lasers with normalized amplitudes a_1 and a_2 are $a_1 a_2 = 1/16$ for local stochastic motion [46] and $a_1 a_2 = 1/2$ for global stochastic motion [47]). Given that the stochastic acceleration is insensitive to the frequency differences of the two laser pulses [47] and it can work without a self-focusing ion channel, it is easier to be achieved than that for coherent motion. It was shown that the most efficient stochastic heating is achieved for the case of two counter-propagating laser waves [45, 63]. Such configuration of two laser beams can be due to the reflection of the dominant incident laser beam from the target surface [75, 76] or Raman backscattering (the Raman backscattering wave

of a driving pulse occurs in plasma at a few percents of the critical density). For a relativistic incident laser pulse, $I\lambda^2 \gtrsim 10^{18} W cm^{-2} \mu m^2$, the reflected wave and Raman backscattering wave will be intense enough to trigger the stochastic acceleration. Therefore the stochastic acceleration in counter-propagating laser waves could be dominant in certain cases in laser interaction with underdense plasma.

However, due to the multidimensional spatio-temporal characteristics of the laser waves and strong nonlinearity of the dynamics of relativistic electrons in these waves, the analytic investigations of stochastic electron acceleration in the colliding laser waves in earlier studies have been limited to either non-relativistic case [4, 61], or the stochastic instability near the separatrices using quite complicated multidimensional Hamiltonian approach [16, 24, 46, 62]. On the other hand, the numerical simulations, which can shed some light on the criterion for stochastic electron motion in multiple laser waves [47, 60, 63], are only valid within the simulated parameter range. Therefore, more complete theoretical analysis is needed to have a better understanding of the electron dynamics in the counter-propagating laser waves.

In this chapter, we will examine the electron dynamics in colliding laser beams by employing the Hamiltonian approach with the proper choices of canonical variables and time, such that the Hamiltonian is time-independent in zero-order approximation [77, 78]. Following Refs. [46, 47, 60, 62], we will focus on the case where one of the laser waves is much stronger than others, which could be considered as a perturbation. We will show that the electron energy gained from the stochastic acceleration due to the presence of a perturbative counter-propagating laser wave can greatly exceed the ponderomotive energy scaling of the dominant laser, where the essential role of the perturbation is to change the dephasing rate between the electron and dominant laser.

The remainder of this chapter is organized as follows. The new Hamiltonian equations will be derived in section 2.1 and the unperturbed electron trajectories are examined. Section 2.2 will investigate the conditions for stochasticity for different laser polarization directions and

initial electron momentum. An impact of the superluminal phase velocity will be discussed in section 2.3. The main results will be summarized and discussed in section 2.4.

2.1 New Hamiltonian equations and unperturbed electron trajectories

In this section, we will derive the new Hamiltonian equations by finding proper canonical variables such that the new Hamiltonian is time-independent without the perturbative laser, and then examine the unperturbed electron trajectories in this new framework. To simplify the expressions, in what follows we will use dimensionless variables, where $\mathbf{r}$ is normalized by the dominant laser wavenumber (k) and t by kc with c being the speed of light in vacuum. The normalized parameter of laser wave, which can be described by vector potential $\mathbf{A}$, is $e\mathbf{A}/mc^2$, where $-e$ and m are the electron charge and mass. In the normalized variables, we take $e = m = c = 1$.

We assume that the dominant laser wave propagates along z direction and is described by the vector potential of $\mathbf{A}(v_p t - z)$, which is arbitrarily polarized in x and y directions (here v_p is the phase velocity). For generality, we consider the perturbative laser wave propagating in the (y,z) plane, which is determined by the vector potential of $\mathbf{A}_1(v_p t + ycos\phi + zsin\phi)$, where ϕ is the angle between the perturbative laser propagation direction and y-axis; and $\mathbf{A}_1$ can have three components in x, y, and z directions, but $A_{1y}/A_{1z} = -tan\phi$ to ensure the orthogonality between the polarization and propagation directions. Then the electron dynamics can be described by the Hamiltonian:

$$\mathcal{H} \equiv \gamma = [1 + (\mathbf{P} + \mathbf{A} + \mathbf{A_1})]^{1/2}, \tag{2.1}$$

where γ is the relativistic factor and $\mathbf{P} = \gamma\mathbf{v} - \mathbf{A} - \mathbf{A_1}$ is the canonical momentum. Although this Hamiltonian was widely used (e.g., see Refs. [46, 16, 62]), the analyses of electron dynamics

accounting for both dominant and perturbative lasers were quite complicated and often incomplete.

We start our analysis with finding the proper canonical variables, Hamiltonian and effective time, such that the new Hamiltonian will be time-independent when the perturbation is absent ($\mathbf{A}_1 = 0$). Taking into account that for $\mathbf{A}_1 = 0$ the combination $\gamma - v_p P_z$ is conserved, it could be considered as a candidate for the new Hamiltonian, while the phase of the dominant laser wave $\eta = v_p t - z$ can be taken as one new canonical variable. It is easy to show that for the laser field $\mathbf{A}(v_p t - z) + \mathbf{A}_1(v_p t + y cos\phi + z sin\phi)$ the canonical momentum P_x is conserved so that the Hamiltonian in Eq. (2.1) is effectively two dimensional. Then, if we treat (η, y) as new canonical coordinates and assume that the corresponding canonical momenta are (χ_η, χ_y), while the new Hamiltonian and time are H and τ, the canonical transformation from the point view of least action principle [79] requires that

$$C(P_z dz + P_y dy - \mathcal{H} dt) = \chi_\eta d\eta + \chi_y dy - H d\tau, \tag{2.2}$$

where C is a constant given that the Lagrangian is not unique. The natural choice of τ is $\tau = v_p t + z sin\phi$. Substituting τ and η into Eq. (2.2) we find $\chi_\eta = -(\gamma sin\phi + v_p P_z)$, $\chi_y = v_p(1 + sin\phi)P_y$, and $H = \gamma - v_p P_z$ for $C = v_p(1 + sin\phi)$. However, for convenience, we will take $\chi_\eta = +(\gamma sin\phi + v_p P_z)$, which is equivalent to choosing η as canonical momentum while treating χ_η as a canonical coordinate. Then the electron dynamics can be described by $H(\chi_\eta, y, \eta, \chi_y, \tau)$, which in the new canonical variables can be found from Eqs. (2.1, 2.2).

For the head-on colliding laser waves ($\phi = \pi/2$), χ_y is a constant. As a result, we have the following 3/2 dimensional (3/2D) Hamiltonian equations

$$\frac{d\chi}{d\tau} = \frac{\partial H}{\partial \eta}, \text{ and } \frac{d\eta}{d\tau} = -\frac{\partial H}{\partial \chi}, \tag{2.3}$$

where $\chi \equiv \chi_\eta = \gamma + v_p P_z$ and the Hamiltonian is

$$H(\chi,\eta,\tau) = \frac{2v_p}{v_p^2-1}\sqrt{\chi^2+(v_p^2-1)P_\perp^2} - \frac{v_p^2+1}{v_p^2-1}\chi, \tag{2.4}$$

with $P_\perp^2 = 1+\sum_{i=x,y}\left[\bar{P}_i + A_i(\eta) + A_{1i}(\tau)\right]^2$ and $\bar{P}_i$ $(i=x,y)$ are the conserved canonical momentum. This 3/2D Hamiltonian, which can also be obtained from the electron equations of motion, will greatly simplify our analysis in comparison with the multidimensional Hamiltonian [46, 62] based on Eq. (2.1).

For simplicity, we first consider the luminal case $v_p = 1$, while the impact of superluminal phase velocity, which mimics the impact of plasma on the laser wave propagation, will be qualitatively discussed in section 2.3. The linearly polarized planar laser waves will be used in the following analysis, i.e., $\mathbf{A} = asin(\eta)\mathbf{e}_x$ and $\mathbf{A}_1 = a_1 sin(k_1\tau)\mathbf{e}_x$ or $\mathbf{A}_1 = a_1 sin(k_1\tau)\mathbf{e}_y$ depending on the relative polarization directions of the counter-propagating waves, where $a_1 \ll a$ and k_1 is the ratio of the perturbative laser frequency (or wavenumber) to that of the dominant one. Then, the Hamiltonian in Eq. (2.4) degenerates to

$$H = \frac{1+\left[asin(\eta)+\delta_x a_1 sin(k_1\tau)+\bar{P}_x\right]^2+\left[\delta_y a_1 sin(k_1\tau)+\bar{P}_y\right]^2}{\chi}, \tag{2.5}$$

where $\delta_{x,y} = 0$ or 1 are switches to controlling the perturbative laser polarization direction. Keep in mind that we are interested in the gain of maximum electron kinetic energy, γ_{max}, which can be expressed in the terms of H, for $v_p = 1$, as follows:

$$\gamma_{max} \equiv \frac{\chi+H}{2} \approx \frac{1}{2}\left(\frac{E_p}{H}+H\right), \tag{2.6}$$

where $E_p = 1+(a+|\bar{P}_x|)^2+\bar{P}_y^2$. Note that the ponderomotive scaling for pre-accelerated electron in the dominant laser wave only is E_p/H_0, where H_0 is the conserved dephasing rate between electron and the dominant laser (which corresponds to the initial Hamiltonian in the present

problem). Therefore, γ_{max} can significantly exceed the ponderomotive scaling either for $H_{min} < H_0$ (which corresponds to the electron moving along with the dominant laser, where $\gamma_{max}/E_p \approx H_0/H_{min}$) or for $H_{max} > E_p/H_0$ (where the electron moves along with the perturbative laser and $\gamma_{max}/E_p \approx H_{max}H_0/E_p$).

For the unperturbed problem ($a_1 = 0$), the new Hamiltonian is conserved and from Eqs. (2.3, 2.5) we find the following implicit dependence $\eta(\tau)$ (we note that η increases with τ provided $d\eta/d\tau > 0$):

$$\tau = \frac{2\bar{P}^2 + a^2}{4H^2}\left[2\eta - \frac{a^2 sin(2\eta)}{2\bar{P}^2 + a^2} - \frac{8a\bar{P}_x cos(\eta)}{2\bar{P}^2 + a^2}\right] + const., \tag{2.7}$$

where $\bar{P}^2 = 1 + \bar{P}_x^2 + \bar{P}_y^2$; and χ depending on time τ:

$$\chi = \frac{1 + [asin(\eta) + \bar{P}_x]^2 + \bar{P}_y^2}{H}. \tag{2.8}$$

From Eq. (2.7) one can find the frequency of unperturbed oscillation of electron canonical coordinate χ:

$$\omega = \frac{2\pi}{T} = \frac{2H^2}{2\bar{P}^2 + a^2}, \tag{2.9}$$

where $T = \tau(\eta = 2\pi) - \tau(\eta = 0)$ is the period of electron oscillation. Therefore, the presence of $\bar{P}_{x,y}$ will decrease (increase) the frequency (period) of electron oscillation via $\bar{P}^2$ and alter the electron trajectories as shown in Eqs. (2.7, 2.8).

From Eq. (2.5) we find that, for relativistic case $a > 1$ (which we will consider in the following), unperturbed (or weakly perturbed) electron trajectories have characteristics of zig-zag time dependence of canonical coordinate χ (e.g., see the upper panel of Fig. 2.1). This feature of electron trajectories enables a long tail of the distribution of the amplitude of m-harmonics, making high-m island overlapping and, therefore, stochastic electron motion possible. Also, from Eq. (2.5) it follows that the strongest impact, "kicks", on both H and canonical variables by the

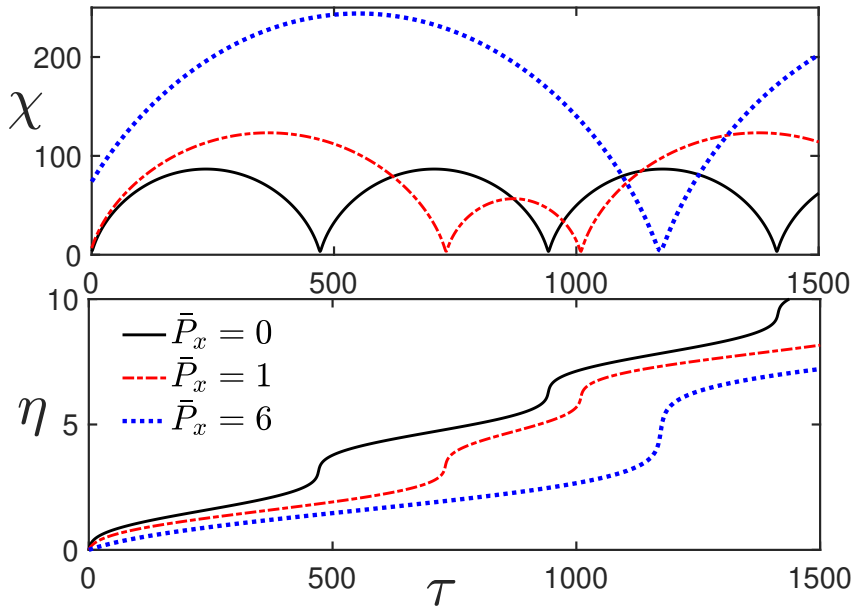

Figure 2.1: Schematic view of the electron trajectories for $a = 5$, $k_1 = 1$, $\bar{P}_y = 0$, and different $\bar{P}_x$. The curves of solid black and dash-dotted red are for $\bar{P}_x = 0$ and $\bar{P}_x = 1$ with $H = 0.3$, and the dotted blue curve is for $\bar{P}_x = 6$ with $H = 0.5$.

perturbative laser occurs at a very short time near the local minimum of χ (e.g., see Fig. 2.2), where the phase between electron and backward laser wave is locally minimized and η undergoes jump. The positions of minima of χ depend both on $\bar{P}_x$ and a: when $|\bar{P}_x| < a$, χ is minimized at $\eta_1 = (2n+1)\pi + \delta$ and $\eta_2 = 2n\pi - \delta$, where $\delta = sin^{-1}(\bar{P}_x/a)$ and n is an integer; whereas, for $\bar{P}_x > a$ ($\bar{P}_x < -a$), the minima of χ are obtained only at $\eta_3 = -\pi/2 + 2n\pi$ ($\eta_4 = \pi/2 + 2n\pi$).

2.2 Threshold for stochastic electron motion

From Hamiltonian in Eq. (2.5) it follows that in the presence of the perturbative laser wave but for $\omega > k_1$, the electron motion is adiabatic and no electron acceleration is possible. However, when $\omega \ll k_1$ the unperturbed electron motion could resonate with the perturbative laser, $m\omega = k_1$ (where m is the harmonics of unperturbed electron motion), and for the case of overlapping of the separatrices of neighbouring resonant islands, $\bar{K} = (\delta\omega + \delta\omega')/2\Delta\omega > 1$, where $\delta\omega$ and $\delta\omega'$ are their widths and $\Delta\omega$ is the distance between them, stochastic heating occurs [56]. However, in

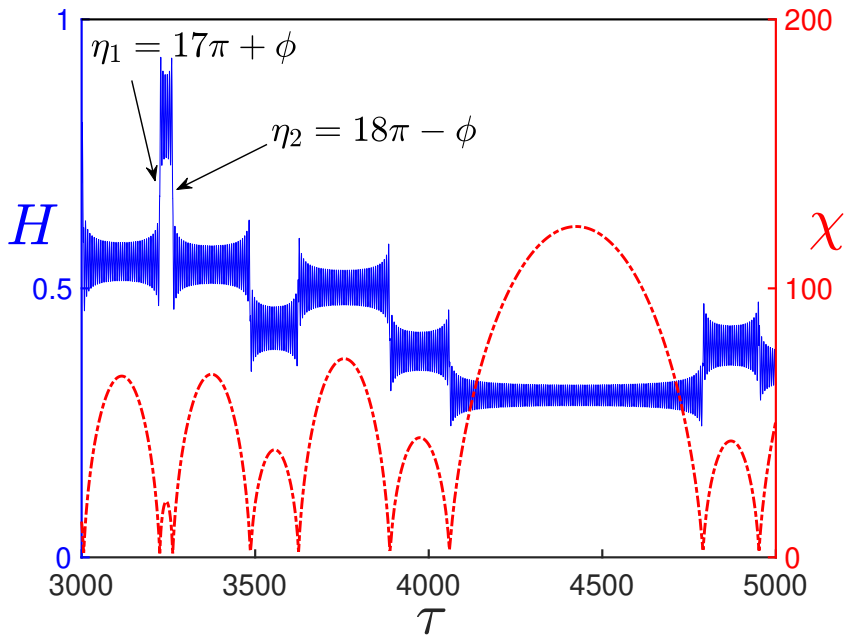

Figure 2.2: Schematic view of the diffusion of Hamiltonian (solid blue) and corresponding χ (dash-dotted red) for $a = 5$, $a_1 = 0.2$, $k_1 = 1$, $\bar{P}_y = 0$, and $\bar{P}_x = 1$.

what follows, we will examine the condition for an onset of stochasticity for the case $\omega/k_1 \ll 1$ by using equivalent, but more convenient Chirikov-like mapping [58] deduced from electron equations of motion.

As discussed in the last section, the kicks due to the perturbative laser of H takes place at a short time near the local minimum of χ (e.g., see Fig. 2.2). Except these short periods of time τ where $\eta \approx \eta_{1,2}$ for $|\bar{P}_x| < a$ and $\eta \approx \eta_3$ (η_4) for $\bar{P}_x > a$ ($\bar{P}_x < -a$), the electron "sees" only fast phase change of the backward laser wave due to large $\chi = \gamma + P_z$ and, therefore, undergoes adiabatic oscillation. Therefore, the Chirikov-like mapping can be formed by using the Hamiltonian H_n and time τ_n, when the electron passes through the nonadiabatic region. Such mapping corresponds to the Poincaré section of electron crossing effectively "fixed" canonical momentum (η) plane. Let's assume that the change of the Hamiltonian due to each nonadiabatic interaction of electron with the perturbative wave is smaller than the Hamiltonian itself, i.e., $\Delta H = |H_{n+1} - H_n| \ll H_n$, then the unperturbed electron trajectory $H_n(\eta, \chi)$ can be used to estimate

the variation of Hamiltonian due to each kick [23]:

$$\Delta H_n \equiv H_{n+1} - H_n = \int_{\eta \approx \eta_i} \frac{\partial H}{\partial \tau} d\tau,\ i = 1, 2 \text{ or } 3 \text{ or } 4. \tag{2.10}$$

However, to make the analysis easier without losing the physics of stochastic electron acceleration, we consider $\bar{P}_x = \bar{P}_y = 0$, which is reasonable if electrons begin to interact with the pre-pulse of lasers (the impacts of $\bar{P}_x$ and $\bar{P}_y$ on the stochastic condition of electrons in colliding lasers with the same polarization direction will be discussed in Appendix A). As a result, the nonadiabatic region (local minimum of χ) corresponds to $\eta \approx n\pi$ with n being an integer.

2.2.1 Lasers with same polarization directions

We first consider the case where the perturbative laser is polarized along the dominant one, i.e., $\mathbf{A}_1 = a_1 sin(k_1\tau)\mathbf{e}_x$ such that $\delta_x(\delta_y) = 1(0)$ in Eq. (2.5). Under the condition of $a_1 \ll a$, we could keep the leading term of $\partial H/\partial\tau = 2aa_1k_1 sin(\eta)cos(k_1\tau)/\chi$. The fact that the main contribution to Hamiltonian variation is from $\eta \approx n\pi$ enables us to do the expansion of the integrand in Eq. (2.10) with respect to $\eta - n\pi$. After some algebra, we find

$$\frac{\Delta H_n}{H_n} = 2(-1)^n a_1 \beta^{1/2} sin(k_1\tau_n) \int_{-\infty}^{\infty} \tilde{\eta} sin\left(\beta\tilde{\eta} + \frac{1}{3}\tilde{\eta}^3\right) d\tilde{\eta}, \tag{2.11}$$

where $\tilde{\eta} = (\eta - n\pi)/\alpha$, $\alpha = (H_n^2/k_1a^2)^{1/3} \sim (\omega/k_1)^{1/3} \ll 1$, and $\beta = (k_1/H_n^2a)^{2/3}$. It should be noted that the fast oscillation for $\tilde{\eta} \tilde{>} 1$ justifies the extension of the integration limits to infinity. We also see that the nonadiabatic interaction of electron motion with backward laser occurs at $|\eta - n\pi| < \alpha \ll 1$ ($|\tilde{\eta}| \tilde{<} 1$).

The integral in Eq. (2.11) could be expressed with the derivative of Airy function, $Ai'(\beta)$, so we have

$$\Delta H_n = 4(-1)^{n+1}\pi a_1 \beta^{1/2} Ai'(\beta) H_n sin(\psi_n), \tag{2.12}$$

where $\psi \equiv k_1\tau_n$. Taking into account the properties of the Airy function, it follows that the requirement of $\Delta H < H_n$ is always satisfied for $a_1 \tilde{<} 1$.

The time interval between two consecutive kicks is equal to the period of the unperturbed electron oscillation and thus the corresponding phase interval is determined by the Hamiltonian:

$$\Delta\psi_n \equiv \psi_{n+1} - \psi_n = k_1 T = \frac{\pi k_1 (2+a^2)}{2H_{n+1}^2}. \tag{2.13}$$

As a result, rearranging Eqs. (2.12, 2.13) could form symplectic mapping conserving phase volume. However, we are interested in the condition for stochasticity, which could be obtained just from Eqs. (2.12, 2.13), and reads as

$$K_x = \left| \frac{d\Delta\psi_n}{dH_{n+1}} \frac{d\Delta H_n}{d\psi_n} \right| \tilde{>} 1, \tag{2.14}$$

where local instability leads to the mixing in phase space. If we disregard the region of phase ψ where chaos appears, we arrive at

$$K_x = 4\pi^2 a a_1 (2+a^2)\beta^2 |Ai'(\beta)| \tilde{>} 1. \tag{2.15}$$

Similar result can be obtained from the point of view of resonance overlapping, where one can show that $K_x \approx \bar{K}^2$.

Introducing the function $f_x(\beta) = 4\pi^2\beta^2|Ai'(\beta)|$, we find that $f_x(\beta)$ increases with β for $\beta < 1$ as

$$f_x(\beta) \approx \pi^2\beta^2; \tag{2.16}$$

reaches maximum, $f^x_{max} \approx 8.83$, at $\beta = \beta^x_s \approx 1.68$; and then falls exponentially at $\beta > \beta^x_s$ (e.g., see Ref. [80]):

$$f_x(\beta) \approx 2\pi^{3/2}\beta^{9/4} exp\left[-(2/3)\beta^{3/2}\right]. \tag{2.17}$$

As a result, from Eq. (2.15) we find that stochastic acceleration is only possible for $a_1 > a_s^x$, where

$$a_s^x = \frac{(f_{max}^x)^{-1}}{a(2+a^2)} \approx \frac{0.11}{a(2+a^2)}. \tag{2.18}$$

We notice that the threshold in Eq. (2.18) is quite different from those in Refs. [46, 47]. The reason for this is that our analysis allows for finding the most stochastically "unstable" range of H (and corresponding electron kinetic energy) and, therefore, gives an exact threshold value of a_1 for the stochasticity onset.

However, for a_1 only slightly larger than a_s^x, the stochastic acceleration occurs only within a narrow region in the vicinity of $H \approx H_s^x$ ($\beta \approx \beta_s^x$), where

$$H_s^x \approx 0.68 \left(\frac{k_1}{a}\right)^{1/2}. \tag{2.19}$$

For $a_1 \gg a_s^x$ stochastic acceleration becomes possible within the range of H: $H_{min}^x < H < H_{max}^x$, where the lower boundary of stochasticity is due to the exponential decay of the width of resonant islands, whereas the upper one is because the distance between the neighboring resonant islands increases faster than their widths. H_{max}^x and H_{min}^x could be found by using asymptotic expressions (2.16, 2.17) of the function $f_x(\beta)$. However, we notice that the inequalities $a \gg a_1 \gg a_s^x$ could be only satisfied for $a \gg 1$, under which we obtain:

$$H_{min}^x \approx \frac{H_s^x}{\sqrt{1.6 + 0.69 ln\,(a_1/a_s^x)}}, \tag{2.20}$$

and

$$H_{max}^x \approx 1.5 \left(\frac{a_1}{a_s^x}\right)^{3/8} H_s^x. \tag{2.21}$$

If we consider initially rest electrons, from Eq. (2.6), we see that γ_{max} can significantly exceed the ponderomotive scaling $E_p/2$ either for $H_{min}^x < 1$ (which corresponds to the electron moving along with the dominant laser wave) or for $H_{max}^x > E_p$ (where the electron moves

along with the perturbative laser). By using expressions (2.20, 2.21) and neglecting numerical factors order of unity, we find that the energy of electrons moving along with dominant laser radiation exceeds the ponderomotive scaling for the case $k_1 < a$ and reaches $\gamma_{max} \sim E_p(a/k_1)^{1/2}$. Whereas the energy of electrons moving along with the perturbative laser could exceed the ponderomotive scaling for the case $k_1 > a^2 > 1$ and $(a^2/k_1)^{4/3} < a_1/a < 1$, where $\gamma_{max} \sim E_p(k_1/a^2)^{1/2}(a_1/a)^{3/8}$. We notice that H^x_{min} and, therefore, corresponding value of γ_{max} have a weak logarithmic dependence on the ratio $a_1/a^x_s > 1$. Moreover, for the case $a^{-2} < k_1 < a$ and $(a^2k_1)^{-4/3} < a_1/a < 1$, we have $H^x_{min} < 1 < H^x_{max}$ and Hamiltonian $H \sim 1$, corresponding to an initially stationary electron, is in the stochastic region. As a result, the stochastic acceleration of an electron, being initially at rest, to kinetic energy exceeding E_p is possible and such energetic electron will move along with dominant laser radiation. Otherwise, pre-acceleration of an electron in the direction along with (for $a_s/a < a_1/a < (k_1a^2)^{-4/3}$ and $k_1 < a$) or opposite to (for $k_1 > a$) the dominant laser propagation is necessary to reach the stochastic region for further acceleration.

Coming back to the expression (2.15), we observe that for $\beta < \beta^x_s$, K increases with increasing β (which for $H^x_{min} < 1$ corresponds to increasing electron energy). It explains the results of numerical simulations from Ref. [47], which demonstrated that the pre-acceleration of electrons reduces the stochastic threshold value of aa_1 (e.g., see Fig. 3(b) in Ref. [47]).

To verify the results of our analytical considerations, we integrate Eqs. (2.3, 2.5) numerically and present the results in the Poincaré maps of (H, ψ) or (γ, ψ), when $\eta = n\pi + \pi/2$, where χ and thus $\gamma = (\chi + H)/2$ reaches their maximum in one unperturbed electron period. The results for $a = 5$, $a_1 = 0.1$, $k_1 = 1$ and $\bar{P}_x = \bar{P}_y = 0$ are displayed in Fig. 2.3, where $k_1 < a$ is satisfied and thus $\gamma_{max} \approx E_p/2H_{min}$. As one can see, a stochastic "sea" is bounded by the KAM invariant [56] at H_{min} and H_{max}, which are, respectively, $H_{min} \approx 0.132$ and $H_{max} \approx 2.92$, and fully agree with Eqs. (2.20) and (2.21). Therefore, the maximum stochastic kinetic energy (γ_{max}), which is insensitive to a_1 as proven in the simulations, is approximately seven times ($1/H_{min}$) larger than that without the backward wave ($E_p/2$). Note that the maximum electron kinetic energy is

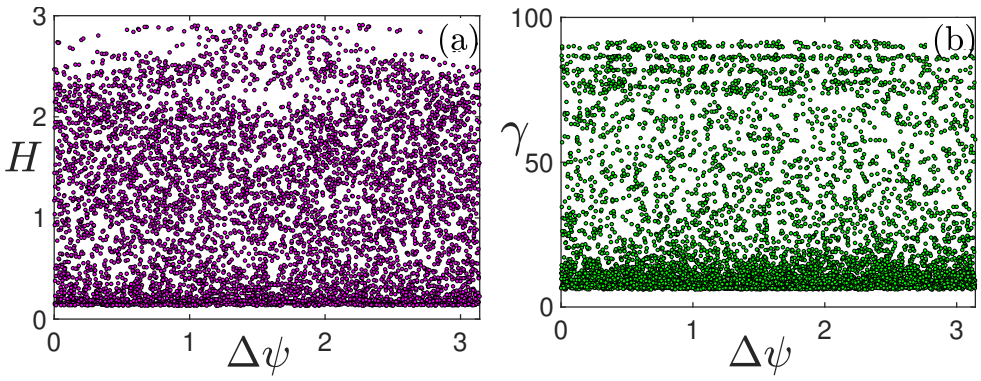

Figure 2.3: Poincaré mappings of (a) $(H,\Delta\psi)$ and (b) $(\gamma,\Delta\psi)$ of electrons when $\eta = n\pi+\pi/2$ for $a=5$, $a_1=0.1$, and $k_1=1$, where $\Delta\psi \equiv \psi - [\psi/\pi]\pi$.

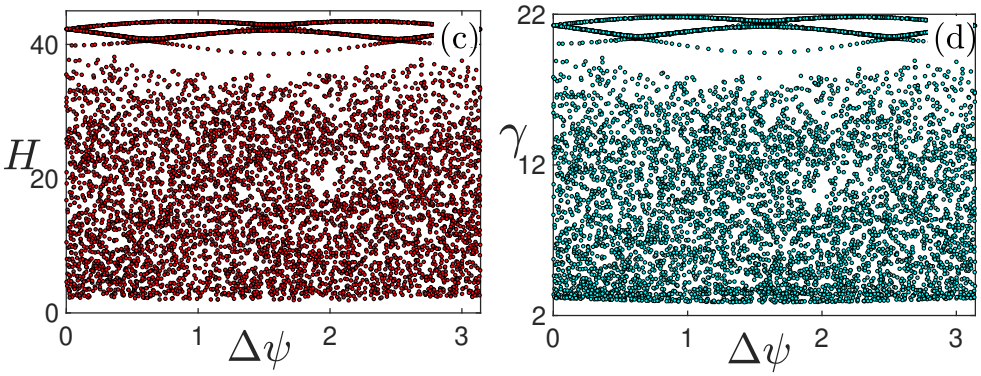

Figure 2.4: Poincaré mappings of (a) $(H,\Delta\psi)$ and (b) $(\gamma,\Delta\psi)$ of electrons when $\eta = n\pi+\pi/2$ for $a=3$, $a_1=0.3$, and $k_1=100$ with the same definition of $\Delta\psi$ with Fig. 2.3.

$E_{max} = \gamma_{max} mc^2 \sim 45MeV$ for the choosing $a=5$ and $k_1=1$. In Fig. 2.4 we show the results for $a=3$, $a_1=0.3$, $\bar{P}_x=\bar{P}_y=0$ but $k_1=100$, where $H_{min}\approx 1.87$ and $H_{max}\approx 37.5$ are, respectively, in agreement with Eq. (2.20) and (2.21). For such large value of $k_1 > a^2$, we see that the maximum stochastic energy satisfies $\gamma_{max}\approx H_{max}/2 > E_p/2$.

2.2.2 Lasers with orthogonal polarization directions

In this section, we consider the case where the colliding laser waves have orthogonal polarization directions, i.e., $\mathbf{A}_1 = a_1 sin(k_1\tau)\mathbf{e}_y$ such that $\delta_y(\delta_x)=1(0)$ in Eq. (2.5). For such case, $\bar{P}_y$ is important since it can be the same order with a_1 in $\partial H/\partial\tau = 2a_1k_1\,[a_1 sin(k_1\tau)+\bar{P}_y]\,cos(k_1\tau)/\chi$. Similar to the last section, we can do expansion of τ with respect to $\eta-\eta_i$ when estimating the

Hamiltonian variation in the nonadiabatic region. As a result, we have

$$\Delta H_n = \frac{2\pi a_1^2 \beta Ai(2^{2/3}\beta)}{(1+\bar{P}_y^2)} H_n sin(2\psi_n) + \frac{4\pi a_1 \bar{P}_y \beta Ai(\beta)}{(1+\bar{P}_y^2)} H_n sin(\psi_n), \tag{2.22}$$

whereas the phase interval between two consecutive kicks is given in Eq. (2.13).

For $\bar{P}_y = 0$, we see that the phase in Eq. (2.22) corresponding to the Chirikov-like mapping is twice of that in Eq. (2.12) for $\mathbf{A}_1$ polarized along with $\mathbf{A}$. As a result, the stochastic condition can be found from Eqs. (2.12, 2.22) as

$$K_y = 4\pi^2 a a_1^2 (2+a^2)\beta^{5/2}|Ai(2^{2/3}\beta)| \tilde{>} 1. \tag{2.23}$$

Introducing the function $f_y(\beta) = 4\pi^2\beta^{5/2}|Ai(2^{2/3}\beta)|$, we find that $f_y(\beta)$ first increases with β for $\beta < \beta_s^y \approx 1.10$; reaches its maximum, $f_{max}^y \approx 2.55$, at β_s^y; and then falls exponentially at $\beta > \beta_s^y$ (e.g., see Ref. [80]) as

$$f_y(\beta) \approx 2^{5/6}\pi^{3/2}\beta^{9/4} exp\left[-(4/3)\beta^{3/2}\right]. \tag{2.24}$$

One can show that for $\beta < \beta_s^y$, f_y can also be approximated by the expression (2.24) with a different factor of order of unity. As a result, from Eq. (2.23) we find that stochastic acceleration is only possible for $a_1 > a_s^y$, where

$$a_s^y = \left[\frac{(f_{max}^y)^{-1}}{a(2+a^2)}\right]^{1/2} \approx \frac{0.63}{[a(2+a^2)]^{1/2}}, \tag{2.25}$$

and the stochastic acceleration occurs in the vicinity of $H \approx H_s^y$ ($\beta \approx \beta_s^y$), where

$$H_s^y \approx 0.93\left(\frac{k_1}{a}\right)^{1/2}. \tag{2.26}$$

It follows that the threshold in Eq. (2.25) is larger than that in Eq. (2.18) for the case of parallel polarized laser waves. For $a_1 \gg a_s^y$, stochastic acceleration becomes possible within the range of

H: $H^y_{min} < H < H^y_{max}$, where H^y_{max} and H^y_{min} could be found by using Eq. (2.24) of the function $f_y(\beta)$ as

$$H^y_{min} \approx \frac{H^y_s}{\sqrt{1.56 + 1.30ln\left(a_1/a^y_s\right)}}, \text{ and } H^y_{max} \approx 1.35\left(\frac{a_1}{a^y_s}\right)^{2/3} H^y_s, \tag{2.27}$$

where we have taken the numeric factor into account when using Eq. (2.24) for $\beta < \beta^y_s$. Considering that a^y_s is much lager than a^x_s for the same parameters, H^y_{min} (H^y_{max}) is relatively lager (smaller) than H^x_{min} (H^x_{max}). As a result, from Eq. (2.6), the maximum energy of electrons in two lasers being orthogonally polarized is smaller than that of electrons in two parallel polarized lasers when $\bar{P}_{x,y} = 0$.

On the other hand, if $|\bar{P}_y| \gg a_1$, the variation of Hamiltonian in Eq. (2.22) is mainly determined by the second term and the stochastic condition reads

$$\bar{K}_y = \frac{4\pi^2 a_1 a \bar{P}_y \left[2(1+\bar{P}^2_y) + a^2\right] \beta^{5/2} |Ai(\beta)|}{(1+\bar{P}^2_y)^{5/2}} \tilde{>} 1. \tag{2.28}$$

As a result, we could find the stochastic condition by using the properties of $\bar{f}_y(\beta) = 4\pi^2\beta^{5/2}|Ai(\beta)|$ as:

$$a_1 > \bar{a}_{sy} = \frac{0.12(1+\bar{P}^2_y)^{5/2}}{a\bar{P}_y\left[2(1+\bar{P}^2_y)+a^2\right]}, \tag{2.29}$$

and the most unstable Hamiltonian:

$$\bar{H}_{sy} \approx 0.66(1+\bar{P}^2_y)^{3/4}\left(\frac{k_1}{a}\right)^{1/2}. \tag{2.30}$$

It follows that the threshold in Eq. (2.29) is smaller than that in Eq. (2.25) for $\bar{P}_y = 0$ if $a_1 \ll |\bar{P}_y| \tilde{<} a^{3/8}$ and even comparable with a^x_s when $|\bar{P}_y| \tilde{>} 1$. However, considering that the lower boundary of stochastic region has a weak dependence on $a_1/\bar{a}^y_s$:

$$\bar{H}^y_{min} \approx \frac{\bar{H}_{sy}}{\sqrt{1.68 + 0.65ln\left(a_1/\bar{a}_{sy}\right)}}, \tag{2.31}$$

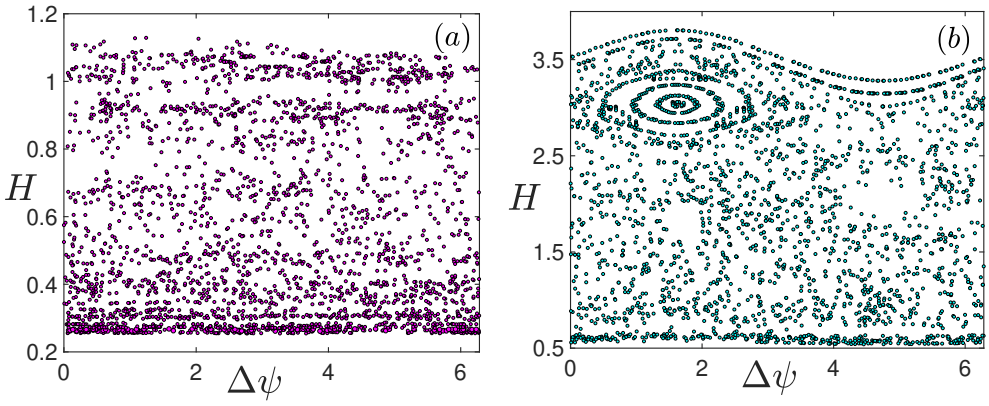

Figure 2.5: Poincaré mappings of (H, ψ) at $\eta = 2n\pi + \pi/2$ with $\Delta\psi \equiv \psi - [\psi/2\pi] \times 2\pi$ for $a = 5$, $\mathbf{A}_1 = 0.2sin(\tau)\mathbf{e}_y$ ($k_1 = 1$), $\bar{P}_x = 0$ and (a) $\bar{P}_y = 0$; (b) $\bar{P}_y = 2$.

the increase of $\bar{H}_{sy}$ with $\bar{P}_y$ will make $\bar{H}^y_{min}$ above H^y_{min} for $\bar{P}_y = 0$ in Eq. (2.27). As a result, the ratio of the maximum electron kinetic energy against the ponderomotive scaling, H_0/H_{min}, will decrease with increasing $\bar{P}_y$. The upper boundary of stochasticity in Hamiltonian space is obtained as

$$\bar{H}^y_{max} \approx 1.32 \left(\frac{a_1}{\bar{a}^y_s}\right)^{1/3} \bar{H}^y_s, \tag{2.32}$$

which is above H^y_{max} for the same parameters except $\bar{P}_y$.

The numerical simulations integrating Eqs. (2.3, 2.5) are performed for the case where the polarization direction of the perturbative laser is orthogonal to that of the dominant one, as shown in Fig. 2.5. It confirms that the lower and upper stochastic boundaries in the Hamiltonian space are, respectively, in agreement with Eq. (2.27) for $\bar{P}_y = 0$, and with Eqs. (2.31, 2.32) for $\bar{P}_y \gg a_1$. For all the cases, the maximum electron kinetic energy is consistent with Eq. (2.6).

2.3 Impact of the superluminal phase velocity

In this section, we examine the impact of superluminal phase velocity, $v_p > 1$, on the stochastic electron dynamics. Here we only consider the case of parallel polarized laser beams assuming that $\bar{P}_{x,y} = 0$. For this purpose, we should again consider the unperturbed electron

trajectories with conserved H, which, from Eq. (2.4), reads

$$\chi = \frac{2v_p\sqrt{H^2+(v_p^2-1)(1+a^2 sin^2\eta)}}{v_p^2-1} - \frac{(v_p^2+1)H}{v_p^2-1}. \tag{2.33}$$

Therefore, χ reaches its maximum and minimum at, respectively, $\eta = \pi/2 + n\pi$ and $\eta = n\pi$ as

$$\begin{aligned} \chi_{max} &= \frac{2v_p\sqrt{H^2+(v_p^2-1)(1+a^2)}}{v_p^2-1} - \frac{(v_p^2+1)H}{v_p^2-1}, \\ \chi_{min} &= \frac{2v_p\sqrt{H^2+v_p^2-1}}{v_p^2-1} - \frac{(v_p^2+1)H}{v_p^2-1}. \end{aligned} \tag{2.34}$$

It follows that both χ_{max} and χ_{min} decrease with increasing H and so is $\gamma_{max} = (\chi_{max}+H)/2 \approx \chi_{max}/2$ (we consider $k_1 \sim 1$ such that γ_{max} is dominated by χ_{max}). Therefore, the maximum electron kinetic energy is obtained at the lower boundary of the stochastic region in the Hamiltonian space (H_{min}). Noticing that $\partial H/\partial\tau$ is maximized at χ_{min}, we know that the strongest impact of the perturbative laser on electron motion for superluminal case also occurs at χ_{min} corresponding to $\eta \approx n\pi$ for $\bar{P}_x = 0$ like in the luminal case. On the other hand, the period of electron oscillation is given by

$$T/2\pi = \frac{v_p^2+1}{v_p^2-1} - \frac{4v_pHK(b^2)}{\pi(v_p^2-1)\sqrt{H^2+(v_p^2-1)(1+a^2)}}, \tag{2.35}$$

where $K(b^2) \equiv \int_0^{\pi/2} d\eta/\sqrt{1-b^2cos^2\eta}$ is the complete elliptic integral of the first kind and $b^2 = (v_p^2-1)a^2/[H^2+(v_p^2-1)(1+a^2)]$.

Then when $H \tilde{>} \sqrt{(v_p^2-1)(1+a^2)}$, $K(b^2 \ll 1) \approx (1+b^2/4)\pi/2$ such that the electron oscillation period T in Eq. (2.35) is approximate to that for the luminal case. This is also true for the extrema of χ in Eq. (2.34). As a result, the electron trajectories and thus the variation of Hamiltonian ΔH in Eq. (2.10) remains almost unchanged compared with those of luminal case. Then the stochastic region in Hamiltonian space with $\sqrt{(v_p^2-1)(1+a^2)} \tilde{<} H$ is not affected by

the superluminal phase velocity. It follows that if the lower boundary of the stochastic region H_{min} for the luminal case satisfies $\sqrt{(v_p^2-1)(1+a^2)}\tilde{<}H_{min}$, the impact of $v_p > 1$ on both H and electron kinetic energy is negligible.

However, if $H_{min} \ll \sqrt{(v_p^2-1)(1+a^2)}$, from Eq. (2.35) we see that T has an approximately linear dependence on H for $H \ll \sqrt{(v_p^2-1)(1+a^2)}$, so that $|d\Delta\psi_n/dH_{n+1}| \approx 12v_pk_1/(v_p^2-1)\sqrt{(v_p^2-1)(1+a^2)}$ is a constant where we use $K(b^2 \to 1) = ln(4/\sqrt{1-b^2}) \approx 3$ (notice that the dominant term of T is the first one on the right hand side of Eq. (2.35) such that T remains almost unchanged with H). The variation of H in the nonadiabatic region for $H \ll \sqrt{(v_p^2-1)(1+a^2)}$ can be estimated as $\Delta H \sim aa_1(v_p-1)^{1/6}$ from Eqs. (2.4, 2.33). Then the stochastic condition in Eq. (2.14) is a constant value as $K_s \sim a_1/(v_p-1)^{4/3}$ for $|H| \ll \sqrt{(v_p^2-1)(1+a^2)}$, where a factor of order of unity has been omitted. It follows that a threshold value of v_p, $v_{ps}-1 \sim a_1^{3/4}$, exists such that for $v_p < v_{ps}$, the region of $|H| \ll \sqrt{(v_p^2-1)(1+a^2)}$ is stochastic and the lower boundary of the stochastic region in luminal case can extend to negative $H \gg -\sqrt{(v_p^2-1)(1+a^2)}$ (for further negative H the stochasticity is impossible since χ increases smoothly from χ_{min} such that the zig-zag temporal dependence of χ is eliminated); whereas for $v_p > v_{ps}$, the stochasticity in small H region is terminated. The maximum electron kinetic energy for the latter case is rather limited, while for the former case ($v_p < v_{ps}$), taking into account that χ_{max} and thus γ_{max} weakly depends on H for $|H| \ll \sqrt{(v_p^2-1)(1+a^2)}$, we have

$$\gamma_{max} \approx \chi_{max}(H=0)/2 = v_p\sqrt{(1+a^2)/(v_p^2-1)}. \tag{2.36}$$

It shows that the maximum electron kinetic energy for superluminal case is much smaller than that for the luminal case, $\gamma_{max} \approx E_p/2H_{min}$ as shown in Eq. (2.6), even though the stochastic regions in H space are almost the same. Moreover, for the superluminal case, the amplitude of oscillation of electron in the adiabatic region, $\delta H \sim 2a_1\sqrt{v_p^2-1}$, is approximately a constant, whereas for luminal case, it decreases with decreasing H.

Numerical results for $a = 5$, $a_1 = 0.2$, $k_1 = 1$ and different $v_p \geq 1$ are shown in Fig. 2.6. We note that the lower boundary of the stochastic region in the Hamiltonian space for $v_p = 1$ in Fig. 2.6(a) satisfies $H_{min} \ll \sqrt{(v_p^2 - 1)(1 + a^2)}$ and thus the threshold value of $v_{ps} \approx 1 + a_1^{3/4} = 1.3$ exists for stochasticity. Comparing Figs. 2.6(b), 2.6(c) with Fig. 2.6(a) we find that, for $v_p < v_{ps}$, the stochastic region in H space remains almost unchanged for large H, whereas the lower boundary of the stochastic region can extend to negative H with small magnitude. The stability islands appear and grow with increasing v_p and will finally destroy the stochasticity when $v_p > v_{ps}$. However, despite the change of the stochastic region in H space for $v_p < v_{ps}$ is small, the maximum electron kinetic energy gained from the stochastic motion is significantly decreased by the impact of the superluminal phase velocity (e.g., see Fig. 2.6(d) and 2.6(e) for $v_p = 1$ and $v_p = 1.1$, respectively). Recalling that $H \approx 0$ is accessible as long as the stochastic region exists and γ_{max} is insensitive to small H, the maximum electron kinetic energy (e.g., see Fig. 2.6(e)) can be well predicted by Eq. (2.36). In Fig. 2.6(f) we sketched the evolution of H for $v_p = 1.1$, which confirms that for small $H \ll \sqrt{(v_p^2 - 1)(1 + a^2)}$, the electron oscillation period remains almost unchanged unlike the luminal case shown in Fig. 2.2. All these results agrees with our analysis.

2.4 Conclusion

In conclusion, we consider the electron dynamics in the fields of colliding laser beams. We show that the proper choice of canonical variables and effective time, such that the new Hamiltonian is conserved for electrons in a dominant laser field, greatly simplifies the analytical treatment of the problem. For example, for the case of counter-propagating planar laser beams and dominant laser with relativistic intensity, $a > 1$, such approach allows an exhaustive analytic analysis of electron dynamics. We find that when the amplitude of the perturbative laser ($a_1 < a$) exceeds some thresholds, the stochastic acceleration of electrons becomes possible within some range of H and thus electron kinetic energy. The maximum electron kinetic energy, which could

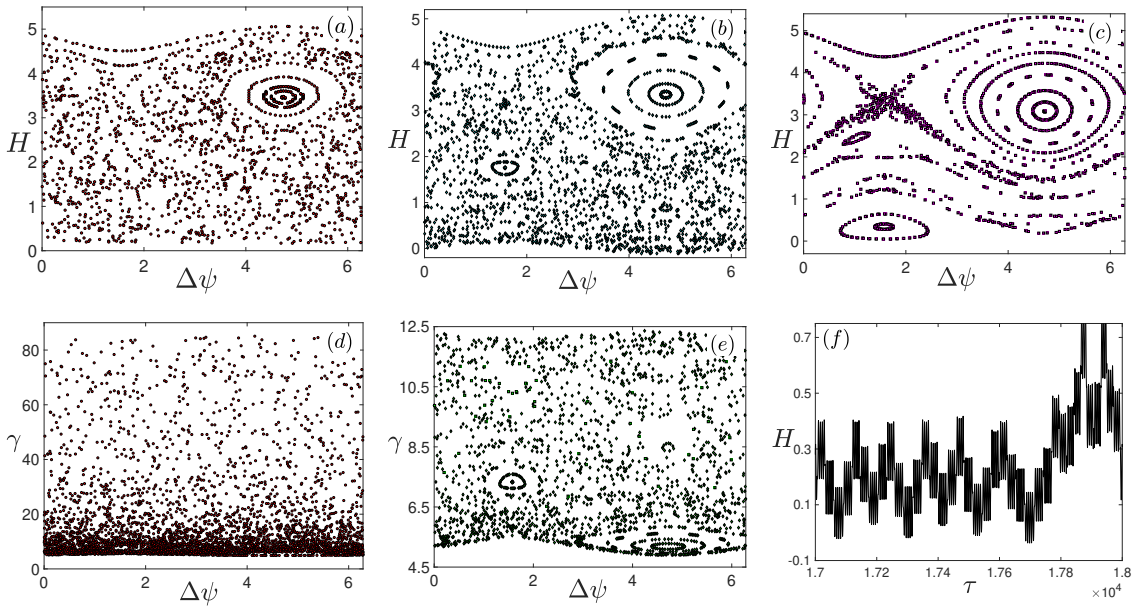

Figure 2.6: Poincaré mappings of (H, ψ) for $a = 5$, $a_1 = 0.2$, $k_1 = 1$ and (a) $v_p = 1$; (b) $v_p = 1.1$; and (c) $v_p = 1.3$. The mappings of (γ, ψ) for (d) $v_p = 1$ and (e) $v_p = 1.1$. (f) Schematic view of the evolution of H for $v_p = 1.1$.

be gained under stochastic acceleration, can significantly exceed the ponderomotive scaling for the electron in the dominant laser only. Moreover, we find that regardless of the orientation of the perturbative laser, H_{min} and thus the maximum electron energy (for k_1 order of unity) have a weak dependence on the amplitude of the perturbative laser above the threshold for stochasticity.

For the case of colliding laser waves polarized in the same direction, the maximum electron kinetic energy can exceed the ponderomotive scaling when the ratio of perturbative to dominant laser frequencies, k_1, is relatively small $k_1 < a$ (in this case, energetic electrons move in the direction of the propagation of the dominant laser beam) and for large k_1, such that $k_1 > a^2 > 1$, providing that $(a^2/k_1)^{4/3} < a_1/a < 1$ (where energetic electrons move in the direction of the propagation of the perturbative laser beam). The results of numerical simulations, shown in Fig. 2.3 and Fig. 2.4, are in a very good agreement with the findings from our analytic theory.

For the case where the polarization direction of the perturbative laser is orthogonal to

that of the dominant laser, the threshold in Eq. (2.25) for $\bar{P}_y = 0$ is much larger than that for lasers being parallel polarized in Eq. (2.18). However, the presence of $\bar{P}_y \neq 0$ could decrease the threshold as shown in Eq. (2.29) when $a_1 < |\bar{P}_y| \lesssim a^{3/8}$ and even to the value comparable to that in Eq. (2.18) when $|\bar{P}_y| > 1$.

The impact of the superluminal phase velocity $v_p > 1$ on the stochastic electron dynamics is qualitatively discussed in section 2.3. It shows that the stochastic region for $H > \sqrt{(v_p^2-1)(1+a^2)}$ will not be affected by the superluminal phase velocity, whereas for $H \ll \sqrt{(v_p^2-1)(1+a^2)}$, both the variation of H due to the kick and the derivative of the time interval between two consecutive kicks with respect to H are approximately constant. As a result, a threshold of v_p exists(v_{ps}). When $v_p < v_{ps}$, new stability islands appear and grow with increasing v_p, until the stochasticity is destroyed when $v_p > v_{ps}$. Although the change of the boundaries in H space is small, the maximum electron kinetic energy is significantly decreased by the impact of the superluminal phase velocity. On the other hand, when $v_p > v_{ps}$, the electron kinetic energy is rather limited.

The work presented in this chapter is a reprint of the material as it appears in *Novel approach to stochastic acceleration of electrons in colliding laser fields* in Physics of Plasmas 26, 050702, by Y. Zhang and S. Krasheninnikov, 2019. The dissertation author was the primary investigator and author of this paper.

Chapter 3

Stochastic electron acceleration in laser and quasi-static periodic electric and magnetic fields

In the DLA of electrons, it has also been reported that efficient electron acceleration in intense laser can be possible if a small transverse stochastic field is added [48], where the electron acceleration exhibits a stochastic nature. Such transverse field can be the Raman backscattered wave or a counter-propagating laser wave with small amplitude [46, 47]. As shown in chapter 2, the essential role of these perturbative transverse fields is not to confine the electron motion or heat the electron directly, but to dephase the electron from main laser pulse and thus allow electron to gain more energy.

In this chapter, we will show that, in the presence of a quasi-static periodic longitudinal electric or transverse magnetic field, electrons in intense laser pulse can also undergo stochastic acceleration [81]. The quasi-static periodic electric or magnetic field has been widely used in studies of electron dynamics, including electric and magnetic undulators [64, 65, 66, 67] and wiggler magnetic field [68, 69]. Moreover, it was shown that the plasma wave can also be taken

as a periodic electrostatic field [7, 70, 71, 72], where electrons in laser and the plasma wave can be stochastically accelerated. Therefore, investigation of the mechanism of stochastic electron acceleration in laser and quasi-static periodic fields are important for the physical understanding of energetic electron generation.

The new Hamiltonian method developed in Ref. [77] will be used in this chapter, where the goal is to find a Hamiltonian which is time-independent without the perturbation. Here, the perturbations are taken as the quasi-static fields under some conditions (which will be later derived), and thus the Hamiltonian is the dephasing rate between the electron and laser wave. We will show that the quasi-static periodic electric and magnetic fields will play a similar role as a perturbative counter-propagating laser wave in chapter 2. As a result, the physics underlying stochastic electron motion and the scaling of maximum electron energy are also similar to that in colliding laser beams. Therefore, in order to keep a connection to chapter 2, the variables in this chapter are similarly defined.

The remainder of this chapter is organized as follows. In section 3.1 we will introduce the new Hamiltonian equations and find the unperturbed electron oscillation in laser pulse only. Section 3.2 will examine the stochastic electron motion in the presence of a periodic transverse magnetic field, while the case for periodic longitudinal electric field will be studied in section 3.3. Section 3.4 will conclude and discuss the main results.

3.1 New Hamiltonian equations and unperturbed electron trajectories

In this section, we will derive the new Hamiltonian and then illustrate the unperturbed electron trajectories without the quasi-static fields. To simplify the analytic expressions, the standard normalization used in chapter 2 will be adopted, where the vector potential of the quasi-static magnetic field, $\mathbf{A_B}$ and the electrostatic potential of the electric field, U, will be

normalized by mc^2/e. Here we only consider the luminal case, where the superluminal impact is similar to that in chapter 2.

We assume that the laser wave propagates along z direction and is described by the vector potential $\tilde{\mathbf{A}}(t-z)$, which is arbitrarily polarized in x and y directions. Both the vector potential $\mathbf{A}_B = A_B(z)\mathbf{e}_x$ for the quasi-static magnetic field and electrostatic potential $U = U(z)$ for electric field are only functions of z. As a result, the electron dynamics can be described by the Hamiltonian in Eq. (2.1) but with $\mathbf{A} = \tilde{\mathbf{A}} + \mathbf{A}_B + t\partial U/\partial z\mathbf{e}_z$ and $\mathbf{P} = \boldsymbol{\gamma}\mathbf{v} - \mathbf{A} \equiv \mathbf{p} - \mathbf{A}$. One can show that for such configuration of EM fields, the x, y-components of canonical momentum are conserved (denoting as $\bar{P}_x$ and $\bar{P}_y$) so that the Hamiltonian in Eq. (2.1) is effectively two dimensional. Keeping in mind of Eq. (2.1), we introduce new variables of $\eta = t - z$, $\chi = \gamma + p_z - 2U$ and time $\tau = t + z$, such that the electron dynamics can be described by a new Hamiltonian $H(\chi, \eta/2, \tau/2) \equiv \gamma - p_z$, since

$$(\eta/2)d\chi - Hd(\tau/2) = P_z dz - \mathcal{H}dt + dF, \tag{3.1}$$

guarantees that such transformation is canonical [79], where $F = \chi\eta/2 - \int U dz + Ut$. From the Hamiltonian equations, it follows that if χ and $\eta/2$ are canonical variables with effective time $\tau/2$, χ and η are also canonical variables with the same Hamiltonian H but effective time τ. The latter will be used in this chapter and thus the new Hamiltonian equations read

$$\frac{d\chi}{d\tau} = \frac{\partial H}{\partial \eta}, \text{ and } \frac{d\eta}{d\tau} = -\frac{\partial H}{\partial \chi}. \tag{3.2}$$

where

$$H = \frac{1 + \left[\tilde{A}_x(\eta) + A_B + \bar{P}_x\right]^2 + \left[\tilde{A}_y(\eta) + \bar{P}_y\right]^2}{\chi + 2U} \equiv \frac{P_\perp^2}{\chi + 2U}. \tag{3.3}$$

Here both A_B and U depend on $z = (\tau - \eta)/2$. These new Hamiltonian equations can also be obtained from the electron equations of motion. For simplicity, in what follows, we will take

$\bar{P}_{x,y} = 0$ and use linearly polarized planar laser wave, where $\tilde{A}_x = asin(\eta)$ and $\tilde{A}_y = 0$ (as indicated by chapter 2 and Eq. (3.3), the impact of A_B is stronger for electron in laser polarized in x-direction than that in laser polarized in y-direction). Moreover, we will assume $A_B = B_1 sin[k_1(\tau - \eta)/2]$ and $U = E_1 sin[k_1(\tau - \eta)/2]$.

The electron kinetic energy, γ, can be obtained from the Hamiltonian as

$$\gamma \equiv \frac{\chi + 2U + H}{2} = \frac{P_\perp^2 + H^2}{2H}. \tag{3.4}$$

Recalling that electrons primarily moves along the laser propagating direction for $k_1 \tilde{<} 1$ due to the ponderomotive force and thus $H = \gamma - p_z$ is small, Eq. (3.4) indicates that the maximum electron energy is obtained at smallest H. As a result, when investigating the electron motion at large energy (small H and thus large χ) region, the quasi-static electric field can be treated as a perturbation when $E_1 \ll \chi_{min} \approx 1/H$ as seen from Eq. (3.3). Whereas the condition $B_1 \ll a$ is required to take the quasi-static magnetic field as a perturbation.

The Hamiltonian in Eq. (3.3) is time-independent and thus conserved when the quasi-static fields (perturbations) are absent. As a result, for the unperturbed problem ($B_1 = E_1 = 0$) where the electron oscillates in the laser field only, from Eqs. (3.2, 3.3) we can find an implicit dependence $\eta(\tau)$ (we note that η increases with τ provided $d\eta/d\tau > 0$):

$$\tau = \frac{2 + a^2}{4H^2}\left[2\eta - \frac{a^2 sin(2\eta)}{2 + a^2}\right] + const., \tag{3.5}$$

and χ

$$\chi = \frac{1 + a^2 sin^2(\eta)}{H}. \tag{3.6}$$

Therefore, the frequency of unperturbed electron oscillation can be found from Eqs. (3.5, 3.6) as

$$\omega = \frac{2\pi}{T} = \frac{4H^2}{2 + a^2}, \tag{3.7}$$

where $T = \tau(\eta = \pi) - \tau(\eta = 0)$ is the period of unperturbed electron oscillation.

Taking into account the fact that the Hamiltonian in Eq. (3.3) has similar structure to that for electrons in colliding laser beams [77], we can conclude that, for $a \gg 1$, the unperturbed (or weakly perturbed) χ will have characteristics of zig-zag time dependence (e.g., see Fig. 3.1). As a result, the unperturbed electron motion will exhibit a long tail distribution of the amplitude of m-harmonics such that high-m resonant islands overlapping and thus stochastic electron motion is possible in the presence of perturbation, where the resonance between unperturbed electron motion and the perturbation takes place when $m\omega = k_1/2$ as seen from equation (3.3). From Eq. (3.3), we can also claim that the strongest impact of the perturbation on H occurs for a short period of time near the local minimum of χ (corresponding to $\eta \approx n\pi$ with n being an integer), while, except these moments, the electron undergoes adiabatic motion. This is because γ and p_z in these nonadiabtic regions are approximately minimized for small H. Therefore, on one hand, the effective mass γm is relatively small compared with that in the adiabatic region such that acceleration of the electron due to the static fields is relatively large. On the other hand, by analogy of the dephasing rate between the electron and laser wave, $\gamma - p_z$, the phase changing rate between the electron and quasi-static fields is p_z such that small p_z in the nonadiabatic region increases the effective interaction time of the electron with the quasi-static fields. These conclusions have been confirmed by numerically solving the Hamiltonian equations in Eq. (3.2) for both quasi-static magnetic and electric fields. For example, in Fig. 3.1 we show the results for $a = 5$, $k_1 = 2$ and (a) $B_1 = 0.1$ for the magnetic case and (b) $E_1 = 0.5$ for the electric case. From the upper panels of Fig. 3.1 and the definition of $\Delta\eta$, we see that the "kicks" of Hamiltonian occurs near $\eta \approx n\pi$, where χ is locally minimized.

The condition for the onset of stochasticity for the case $\omega/k_1 \ll 1$ can be found by using Chirikov-like mapping [58], which describes the recurrence relations of electron Hamiltonian and time when it passes through some fixed canonical plane. In our case, the fixed canonical plane can be chosen as the nonadiabatic region, which corresponds to an effectively "fixed" η, provided

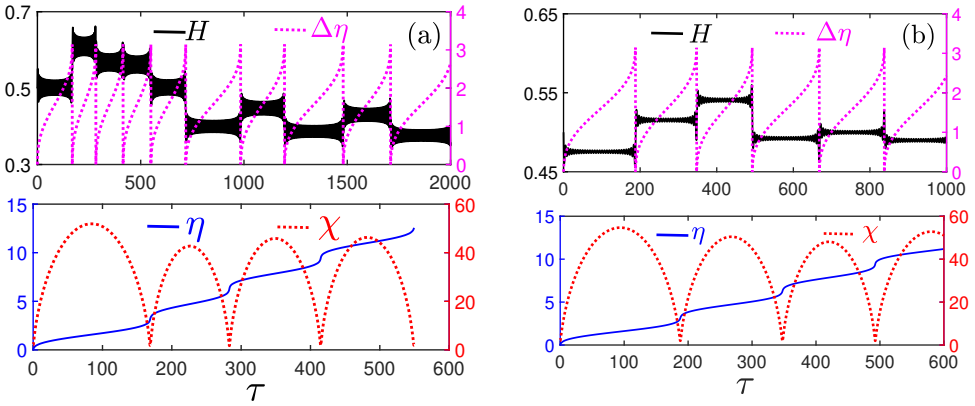

Figure 3.1: Schematic view of the electron trajectories and diffusion of Hamiltonian for $a = 5$, $k_1 = 2$ and (a) $B_1 = 0.1$ for the magnetic case and (b) $E_1 = 0.5$ for the electric case. The definition of $\Delta\eta$ is $\Delta\eta \equiv \eta - [\eta/\pi]\pi$.

that the Hamiltonian is a periodic function of η with a period of π. Therefore, in order to find the Chirikov-like mapping, we should derive the changes of Hamiltonian and time between two consecutive kicks

$$\Delta H_n \equiv H_{n+1} - H_n = \int_{\tau_n}^{\tau_{n+1}} \frac{\partial H}{\partial \tau} d\tau, \text{ and } \Delta\tau_n = \tau_{n+1} - \tau_n. \tag{3.8}$$

However, if we assume the change of Hamiltonian due to each kick is small, $|\Delta H_n| \ll H_n$, then the changes of Hamiltonian and time in Eq. (3.8) can be estimated using the unperturbed electron trajectory $H_n(\eta, \chi)$. Moreover, recalling the fact that the main contribution to Hamiltonian variation is from $\eta \approx n\pi$, the integration in equation (3.8) for Hamiltonian variation can be first transformed into the integration over $\eta - n\pi$ and then is computed by using expansion of integrand in terms of $\eta - n\pi$. In what follows, we will use these techniques to examine the stochastic electron dynamics in periodic magnetic and electric fields, respectively.

3.2 Stochastic electron motion in laser and periodic magnetic field

In this section, we consider the impact of a periodic magnetic field $B(z)\mathbf{e}_y$ on the electron dynamics in laser radiation. Taking into account the assumption of $B_1 \ll a$, we can keep the leading term of $\partial H/\partial\tau \approx ak_1B_1 sin(\eta)cos\left[k_1(\tau-\eta)/2\right]/\chi$. After some algebra, from Eq. (3.8) we find

$$\Delta H_n^b = (-1)^n 2^{2/3} B_1 \left(\frac{k_1 H_n}{a}\right)^{1/3} sin\left[k_1(\tau_n - n\pi)/2\right] \int_{-\infty}^{\infty} \tilde{\eta} sin\left(\beta\tilde{\eta} + \frac{1}{3}\tilde{\eta}^3\right) d\tilde{\eta}, \tag{3.9}$$

where $\tilde{\eta} = (\eta - n\pi)/\alpha$, $\alpha = (2H_n^2/k_1a^2)^{1/3} \sim (\omega/k_1)^{1/3} \ll 1$, $\beta = (k_1/2H_n^2a)^{2/3}(1-H_n^2)$. Here we use superscript b to denote the quantities in the case of quasi-static magnetic field in this section and e for those in electric field case discussed in next section. The fact that the integral in Eq. (3.9) oscillates rapidly for $\tilde{\eta} \tilde{>} 1$ ensures that the nonadiabatic interaction of the electron motion with the perturbation occurs at small region of $|\eta - n\pi| < \alpha \ll 1$ ($|\tilde{\eta}| \tilde{<} 1$) and justifies the extension of the integration limits to infinity. As a matter of fact, the integral in Eq. (3.9) is related to the derivative of Airy function, $Ai'(\beta)$, so we have

$$\Delta H_n^b = (-1)^{n+1} 2^{5/3} \pi B_1 \left(\frac{k_1 H_n}{a}\right)^{1/3} Ai'(\beta) sin(\psi_n), \tag{3.10}$$

where $\psi_n \equiv k_1(\tau_n - n\pi)/2$ is the phase where nth "kick" occurs. As a result, for small H of interest, we have $|\Delta H_n^b/H_n| \approx 4\pi B_1 \beta^{1/2} |Ai'(\beta)|$. Considering that $4\pi\beta^{1/2}|Ai'(\beta)|$ has a maximum order of unity at $\beta \approx 0.73$ and decays to zero for both larger and smaller β, a sufficient condition for the assumption $|\Delta H_n^b| < H_n$ used in estimate of Eq. (3.8) is $B_1 \tilde{<} 1 \tilde{<} a$.

The phase interval $\Delta\psi_n = \psi_{n+1} - \psi_n = k_1(\Delta\tau_n - \pi)/2$ between two consecutive kicks can be found by using approximation of $\Delta\tau_n$ by the period of unperturbed electron oscillation, where

$\Delta\tau_n$ is defined in Eq. (3.8). As a result,

$$\Delta\psi_n \equiv \psi_{n+1} - \psi_n = \frac{\pi k_1(2+a^2)}{4H_{n+1}^2} - k_1\pi/2. \tag{3.11}$$

The second term on the right hand side of Eq. (3.11) only affects the region of phase where chaos occurs, which can be disregard when deriving the condition for stochasticity [56]

$$K^b = \left|\frac{d\Delta\psi_n}{dH_{n+1}}\frac{d\Delta H_n^b}{d\psi_n}\right| = \frac{4\pi^2 B_1(2+a^2)a\beta^2|Ai'(\beta)|}{(1-H^2)^2} \tilde{>} 1. \tag{3.12}$$

For electrons with small $H \ll 1$ (large energy), the stochastic condition in Eq. (3.12) is the same with that for electrons in colliding laser beams [77]. Therefore, we can introduce a function $f^b(\beta) = 4\pi^2\beta^2|Ai'(\beta)|$, which increases with β for $\beta < \beta_s^b \approx 1.68$; reaches maximum, $f_{max}^b \approx 8.83$, at $\beta = \beta_s^b$; and then falls exponentially at $\beta > \beta_s^b$ (e.g., see Ref. [80]):

$$f^b(\beta) \approx 2\pi^{3/2}\beta^{9/4} exp\left[-(2/3)\beta^{3/2}\right]. \tag{3.13}$$

As a result, from Eq. (3.12) we find that stochastic motion is only possible for $B_1 > B_s$, where

$$B_s = \frac{1}{f_{max}^b}\frac{1}{a(2+a^2)} \approx \frac{0.11}{a(2+a^2)}. \tag{3.14}$$

The Hamiltonian corresponding to the threshold B_s is governed by β_s^b

$$H_s^b = H(\beta_s^b) \approx 0.48\left(\frac{k_1}{a}\right)^{1/2}. \tag{3.15}$$

For $B_1 \gg B_s$ stochastic acceleration becomes possible within the range of H: $H_{min}^b < H < H_{max}^b$, where the lower boundary of stochasticity is due to the exponential decay of the widths of resonant islands, whereas the upper one is because of the larger distance between the neighboring resonant islands than their widths. H_{max}^b and H_{min}^b could be found by using asymptotic expressions of the

function $f^b(\beta)$. As a result, we have

$$H^b_{min} \approx \frac{H^b_s}{\sqrt{1.6+0.69ln\,(B_1/B_s)}},\ H^b_{max} \approx 1.5\left(\frac{B_1}{B_s}\right)^{3/8} H^b_s. \tag{3.16}$$

From Eq. (3.4) we see that, without the quasi-static fields, the maximum electron energy gained from laser only is $\gamma^0_{max} = (1+a^2+H_0^2)/2H_0$ (where H_0 is the initial Hamiltonian and conserved), which can be regarded as the vacuum ponderomotive energy. However, in the presence of magnetic field, when $H^b_{min} < H_0 < H^b_{max}$, the stochastic electron motion can significantly increase the maximum electron energy $\gamma^b_{max} \approx (1+a^2)/2H^b_{min}$ for $a \gg 1$ as seen from Eq. (3.16). Moreover, Eq. (3.16) demonstrates that γ^b_{max}, which corresponds to H^b_{min}, has a weak logarithmic dependence on the ratio B_1/B_s.

These results are confirmed by the numerical simulations, where the Poincaré mappings of (H, ψ) and (γ, ψ) are shown in Fig. 3.2. Here, the data chosen for the Poincaré mappings are those for $\eta = n\pi + \pi/2$, which corresponds to the local maximum of γ. It illustrates that a stochastic "sea" is bounded by the KAM invariants at both large and small H, where the boundaries of the stochastic region in H agree with Eq. (3.16) for both $B_1 = 0.1$ in Fig. 3.2(a) and $B_1 = 0.01$ in Fig. 3.2(d) (in order to have a close-up view of H^b_{min}, we have zoomed in the lower boundary regions, e.g., see Fig. 3.2(c) and Fig. 3.2(f), respectively). Fig. 3.2(b) and Fig. 3.2(e) confirm that the maximum electron energy weakly depends on B_1.

3.3 Stochastic electron motion in laser and periodic electric field

In this section, the electric motion in laser and quasi-static electric field will be considered by using the same method in section 3.2. In order to take $U(z)$ as a perturbation, we will focus on small H such that $\chi \gg E_1$. From Eq. (3.3), we find that $\partial H/\partial\tau = -k_1E_1cos\,[k_1(\tau-\eta)/2] \times d\eta/d\tau$

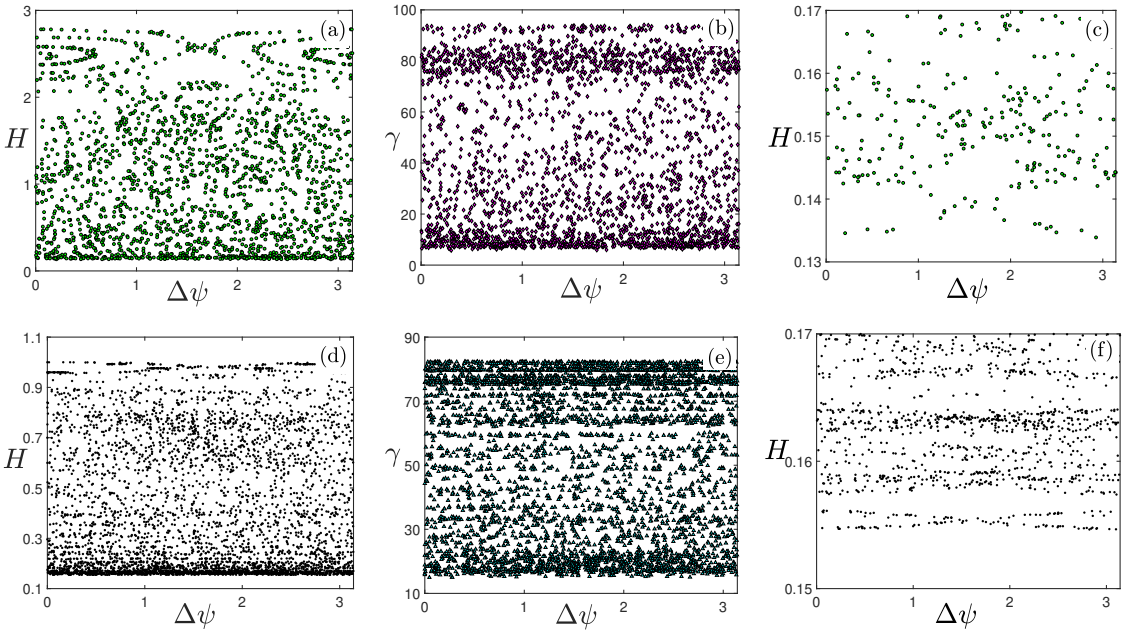

Figure 3.2: Poincaré mappings of $(H,\Delta\psi)$, $(\gamma,\Delta\psi)$ and zoomed-in view of $(H,\Delta\psi)$ for $B_1 = 0.1$ in (a-c) and $B_1 = 0.01$ in (d-f), when the electron passes through $\eta = n\pi + \pi/2$. $a = 5$, $k_1 = 2$ and $\Delta\psi \equiv \psi - [\psi/\pi]\pi$.

and thus from Eq. (3.8) we obtain

$$\Delta H_n^e = -2^{4/3}\pi E_1 \left(\frac{k_1 H_n}{a}\right)^{2/3} Ai(\beta)cos(\psi_n), \tag{3.17}$$

where $Ai(\beta)$ is the Airy function, β and ψ_n have been defined in section 3.2. Therefore, we have $|\Delta H_n^e/H_n| \approx 2^{3/2}\pi E_1 (k_1/a)^{1/2}\beta^{1/4}|Ai(\beta)|$, where $2^{3/2}\pi\beta^{1/4}|Ai(\beta)|$ has a maximum order of unity at $\beta \approx 0.29$. As a result, if $E_1 \tilde{<} (a/k_1)^{1/2}$, $|\Delta H_n^e| < H_n$ if true for all H.

Taking into account the phase interval between two consecutive kicks in Eq. (3.11), the condition for stochasticity is obtained as

$$K^e = \frac{2^{3/2}\pi^2 E_1 (2+a^2)(ak_1)^{1/2}\beta^{7/4}Ai(\beta)}{(1-H^2)^{7/4}} \tilde{>} 1. \tag{3.18}$$

Therefore, if we focus on small $H \ll 1$, we can introduce a function $f^e(\beta) = 2^{3/2}\pi^2\beta^{7/4}Ai(\beta)$. It increases with β for $\beta < \beta_s^e \approx 1.34$; reaches maximum $f_{max}^e \approx 4.14$ at β_s^e; and then falls

exponentially at $\beta > \beta_s^e$ (e.g., see Ref. [80]):

$$f^e(\beta) \approx 2^{1/2}\pi^{3/2}\beta^{3/2} exp\left[-(2/3)\beta^{3/2}\right]. \tag{3.19}$$

As a result, from Eq. (3.18) we find that stochastic electron motion is only possible for

$$E_1 > E_s \approx \frac{0.24}{(2+a^2)(ak_1)^{1/2}}, \tag{3.20}$$

where the Hamiltonian corresponding to E_s is given by β_s^e

$$H_s^e = H(\beta_s^e) \approx 0.454(k_1/a)^{1/2}. \tag{3.21}$$

For $E_1 \gg E_s$, efficient stochastic acceleration is possible, where the lower and upper boundaries of stochastic region in H space are

$$H_{min}^e \approx \frac{H_s^e}{\sqrt{1.8+0.62ln\,(E_1/E_s)}},\ H_{max}^e \approx 2.2\left(\frac{E_1}{E_s}\right)^{3/7} H_s^e. \tag{3.22}$$

Therefore, we come to the similar conclusions to those in section 3.2: as along as $H_{min}^e < H_0 < H_{max}^e$, the stochastic motion can facilitate electron acceleration beyond the vacuum ponderomotive energy and the maximum electron energy gained from laser, $\gamma_{max}^e = (1+a^2)/2H_{min}^e$, has a weak dependence on E_1/E_s.

Numerical simulations are performed to check these analytic results. In Fig. 3.3 we show the Poincaré mappings of (H, ψ) and (γ, ψ) for $a = 5$, $k_1 = 2$ and $E_1 = 0.1$. The boundaries of the stochastic region in H agree with Eq. (3.22), where the lower boundary is the same order with that for the magnetic case in Fig. 3.2. From Eqs. (3.20, 3.21) we see $E_s \approx 2.8 \times 10^{-3}$ and $H_s^e \approx 0.29$ for $a = 5$ and $k_1 = 2$. These two quantities are confirmed by the simulations, which show that for E_1 slightly larger than E_s, stochasticity occurs only in a narrow region in the vicinity of H_s^e.

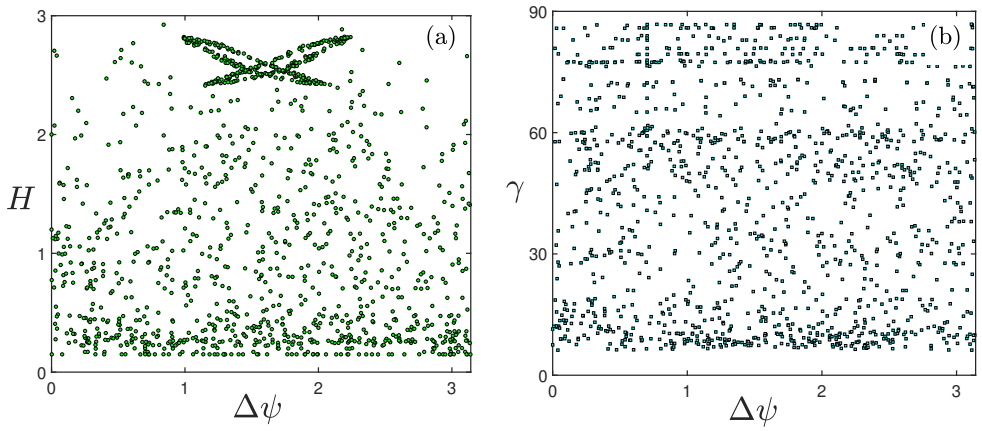

Figure 3.3: Poincaré mappings of (a) $(H,\Delta\psi)$ and (b) $(\gamma,\Delta\psi)$ for $a=5$, $k_1=2$ and $E_1=0.1$ when $\eta = n\pi+\pi/2$.

3.4 conclusion

In conclusion, we investigated the electron dynamics in laser radiation and quasi-static periodic magnetic and electric fields by using a novel Hamiltonian method, where the Hamiltonian is time-independent when the quasi-static fields are absent. We find that the periodic fields play a similar role to that of a counter-propagating laser wave, which can stochastically change the new Hamiltonian and thus enable net energy transfer between the electron and laser wave. The stochastic electron motion occurs when the amplitudes of quasi-static fields exceed some thresholds. We find that the maximum electron energy gained under stochastic acceleration, which is associated with the lower boundary of the stochastic region in Hamiltonian space, weakly depends on the amplitude of quasi-static fields. However, decreasing the wavenumber of quasi-static fields will largely increase the maximum electron energy.

For the case of the periodic magnetic field, the assumption of $B_1 \ll a$ is necessary to validate these analyses, whereas for the electric case it requires $E_1 \ll \chi$ and thus $E_1 \ll 1/H$ as seen from Eq. (3.3). In both cases, we mainly focus on a small H region, which is reasonable provided that the intense laser will push the electron moving with it and thus $H = \gamma - p_z$ is small. Although the physical orientations of these two periodic fields are different, the physical pictures

of stochastic electron motion for these two cases are similar: the Hamiltonian is "periodically kicked" by the perturbative field when $\chi = \gamma + p_z$ is locally minimized. Except for these short periods of time, the impact of perturbative field is small and the electron motion is adiabatic.

Numerical simulations have been conducted to integrate the Hamiltonian equations. The results are presented in the Poincaré mappings, which are in a very good agreement with the findings from our analytic theory. It shows that the lower (upper) boundary of the stochastic region in Hamiltonian (energy) space has a logarithmic dependence on the amplitude of the perturbative field.

The work presented in this chapter is a reprint of the material as it appears in *Stochastic electron acceleration in relativistic laser pulse and stationary periodic electric and magnetic fields* in Physics of Plasmas 26, 113112, by Y. Zhang and S. Krasheninnikov, 2019. The dissertation author was the primary investigator and author of this paper.

Chapter 4

Stochastic electron acceleration in laser and confining quasi-static electric and magnetic fields

The mechanisms of electron heating to obtain high energy have been suggested and studied analytically, numerically, and experimentally over many years. Many of these works (see e.g. Refs. [10, 11, 15, 18, 21, 22, 25, 29, 82, 83, 84, 85, 86, 87, 88, 89, 90]) reveal that the presence of self-generated or externally applied QEM fields could significantly increase the electron energy gained from the laser well beyond the ponderomotive scaling [91]. Furthermore, the available experimental data (e.g., see Refs. [7, 20, 36, 92, 93] and the references therein) also support these conclusions.

However, the mechanism(-s) of such synergistic effects is still under debate. In Ref. [21], the synergy of the linearly polarized laser radiation propagating in the z-direction with only the y-component of the vector potential, static electric field (in the y-direction) and magnetic field (in the x-direction), was attributed to the betatron resonance. However, in Ref. [22], it was shown that the synergy persists for arbitrary orientation of the laser vector potential and the static electric

field, while the synergistic effect of the laser and static electric field is due to the "parametric amplification". In Ref. [15], it was shown that the synergistic effects, causing electron heating beyond the ponderomotive scaling, are also present in the case where electrostatic potential, U, depends on the z-coordinate (the direction of laser beam propagation). In Ref. [25], it was demonstrated that in the case of a V-shape electrostatic potential, $U = E_0 z$, the electron dynamics can be described by a Chirikov-like map [58] and a strong electron heating is due to an onset of stochasticity which is determined by a particular relationship between normalized laser vector potential and E_0. Later on, the synergy between laser radiation and electrostatic potential $U(z)$ was also reported in Refs. [86, 88, 89]. In Refs. [23, 94], it was shown that an onset of stochastic electron motion can also be triggered by the synergy of laser radiation and the constant magnetic field perpendicular to the laser propagation direction. The impact of a longitudinal decelerating electric field on electron acceleration in the laser and transverse electric field was investigated in Ref. [13] where the decelerating electric field helps with maintaining high-amplitude betatron oscillations. Moreover, the generation of strong spontaneous longitudinal magnetic field in the laser-plasma interaction [18, 95] has made the resonant acceleration of electrons, which requires a matching condition [11, 96, 97] between the electron gyro-frequency and laser frequency, possible.

Although starting from different considerations, the maximum electron energy has been estimated as a function of the parameters of the laser radiation and QEM fields through simplified analyses and particle-in-cell (PIC) simulations (e.g., see Refs. [10, 11, 13, 22, 25]) , the identification of the synergistic mechanism(-s) is poorly understood due to the strong nonlinearity of the relativistic electron motion in these fields.

Recently, it was shown that the electron dynamics can be described by the 3/2 dimensional (3/2D) Hamiltonian approach for a homogeneous magnetic field and linearly polarized laser plane wave [9]. This approach can be extended to the cases of arbitrarily polarized laser radiation depending only on the phase variable $(v_p t - z)/\lambda$ and arbitrary QEM fields in the directions both

along and across to the laser propagation direction. Here λ is the laser pulse wavelength; $v_p \geq c$ is the phase velocity; t and z are, respectively, the time and coordinate along the laser propagating direction. This method can greatly simplified the analysis of electron dynamics benefiting from the fundamental results of previous studies on regular and stochastic motion in Hamiltonian systems (see e.g. Refs. [56, 57] and the references therein) and thus will be used in this chapter.

In contrast to chapter 3, the electron motions will be confined within the potential wells of the QEM fields and thus we call them as confining QEM fields. As a result, the QEM fields cannot be taken as perturbations as in chapter 3. However, we will show that the laser wave can play the role of a perturbation in analysis of the electron dynamics if we consider relativistic electrons (electron energy above the ponderomotive scaling). Therefore, our new Hamiltonian will be the total electron energy in the QEM fields, which is conserved without the laser radiation. We will show that, in the presence of QEM fields, an onset of stochasticity can be accounted for the electron acceleration in laser-plasma interaction.

The role of the static fields in this mechanism is to reduce the longitudinal dephasing rate $\gamma - p_z/m_e c$ between the electron and laser beam such that the electron could stay in phase with the laser and effectively exchange energy with laser, instead of directly transferring substantial energy to the electron. Here γ is the relativistic factor and p_z and m_e are the electron momentum along laser propagation direction and mass, respectively. The smallest dephasing rate is corresponding to the strongest interaction between the electron and laser wave which is also called the nonadiabatic interaction or "collisions" in the rest of this chapter.

In the rest of this chapter, we will use again the standard dimensionless variables. For the sake of simplicity, we will use plane wave of laser radiation which has been justified by the numerical simulations (e.g. Ref. [12]) where the laser field in the ion channel has a planar structure with superluminal phase velocity. As a result, the laser can be described by $\vec{\tilde{A}} = \tilde{A}_x(t - z/v_p)\vec{e}_x + \tilde{A}_y(t - z/v_p)\vec{e}_y$, where $\tilde{A}_x$ and $\tilde{A}_y$ are used to distinguish the laser polarizations and v_p here denotes the dimensionless laser phase velocity normalized by c.

For all the cases, we start with general Hamiltonian for arbitrarily polarized laser with superluminal phase velocity and QEM fields but the impacts of the electric and magnetic fields are discussed separately. The rest of this chapter is organized as follows. In section 4.1 we examine the electron dynamics in the transverse QEM fields and laser radiation. Section 4.2 will study the role of the longitudinal electric field for general power form of $U(z) \propto k_u|z|^p$, where $p = 1$ was studied in Refs. [25, 26]. However, we will show that the electron dynamics for $p > 1$ is quite different from that for $p = 1$. In section 4.3, the electron motion in transverse electric but longitudinal magnetic fields will be discussed. The results will discussed and summarized in section 4.4.

4.1 Electron in transverse electric and magnetic fields

In this section, we consider electron motion in the QEM fields, both of which are across to the laser propagation direction. These fields have been found in the ion channels, where the charge separation is balanced by a transverse gradient of the ponderomotive pressure of the laser beam. An electron injected into the channel would be accelerated in the forward direction by the fields of the laser beam, where the QEM fields play an important role in the electron acceleration via low harmonic resonance between electron betatron oscillation frequency and laser frequency (e.g., see Refs. [21, 22]). However, here we will consider different acceleration mechanism of electrons due to an onset of stochastic motion.

Without loosing the physics, we assume that the quasi-static electric fields is in the y-direction while the magnetic field as a function of y-coordinate is in the x-direction, i.e.,

$$\vec{A} = \tilde{\vec{A}} - \vec{e}_y t \partial U(y)/\partial y + \vec{e}_z A_B(y). \tag{4.1}$$

Notice that $E_{stat} = \nabla U$ in order to denote an attractive electrostatic potential well.

Unlike chapters 2 and 3, here we derive the new Hamiltonian from the equations of motion

of relativistic electrons

$$\frac{dP_\alpha}{dt} = \frac{dA_\alpha}{dt} - \frac{\partial A_\beta}{\partial x_\alpha} v_\beta, \tag{4.2}$$

$$\frac{d\gamma}{dt} = \frac{\partial A_\beta}{\partial t} v_\beta, \tag{4.3}$$

where $P_\alpha = \gamma dx_\alpha/dt \equiv \gamma v_\alpha$ and $\gamma^2 = 1 + \vec{P}^2$. From Eqs. (4.2, 4.3), one can find

$$\frac{d(P_x - \tilde{A}_x)}{dt} = 0 \rightarrow P_x = \tilde{A}_x + \bar{P}_x, \tag{4.4}$$

$$\frac{d\left(P_y - \tilde{A}_y\right)}{dt} = -\frac{\partial U(y)}{\partial y} - \frac{\partial A_B(y)}{\partial y} v_z, \tag{4.5}$$

$$\frac{d\left(P_z - A_B\right)}{dt} = -\frac{\partial \tilde{A}_x}{\partial z} v_x - \frac{\partial \tilde{A}_y}{\partial z} v_y = \frac{1}{v_p}\frac{\partial \tilde{A}_x}{\partial t} v_x + \frac{1}{v_p}\frac{\partial \tilde{A}_y}{\partial t} v_y, \tag{4.6}$$

$$\frac{d(\gamma + U)}{dt} = \frac{\partial \tilde{A}_x}{\partial t} v_x + \frac{\partial \tilde{A}_y}{\partial t} v_y, \tag{4.7}$$

where $\bar{P}_x = P_x - \tilde{A}_x\big|_{t=0}$. From Eqs. (4.6, 4.7), we arrive to the constant of motion

$$\gamma - v_p P_z + W_p^B(y) = C_\perp \equiv \left\{\gamma - v_p P_z + W_p^B(y)\right\}_{t=0}, \tag{4.8}$$

where $W_p^B(y) \equiv U(y) + v_p A_B(y)$. Combining Eqs. (4.1, 4.8), we can obtain

$$P_z = \frac{v_p\left(W_p^B - C_\perp\right)}{v_p^2 - 1} + \frac{\sigma}{v_p^2 - 1}\sqrt{\left(W_p^B - C_\perp\right)^2 + \left(v_p^2 - 1\right) P_{\perp,y}^2}, \tag{4.9}$$

where $\sigma = \pm 1$ and

$$P_{\perp,y}^2 = 1 + \left(\bar{P}_x + \tilde{A}_x\right)^2 + \left(\tilde{p}_y + \tilde{A}_y\right)^2, \tag{4.10}$$

with $\tilde{p}_y \equiv P_y - \tilde{A}_y$. Noticing that Eqs. (4.8, 4.9) yield $\sigma\sqrt{\left(W_p^B - C_\perp\right)^2 + \left(v_p^2 - 1\right) P_{\perp,y}^2} = v_p\gamma - P_z > 0$, we find that σ in Eq. (4.9) should be taken positive ($\sigma = +1$). Introducing the variable

$\xi_1 = t - z/v_p$, we have

$$\frac{d\xi_1}{dt} = 1 - \frac{P_z}{v_p\gamma}. \tag{4.11}$$

Then from Eqs. (4.3, 4.5) we find

$$\frac{d\tilde{p}_y}{d\xi_1} = \left[-\frac{\partial U(y)}{\partial y} - \frac{\partial A_B(y)}{\partial y}\frac{P_z}{\gamma}\right]\frac{v_p\gamma}{v_p\gamma - P_z} = -\frac{v_p\gamma}{v_p\gamma - P_z}\frac{\partial W_p^B(y)}{\partial y} + v_p\frac{\partial A_B(y)}{\partial y}, \tag{4.12}$$

$$\frac{dy}{d\xi_1} = \frac{v_p(\tilde{p}_y + \tilde{A}_y)}{v_p\gamma - P_z}. \tag{4.13}$$

Substitute Eqs. (4.8, 4.9) into (4.12, 4.13), we arrive to the Hamiltonian equations

$$\frac{d\tilde{P}_y}{d\xi_1} = -\frac{\partial H_y^p}{\partial y},\ \frac{dy}{d\xi_1} = \frac{\partial H_y^p}{\partial \tilde{p}_y}, \tag{4.14}$$

where

$$H_y^p(\tilde{p}_y, y, \xi_1) = \frac{v_p}{v_p^2 - 1}\left\{\sqrt{\left(W_p^B - C_\perp\right)^2 + \left(v_p^2 - 1\right)P_{\perp,y}^2} + W_p^U - C_\perp\right\}, \tag{4.15}$$

$W_p^U = v_p U(y) + A_B(y)$ and $P_{\perp,y}^2$ is given by equation (4.10) with $\tilde{A}_{(...)} = \tilde{A}_{(...)}(\xi_1)$. Noticing that $W_p^U - W_p^B = (v_p - 1)W^{(-)}$ and $W_p^U + W_p^B = (v_p + 1)W^{(+)}$ where $W^{(\pm)} \equiv U \pm A_B$, we find that at $v_p = 1$ the Hamiltonian in Eq. (4.15) becomes

$$H_y = \frac{1}{2}\left\{\frac{1 + \left(\bar{P}_x + \tilde{A}_x\right)^2 + \left(\tilde{p}_y + \tilde{A}_y\right)^2}{C_\perp - W^{(+)}(y)} + W^{(-)}(y) + C_\perp\right\} = \gamma + U = E, \tag{4.16}$$

where E is the total electron energy.

4.1.1 Stochastic electron motion in laser and quasi-static fields

The Hamiltonians in Eq. (4.15) and (4.16) are valid for arbitrary $U(y)$ and $A_B(y)$. However, to study the electron motion, in the following, we specify $U = \kappa_u y^2/2$ and $A_B = \kappa_b y^2/2$ where κ_u

and κ_b are constants denoting, respectively, the electric and magnetic fields strength, like in the ion channel [21] (the dimensionless parameter κ_u for self-generated electric field is dependent on the ion density in the channel, $\kappa_u = \omega_{pe}^2/\omega^2$, where $\omega_{pe} = \sqrt{4\pi n_0 e^2/m_e}$ is the plasma frequency).

The nonadiabatic region corresponds to the minimum of the dephasing rate $\gamma - p_z = C_\perp - W_p^B(y) + (v_p - 1)p_z$, which indicates that the presence of the static fields could enhance the electron-laser interaction when $W_p^B(y)$ approaches $C_\perp$ if $\kappa_u + v_p\kappa_b > 0$ while the superluminal phase velocity of laser radiation, $v_p > 1$, would reduce it [27, 28]. For simplicity, in what follows, we will consider the luminal case ($v_p = 1$) in Eq. (4.16). Then in order to have strong electron laser interactions, we would consider $\kappa_u + \kappa_b > 0$ and Eq. (4.16) indicates that such strong interaction occurs at small denominator of Hamiltonian, $C_\perp - W^{(+)}(y) = \gamma - p_z$. For relativistic electrons with energy $E \gg W^{(-)}(y_{\max,\min}) + C_\perp \sim (\kappa_u - \kappa_b + 1)C_\perp$, where $y_{\max,\min} \approx \pm\sqrt{2C_\perp/(\kappa_u + \kappa_b)}$ correspond to the nonadiabatic regions, the impact of the $W^{(-)}(y)$ is negligible in the nonadiabatic region. As a result, the electric and magnetic fields play a similar role in the electron dynamics and we can ignore the magnetic field, taking $\kappa_u + \kappa_b$ as the "effective" electric coefficient. In the rest of this section we would take $\kappa_u > 0$ and $\kappa_b = 0$.

First we consider electron trajectory without the impact of laser radiation so that the electron energy is conserved. From Eq. (4.16), we see that the electron motion is bounded between $y_{\max,\min} \approx \pm\sqrt{2C_\perp\kappa_u^{-1}}$ and we find

$$\tilde{p}_y = -\sqrt{2EC_\perp}\sin\theta,\ y = \sqrt{2C_\perp\kappa_u^{-1}}\cos\theta,\ d\theta/d\xi = \sqrt{E\kappa_u}C_\perp^{-1}\sin^{-2}\theta, \tag{4.17}$$

where the angle θ goes clockwise direction (see Fig. 4.1) with $\theta = 0$ ($\theta = \pi$) corresponding to y_{max} ($y_{\min}$). Here $\xi = t - z$ for $v_p = 1$. The last expression in Eq. (4.17) reads

$$\zeta \equiv \xi - \xi_n = \frac{C_\perp(2\theta - \sin 2\theta)}{4\sqrt{E\kappa_u}}, \tag{4.18}$$

where ξ_{2n} is the time of the nth passage of the electron through $y_{\max}$. Substituting $\theta = 2\pi$ in the

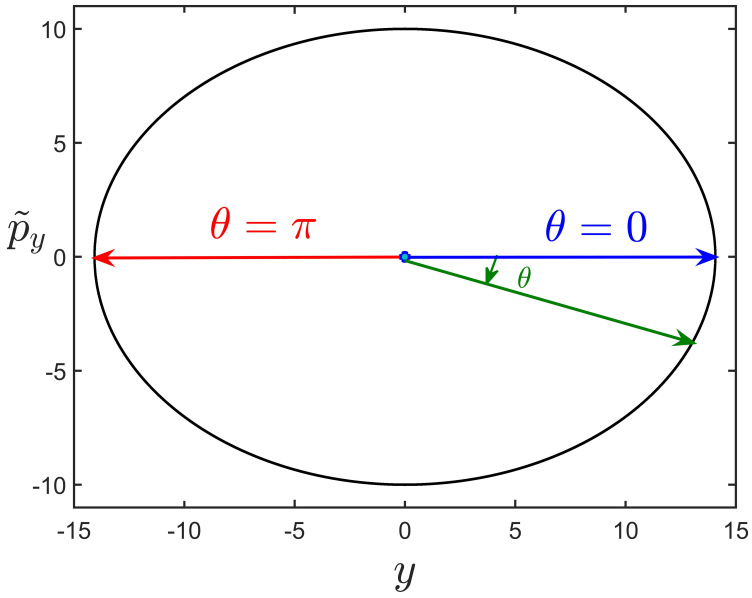

Figure 4.1: Schematic view of the ultra-relativistic electron trajectory in the transverse electric field for $C_\perp = 1$, $\kappa_u = 0.01$ and $E = 50$.

above expression provides the unperturbed electron frequency over closed orbit

$$\Omega = \frac{2\sqrt{E\kappa_u}}{C_\perp}. \tag{4.19}$$

Eq. (4.19) could also be derived from the calculation of the action, I, of the electron from Eq. (4.17), where $I = \oint \tilde{p}_y dy/2\pi = C_\perp \kappa_u^{-1/2} E^{1/2}$ and thus $\Omega = \partial E/\partial I$.

However, from Eq. (4.16) we find that an impact of laser radiation on electron trajectory could be largely ignored (with exception rather narrow regions in the vicinity of $\theta = 0$ and $\theta = \pi$, where $\tilde{p}_y$ approaches zero) only for the energies

$$E > E_{pond} = a_0^2/2C_\perp, \tag{4.20}$$

where E_{pond} in our case could be considered as a ponderomotive energy scaling. For such electron energy, the unperturbed electron orbit in Eq. (4.20) is significantly stretched along $\tilde{p}_y$, where

its dynamics is to some extent similar to that of oscillating particles in a "square well" [56] in the sense that it moves freely in the adiabatic region and gets "kicked" within the nonadiabatic regions ($y_{\max,\min}$). It follows that the zigzag-like dependence of y on the time ξ and "step-shape" of $\tilde{p}_y$ would have harmonics with long tail distribution of the amplitude (the amplitude of the nth harmonic is approximately to $a_n \approx 1/n$ for the particle in the square well). As a result, the resonance of electron frequency Ω with laser frequency (which is unity in our normalization) occurs at $n\Omega = 1$ with $n \geq 1$ being an integer number. The resonant islands could be largely broadened such that their overlapping, which causes stochastic electron heating, is possible. Thus, the requirement $\Omega \leq 1$ sets the limit for efficient electron-laser interactions since at $\Omega > 1$ an impact of laser field becomes adiabatic. As a result, an absolute maximum energy where electron can be heated up via interactions with the laser radiation and the transverse electric field is considered as

$$E_{\max}^{abs} = C_{\perp}^2/4\kappa_u. \tag{4.21}$$

From Eqs. (4.20, 4.21), we find that in order to accelerate electrons beyond the ponderomotive scaling, we should have

$$\varepsilon \equiv \sqrt{2}a_0\kappa_u^{1/2}C_{\perp}^{-3/2} \ll 1. \tag{4.22}$$

This parameter ε was also introduced in Ref. [22] for the parametric amplification of laser-drive electron acceleration with $\varepsilon \sim 1$, and in Ref. [29] as result of time-average theory for $\varepsilon \tilde{<} 1$. Then from Eqs. (4.20-4.22) we have $E_{\max}^{abs} = E_{pond}\varepsilon^{-2}$ and thus, in what follows, we would use $E_{\max}^{abs}$ to scale the electron energies.

The energy variation of the electron, $\Delta E = \int \frac{\partial H}{\partial \xi} d\xi$, in the vicinity of the nonadiabatic region y_{max} for the polarization of $\vec{\tilde{A}} = a_0 \sin(\xi)\vec{e}_y$ and $\vec{\tilde{A}} = a_0 \sin(\xi)\vec{e}_x$ is given, respectively, by

$$E_y(\xi) - E_y(\xi_{\max}) = \int_{\xi_{\max}}^{\xi} \frac{a_0(a_0 \sin\xi + \tilde{p}_y)\cos\xi}{C_{\perp} - U(y)} d\xi, \tag{4.23}$$

and

$$E_x(\xi) - E_x(\xi_{\max}) = \int_{\xi_{\max}}^{\xi} \frac{a_0^2 \sin\xi\cos\xi}{C_\perp - U(y)} d\xi. \tag{4.24}$$

We consider the case $\Omega \ll 1$ and thus electron heating is due to the overlapping of high-n resonances ($n\Omega = 1$). Then the electron energy changes during relatively short time of strong interactions of electron with laser radiation in the vicinity of $y = y_{max}$ and $y = y_{\min}$. We assume that the electron energy variation during such collisions, ΔE, is small $|\Delta E| \ll E$ such that the unperturbed electron trajectories in Eq. (4.17) can be applied to assess the electron energy change between two consecutive collisions in Eqs. (4.23, 4.24). As a result, we have

$$\Delta E_x = \frac{a_0^2}{2\sqrt{E\kappa_u}} \sin(2\xi_j) \int_{-\pi/2}^{\pi/2} \cos\left[2\Omega^{-1}\left(\theta - \frac{\sin 2\theta}{2}\right)\right] d\theta, \tag{4.25}$$

$$\Delta E_y = a_0\sqrt{2C_\perp/\kappa_u}\sin\xi_j \int_{-\pi/2}^{\pi/2} \sin\theta \sin\left[\Omega^{-1}\left(\theta - \frac{\sin 2\theta}{2}\right)\right] d\theta + \Delta E_x, \tag{4.26}$$

where ξ_j is the time of previous collision in the vicinity of $y_{\min}$.

Under the condition of $\Omega \ll 1$, we notice the fact that $|\theta| \ll 1$ mostly contributes to the integrals in equations (4.25, 4.26). This enables the Taylor expansion of the terms in the brackets as $\theta - \sin(2\theta)/2 = 2\theta^3/3$. Moreover, the integral limits can be extended to infinity such that the integrals in Eqs. (4.25, 4.26) are degenerated to the Airy function $Ai(x)$ and its first derivative $Ai'(x)$ at zero, and after some algebra we obtain

$$\Delta E_x = 2^{1/3}3^{-1/6}\Gamma(1/3)\left(E_{\max}^{abs}\right)^{4/3}\varepsilon^2 E^{-1/3}\sin(2\xi_{2n}), \tag{4.27}$$

$$\Delta E_y = 2^{4/3}3^{1/6}\Gamma(2/3)\left(E_{\max}^{abs}\right)^{2/3}\varepsilon E^{1/3}\sin(\xi_j) + \Delta E_x, \tag{4.28}$$

where $\Gamma(x)$ is the gamma function. Then condition of $|\Delta E| \ll E$ requires that

$$E \gg E_{\max}^{abs}\varepsilon^{3/2} = E_{pond}\varepsilon^{-1/2}. \tag{4.29}$$

Therefore, our analysis is only valid for the electron with energy of $\varepsilon^{3/2} \ll E/E_{\max}^{abs} \ll 1$ under the condition of $\varepsilon \ll 1$. For electron with energy smaller than that in Eq. (4.29), the change of the electron orbit due to the electron laser interaction is large and our estimate in Eqs. (4.27, 4.28) using the unperturbed electron orbit is not accurate. However, from the numerical simulations we find that the electrons with energy $E < E_{max}^{abs}\varepsilon^{3/2}$ could still undergo stochastic acceleration. Here we are interested in the maximum electron energy gain and thus we consider electrons satisfying Eq. (4.29). One important result drawn from condition (4.29) is that the first term on the right hand side of Eq. (4.28) is dominated over the second one such that

$$\Delta E_y \approx 2^{4/3}3^{1/6}\Gamma(2/3)\left(E_{\max}^{abs}\right)^{2/3}\varepsilon E^{1/3}\sin(\xi_j) \gg \Delta E_x. \tag{4.30}$$

By using the same procedure or considering symmetry of this system, we can show that the energy variation in the vicinity of $y_{\min}$ is also given by expressions (4.27, 4.30) except a "-" sign in front for ΔE_y as the work done by the laser depends on the direction of $\tilde{p}_y$. Therefore, we can ignore the difference between y_{max} and $y_{\min}$ and obtain the following mappings from Eqs. (4.19, 4.27, 4.30) as

$$\Pi_{n+1}^{x(y)} = \Pi_n^{x(y)} + Q_{x(y)}\sin\psi_n^{x(y)}, \psi_{n+1}^{x(y)} = \psi_n^{x(y)} + \Pi_{n+1}^{\alpha_{x(y)}}, \tag{4.31}$$

where $\Pi_n^x = (2\pi)^{-8/3}(E_n/E_{\max}^{abs})^{4/3}$, $\psi_n^x = 2\xi_n$, $Q_x = 2^{-1/3}3^{-7/6}\Gamma(1/3)\pi^{-8/3}\varepsilon^2$, $\alpha_x = -3/8$ and $\Pi_n^y = (\pi)^{-4/3}(E_n/E_{\max}^{abs})^{2/3}$, $\psi_n^y = \xi_n$, $Q_y = (-1)^n 2^{7/3}3^{-5/6}\Gamma(2/3)\pi^{-4/3}\varepsilon$, $\alpha_y = -3/4$ are the quantities corresponding to different polarizations. The mappings in Eq. (4.31) are rather similar to the "Chirikov standard Map" [58] and it can be easily shown that they are symplectic and thus conserve the phase volume.

To see the stochasticity boundary, the relation $K_{x(y)} = \left| d\psi_{n+1}^{x(y)}/d\psi_n^{x(y)} - 1 \right| \geq 1$ should be

satisfied [23, 56], which yields

$$K_x = k_x \left(E_{\max}^{abs} E^{-1}\right)^{11/6} \varepsilon^2 > 1, \text{ and } K_y = k_y \left(E_{\max}^{abs} E^{-1}\right)^{7/6} \varepsilon > 1, \tag{4.32}$$

where $k_x = 2^{1/3}3^{-1/6}\pi\Gamma(1/3)$ and $k_y = 2^{1/3}3^{1/6}\pi\Gamma(2/3)$ are the numerical factors order of unity. The satisfaction of relation in Eq. (4.32) leads to the mixing in phase space and gives the stochasticity criterion as a function of the electron energy E, laser field amplitude a_0 and the electric field strength κ_u, where we have disregarded the region of phase ψ in which chaos appears. It follows that for both polarizations there exits upper limit of the stochastic heating energy as

$$E_{\max}^{x} \approx E_{\max}^{abs} \varepsilon^{12/11} = E_{pond} \varepsilon^{-10/11}, \text{ and } E_{\max}^{y} \approx E_{\max}^{abs} \varepsilon^{6/7} = E_{pond} \varepsilon^{-8/7}, \tag{4.33}$$

We see that the maximum stochastic energy in Eq. (4.33) are smaller than $E_{\max}^{abs}$ but they are above the ponderomotive scaling under the condition of $\varepsilon \ll 1$. Also it shows that $E_{\max}^{y} \gg E_{\max}^{x}$ and thus the electrons can gain more energy in the case where the laser electric field along the quasi-static electric field than that across to it. This is not surprising because the electron transverse velocity anti-parallel to the laser electric field is larger in the former case and thus if we choose large $\bar{P}_x$ in the latter this difference can be eliminated. Moreover, Eq. (4.33) indicates that the upper energy boundary is relaxed for weak electric field.

4.1.2 Results of numerical simulations

In order to confirm the analyses, we have numerically solved the Hamiltonian equations in Eq. (4.14) for different parameters of laser radiation and electric field. Note that the upper limit of the stochastic energy would be larger for smaller electric field strength, which is not surprising since the weaker electric field allows the electron to stay in the nonadiabatic region for longer time

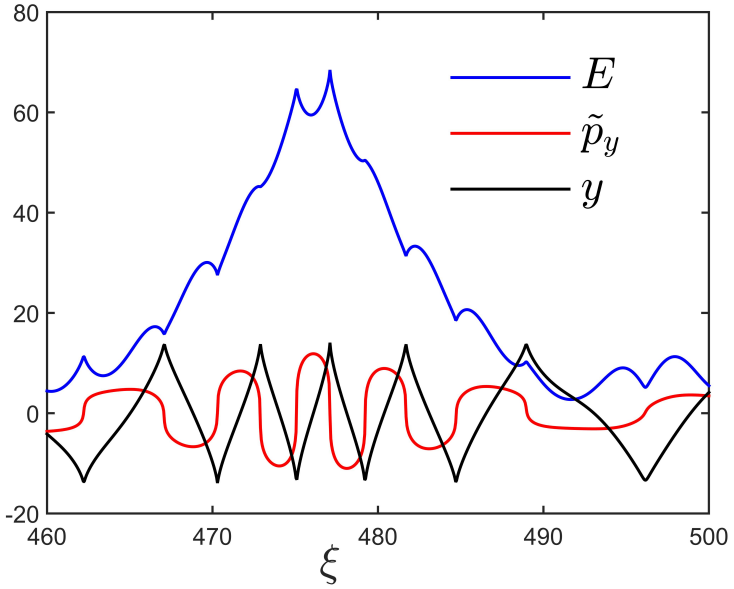

Figure 4.2: Electron motion in the transverse electric field for $C_\perp = 1$, $\kappa_u = 0.01$, y-polarized laser amplitude $a_0 = 1$ and initial energy $E = 13$.

such that it could gain more energy from the laser wave. Moreover, a weak electric field should be employed to have $\varepsilon \ll 1$ since the stochastic heating occurs at high harmonic resonances $\Omega = \varepsilon\sqrt{E/E_{pond}} = \sqrt{E/E^{abs}_{\max}} \ll 1$ and we are interested in electron energy accelerated beyond the ponderomotive scaling ($E > E_{pond}$). For electrons with large energy such that $\Omega \sim 1$, the strong interaction of electron with laser pulse could take place along the whole electron orbit in Fig. 4.1 ($|\theta| \sim 1$) and the analytical results in Eqs. (4.27-4.33) are not accurate and thus the stochastic heating is hardly distinguished. For example, Fig. 4.2 (which looks like Fig. 10 in Ref. [12]) shows the electron dynamics for $C_\perp = 1$, $\kappa_u = 0.01$, y-polarized laser with amplitude $a_0 = 1$ (thus $\varepsilon \sim 0.1$) and initial energy $E = 13$. For these parameters, $\Omega \sim 1$ for large electron energy $E \sim 25$ where the electron wanders near the boundary of stochasticity and its dynamics is complex. Therefore, in order to check the result in Eq.(4.33) which only holds for $\Omega \ll 1$ and thus only $|\theta| \ll 1$ contributes to the electron energy variation, we requires $\Omega_{\max} = \sqrt{E^x_{\max}/E^{abs}_{\max}} \approx \varepsilon^{1/2} \ll 1$. Here we take $\kappa_u \leq 10^{-4}$, $a_0 \sim 1$ and $C_\perp = 1$ such that $\varepsilon \sim 0.01$.

On the other hand, the laser polarization is of great importance for the electron dynamics

since the electron motion is more stochastic for laser polarized along the quasi-static electric field than that for laser across to the electric field. Taking into account that $\Omega^x_{\max} \approx \varepsilon^{6/11} < \Omega^y_{\max} \approx \varepsilon^{3/7}$, the latter case is preferable to distinguish the stochastic heating. Therefore, we will present only the numerical results for the laser polarization of $\tilde{\vec{A}} = a_0 \sin(\xi)\vec{e}_x$. All the simulations are set to $C_\perp = 1$. In contrast to the low harmonic resonance [29], where "preheated" electrons are required to obtain high energy well beyond the ponderomotive scaling due to the existence of the threshold-type dependence of the final energy gain on ε, the stochastic motion can accelerate electrons from very low energy even though our analysis validate only for $E > E_{pond}$.

The Poincaré mappings in numerical simulations are formed in the following way: it's on 2D energy E and laser phase $\Delta\xi$ ($0 < \Delta\xi < \pi$) space where $\Delta\xi \equiv \xi_n - m\pi$ with $m \equiv [\xi_n/\pi]$. E_n and ξ_n are picked when electron passes through $y_{\max,\min}$. In Fig. 4.3 we have shown the numerical results of the maximum stochastic energy of electrons, in unit of $E^{abs}_{\max}$, picking from the Poincaré mappings as a function of the parameter ε in the logarithmic diagram as well as their fitting by the linear polynomial. The blue squares correspond to the data of $\kappa_u = 10^{-4}$ and varying a_0 while the red diamonds are for $a_0 = 8$ and varying κ_u. As we can see, the numerical simulations agree well with the analytic results in Eq. (4.33).

The inaccuracy in the fitting reflects the difficulty to determine the maximum stochastic energy from the mappings. This is because, when the stochastic parameter K closes to unity [23], "the structure of the phase space becomes complicated where the fraction of stable components of the motion plays an important role". Fig. 4.4 has displayed the Poincaré mapping of electron for $a_0 = 8$ and $\kappa_u = 5 \times 10^{-5}$ as an example. The large excursion at high energy is the well-known phenomenon at the boundary of stochasticity. In the simulations, the energy below the large excursion in the transverse case has been taken as the maximum stochastic energy.

The stability island in the Poincaré mapping can be studied as following. The stationary

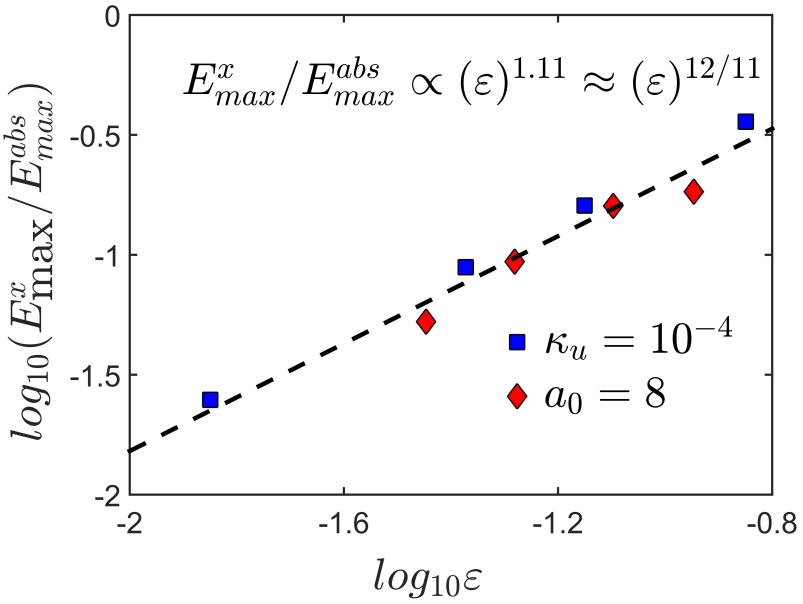

Figure 4.3: The maximum stochastic energy $E^x_{\max}/E^{abs}_{\max}$ versus ε of electrons for the laser polarized across to the transverse electric field in the logarithmic diagram and its fittings by a linear polynomial (the blue squares are for $\kappa_u = 10^{-4}$ and varying a_0, whereas the red diamonds are for $a_0 = 8$ and different κ_u).

points in the phase space are determined according to Eq. (4.31) by the solutions of

$$Q_x \sin\psi^x_0 = 0, (\Pi^x_0)^{-3/8} = 2\pi N, \tag{4.34}$$

where N is integer. As a result, $\psi^x_0 = (2n+1)\pi$ ($\Delta\xi = \pi/2$) and $\psi^x_0 = 2n\pi$ ($\Delta\xi = 0$ or $\Delta\xi = \pi$) are stationary points. The stability of these stationary points are determined by the eigenvalues, $\lambda_{1,2}$, of the Jacobian of the map [23] in the neighborhood of ψ^x_0 and Π^x_0

$$\begin{bmatrix} \partial\Pi^x_{n+1}/\partial\Pi^x_n & \partial\Pi^x_{n+1}/\partial\psi^x_n \\ \partial\psi^x_{n+1}/\partial\Pi^x_n & \partial\psi^x_{n+1}/\partial\psi^x_n \end{bmatrix} \begin{bmatrix} x \\ y \end{bmatrix} = \lambda_{1,2} \begin{bmatrix} x \\ y \end{bmatrix}. \tag{4.35}$$

where the stability condition requires that $\lambda_{1,2} < 1$. As a result, we have

$$|2 - 3/8(\Pi^x_0)^{-11/8} Q_x \cos\psi^x_0| < 2, \tag{4.36}$$

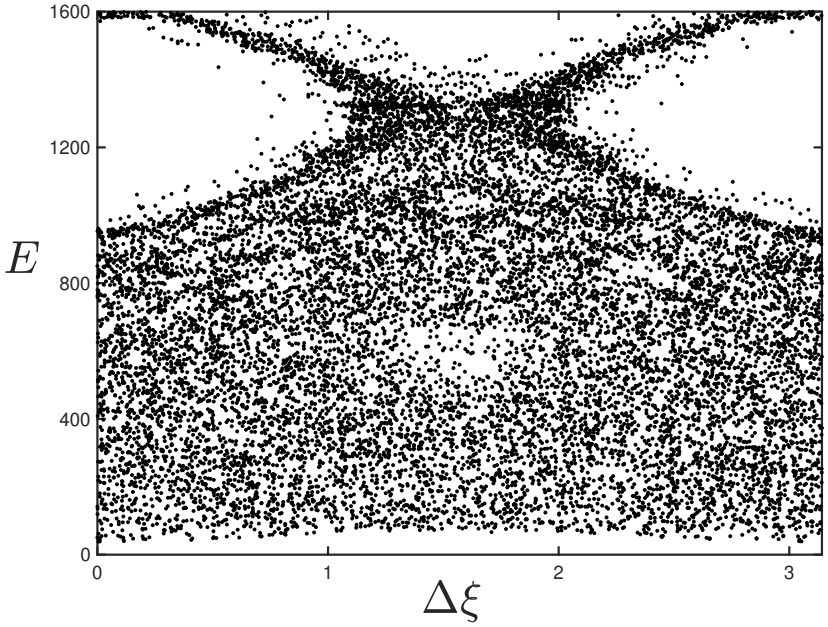

Figure 4.4: Poincaré mapping of electrons in the transverse electric field with $\kappa_u = 5 \times 10^{-5}$, laser polarized across to the electric field with $a_0 = 8$ and $C_\perp = 1$.

which shows that, $\psi_0^x = (2n+1)\pi$ ($\Delta\xi = \pi/2$) are always unstable stationary points and the points of $\psi_0^x = 2n\pi$ ($\Delta\xi = 0$ or $\Delta\xi = \pi$) are stable for

$$E > E_{\max}^x, \tag{4.37}$$

where a factor of order of unity has been omitted. Therefore, the stability island is present only for electron energy above the completely stochastic region as shown in Fig. 4.4.

Fig. 4.5 has shown the evolution of electron trajectories and energy. As one can see, it agrees with the analytic results including the electron oscillating frequency, electron trajectories (zig-zag shape of y and step-shape of $\tilde{p}_y$) which could have long tail distribution of Fourier spectrum, and energy "kicks" for highly stochastic motion, etc.

We see that the variation of electron energy occurs primarily within a certain time interval much smaller than its characteristic periods. The energy change mainly occurs around $y_{\max}$ and $y_{\min}$ where $|\theta| \ll 1$ corresponds to the energy jump. Except for these time moments of "kick",

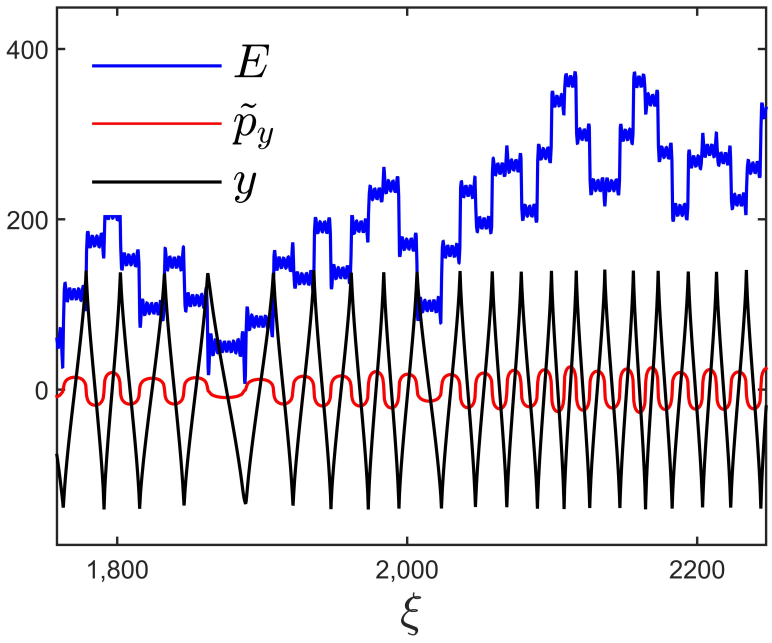

Figure 4.5: Electron motion for $C_\perp = 1$, $a_0 = 5$ and $\kappa_u = 10^{-4}$. To make them readable, the canonical coordinates have been shrunk by some factors to illustrate their shapes.

the electron motion experiences oscillations in the adiabatic region.

To confirm the role of superluminal phase velocity, numerical simulation for the same parameters with Fig. 4.4 but $v_p = 1.001$ is exhibited in Fig. 4.6. Compared with Fig. 4.4, it demonstrates that the superluminal phase velocity indeed weakens the stochastic acceleration by reducing the maximum stochastic energy.

The effect of magnetic field has been discussed before, where $\kappa_u + \kappa_b$ acts as the "effective" strength of the electrostatic potential for the same dependence of U and A_B on the coordinate y. Therefore, we could conclude that: if $\kappa_b > 0$, the magnetic field would weaken the stochastic electron motion by increasing the "effective" electric strength; if $\kappa_b < 0$ but $|\kappa_b| < \kappa_u$, it will enhance it; while the stochasticity no longer exists when $\kappa_u + \kappa_b < 0$. This has been verified by the numerical simulations.

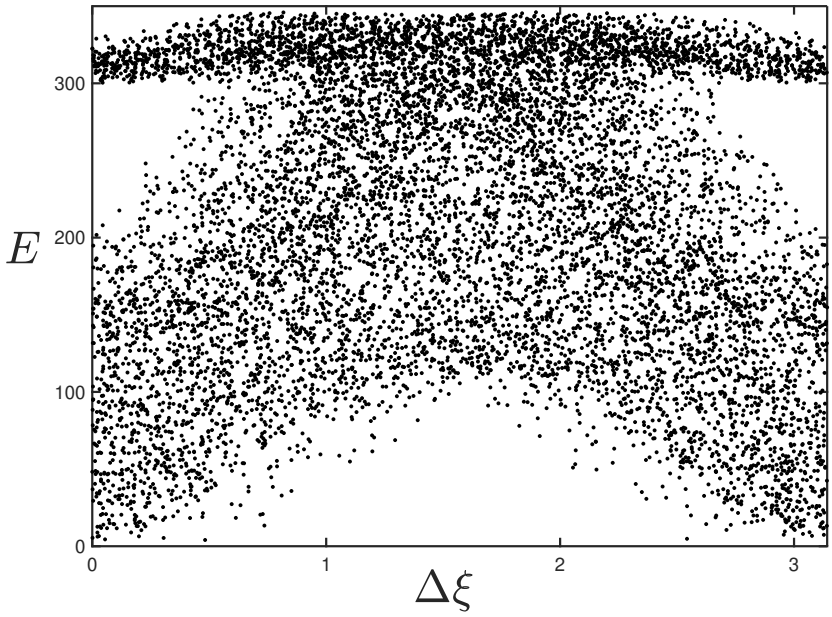

Figure 4.6: Poincaré mapping of electrons for the same parameters with Fig. 4.4 but $v_p = 1.001$.

4.2 Electron in longitudinal electric and transverse magnetic fields

In this section, we will study the stochastic electric motion in the quasi-static longitudinal electric and transverse magnetic fields. The longitudinal electric field can be formed inside the pre-plasma in order to balance the increased electron pressure due to laser heating [15, 98, 99], within which electrons can be stochastically accelerated. The mechanism underlying the stochastic electron motion has been studied by using the simplified V-shape of the electrostatic potential [25, 26]. It showed that the electron can be stochastically accelerated to infinite energy for "infinite potential well" (the potential well is deep enough that the electron inside such potential well can never escape) when the laser strength exceeds the electric field. However, the actual shape of the potential well [15, 98] inside the pre-formed plasma may be different from the V-shape considered in [25, 26] and thus more realistic form of $U(z)$ should be investigated. In the following, we will consider $U(z) = k_u|z|^p$ (where $p = 1$ is for the V-shape of U) and show

that the electron dynamics for $p > 1$ is quite different from that for $p = 1$. Moreover, we include a transverse quasi-static magnetic field, which also depends only on the z-coordinate and is in the y-direction. As a result, the vector potential including all the QEM fields can be

$$\vec{A} = \tilde{\vec{A}} - \vec{e}_z t \partial U(z)/\partial z + \vec{e}_y A_B(z). \tag{4.38}$$

Then, from Eqs. (4.2, 4.3) we can obtain again Eq. (4.4) as well as

$$P_y - \tilde{A}_y - A_B = \bar{P}_y \equiv \left(P_y - \tilde{A}_y - A_B\right)_{t=0}, \tag{4.39}$$

$$\frac{dP_z}{dt} = -\frac{\partial U(z)}{\partial z} - \frac{\partial A_B(z)}{\partial z} v_y - \frac{\partial \tilde{A}_x}{\partial z} v_x - \frac{\partial \tilde{A}_y}{\partial z} v_y, \tag{4.40}$$

$$\frac{d(\gamma + U)}{dt} = \frac{\partial \tilde{A}_x}{\partial t} v_x + \frac{\partial \tilde{A}_y}{\partial t} v_y. \tag{4.41}$$

We introduce variables $\delta = \gamma - P_z$, $\xi = t - z$ and $\tilde{z} = z$, and thus

$$\tilde{A}_{(...)}(\xi, \tilde{z}) = \tilde{A}_{(...)}\left(\xi + \left(1 - \frac{1}{v_p}\right)\tilde{z}\right). \tag{4.42}$$

Then from Eqs. (4.4,4.39-4.41) and using the chain rule we obtain

$$\frac{d\delta}{d\xi} = \frac{1}{2\delta}\frac{\partial}{\partial \tilde{z}} P_{\perp,z}^2 + \frac{\partial U}{\partial \tilde{z}}, \tag{4.43}$$

where

$$P_{\perp,z}^2 = 1 + \left(\bar{P}_x + \tilde{A}_x(\xi, \tilde{z})\right)^2 + \left(\bar{P}_y + \tilde{A}_y(\xi, \tilde{z}) + A_B(\tilde{z})\right)^2. \tag{4.44}$$

Applying the expression of δ to the expressions of P_z and γ, we obtain

$$P_z = \frac{P_{\perp,z}^2}{2\delta} - \frac{\delta}{2}, \text{ and } \frac{d\tilde{z}}{d\xi} = \frac{P_z}{\delta} = \frac{P_{\perp,z}^2}{2\delta^2} - \frac{1}{2}, \tag{4.45}$$

Observing Eqs.(4.43, 4.45) we arrive to the following Hamiltonian equations

$$\frac{d\tilde{z}}{d\xi} = -\frac{\partial H_z^p}{\partial \delta} \text{ and } \frac{d\delta}{d\xi} = \frac{\partial H_z^p}{\partial \tilde{z}}, \tag{4.46}$$

where

$$H_z^p(\tilde{z}, \delta, \xi) = \frac{1}{2}\left\{ \frac{P_{\perp,z}^2}{\delta} + \delta \right\} + U(\tilde{z}). \tag{4.47}$$

Notice that the superluminal phase velocity appears only in the vector potential in Eq.(4.42), which depends not only on ξ but also on $\tilde{z}$ due to an impact of $v_p - 1 > 0$. In the following, we will specify the electrostatic potential of electric field as $U(z) = k_u|z|^p$, where $p = 1$ was considered in Refs. [25, 26]. We will first consider $A_B = 0$ and the effect of the quasi-static magnetic field will be discussed separately.

4.2.1 Electron motion in laser and longitudinal electric field only

Here we consider electron motion in the laser and longitudinal electric field only. As a result, the laser polarization in Eq. (4.47) is not important so that the use of $\tilde{\vec{A}} = a_0 \sin(\xi - (1 - 1/v_p)\tilde{z})\vec{e}_x$ will be applied in the following and for the sake of simplicity, we shall assume $\bar{P}_x = \bar{P}_y = 0$.

From Eq. (4.47) we see that the strongest electron interaction with the laser locates at small $\delta = \gamma - P_z$ when the electron passes through the bottom of the electrostatic potential well $\tilde{z} = 0$. Therefore, whereas the transverse electric field reduces the electron dephasing rate from laser directly when it departures from the bottom of the electrostatic potential well, the longitudinal electric field seems to only confine the electrons such that they could enter the nonadiabatic region multiple times.

By using the same method as in section 4.1, the energy exchange between two consecutive

collisions between the electron and the laser wave is given by

$$\Delta E_z = \int_{\xi_n}^{\xi_{n+1}} \frac{dH_z}{d\xi} d\xi = \int_{\xi_n}^{\xi_{n+1}} \frac{a_0^2 \sin\left[2\xi + (1-1/v_p)\tilde{z}\right]}{2\delta} d\xi, \tag{4.48}$$

where $\xi = \xi_n$ is the time of nth passage of the electron through the nonadiabatic region $\delta \approx \delta_{\min}$ from the negative $\tilde{z}$ (z) side. From Eq. (4.47) we see that $\tilde{z}$ can be large when relativistic electrons oscillate in the electric field. As a result, the superluminal phase velocity $v_p > 1$ could introduce a fast oscillation to the integral in Eq. (4.48) and thus reduce the electron laser interactions. Therefore, in the following we will consider the luminal case ($v_p = 1$), where the impact of superluminal phase velocity on the electron motion will be investigated by using the numerical simulations.

For the action-angle variables (I, ϑ) of the unperturbed particle, from Eq. (4.47) we obtain

$$I = \frac{2p}{\pi(p+1)} E^{1+1/p} k_u^{-1/p}. \tag{4.49}$$

Therefore, the electron oscillating frequency $\Omega = \partial E/\partial I$ in the electric field reads

$$\Omega = 2^{-1} \pi k_u^{1/p} E^{-1/p}. \tag{4.50}$$

As a result, in order to have efficient electron-laser interactions we should have the resonances between the electron oscillating frequency with the laser frequency, i.e., $n\Omega = 1$ where $n \geq 1$ is an integer number. Therefore, we would consider $\Omega \leq 1$ and thus $E \geq k_u$ for stochastic motion. Moreover, we are interested in electron acceleration beyond the ponderomotive scaling and thus $E \geq \max\{k_u, E_{pond} = a_0^2/2\}$ is considered.

Noting that for $p = 1$, from Eq. (4.46) we have $\delta = \delta_{\min} + k_u(\xi - \xi_n)$ ($\delta_{\min}$ denotes the local minimum of the coordinate δ at the center of the nonadiabatic region), the integral in Eq. (4.48) could be easily estimated as shown in Refs. [25, 26]. For the general case of $p > 1$,

analyzing Eq. (4.46) we know that $d\tilde{z}/d\xi \gg 1$ and $d\delta/d\xi \ll 1$ in the vicinity of $(\delta = \delta_{\min}, \tilde{z} = 0)$. As a result, the electron will leave the vicinity of $(\delta_{\min}, \tilde{z} = 0)$ and reach $(\delta_{\min}, \tilde{z}_{\max})$ in an extremely short time period, where $\tilde{z}_{\max} \approx pE^{1/p}k_u^{-1/p}$. Therefore, the electron trajectory in the nonadiabatic region $\delta \tilde{<} 1$ can be largely described by $\delta \approx \delta_{\min} + pk_u\tilde{z}_{\max}^{p-1}(\xi - \xi_n)$ and $\tilde{z} \approx \tilde{z}_{\max}$ (notice that $\delta \approx \delta_{\min} + pk_u\tilde{z}_{\max}^{p-1}(\xi - \xi_n)$ is consistent with the exact solution of $p = 1$). This argument has been confirmed by the numerical simulations (e.g., see Fig. 4.9). This situation is not surprising since the relativistic electron has speed of $v_z \approx c$ around $\delta_{\min}$ and thus moves fast toward $\tilde{z}_{\max}$, where it is significantly decelerated.

The condition of $\delta \sim 1$ corresponds to $\xi - \xi_n \sim p^{-1}k_u^{-1/p}E^{1/p-1} \equiv \zeta_f$, which can be seen as the boundary of the nonadiabatic region. As we can see, for $p > 1$, $\zeta_f \ll 1$ and thus the variation of the numerator in Eq. (4.48) can be negligible. As a result, we find

$$\Delta E_z = a_0^2 \sin 2\xi_n \int_0^{\zeta_f} \frac{1}{pk_u^{1/p}E^{1-1/p}\zeta + \delta_{\min}} d\zeta = \frac{a_0^2 \Lambda \sin 2\xi_n}{pk_u^{1/p}E^{1-1/p}}, \tag{4.51}$$

where $\Lambda \sim \ln(E)$. We see that Eq. (4.43) is consistent with the result for $p = 1$ with a slight difference of the coefficient [25, 26].

Eqs. (4.50) and (4.51) form the following symplectic Chirikov-like mapping

$$\Pi_{n+1} = \Pi_n + Q\sin\psi_n,\ \psi_{n+1} = \psi_n + \Pi_{n+1}^{1/(2p-1)}, \tag{4.52}$$

where $\Pi_n = 8^{2p-1}k_u^{1/p-2}E_n^{2-1/p}$, $\psi_n = 2\xi_n$ and $Q = (2p-1)8^{2p-1}k_u^{-2}\Lambda a_0^2/p^2$. Therefore, an onset of stochasticity requires

$$K = 8p^{-2}k_u^{-2/p}\Lambda a_0^2 E^{2(1-p)/p} \geq 1. \tag{4.53}$$

We can see that for $p > 1$, an upper boundary of the stochastic energy exits as

$$E^L_{\max} \propto k_u^{-1/(p-1)} a_0^{p/(p-1)}, \tag{4.54}$$

which is quite different from the $p = 1$ case where there is no energy limit under the stochastic condition $a_0 > k_u$ [25, 26]. Like in the case of transverse electric field, higher energy boundary can be achieved at smaller k_u. The resonant condition of $\Omega < 1$ ($E > k_u$) now requires $a_0 > k_u$ while electron stochastic acceleration above the ponderomotive scaling requires $a_0^{p-2} k_u < 1$. Therefore, we are interested in the region of $k_u < \min\{a_0, a_0^{2-p}\}$.

4.2.2 Impact of transverse quasi-static magnetic field

Here we consider the impact of quasi-static magnetic field $A_B(z)$. As a result, from Eq. (4.47) we see that the laser polarization becomes important. For the laser polarized along the magnetic field (x-direction), the stochastic electron motion would always be suppressed as shown in the following. By analyzing Eq. (4.47) with magnetic field, we find that the electron will have a different unperturbed orbit $\delta_B(\tilde{z}) > \delta(\tilde{z})$ in the nonadiabatic region, where $\delta_B(\tilde{z})$ and $\delta(\tilde{z})$ are, respectively, the quantities with and without the quasi-static magnetic field for the same electron energy E. Then the energy variation in Eq. (4.48) for the laser wave polarized in x-direction has the form of

$$\Delta E_z = \int_{\xi_n}^{\xi_{n+1}} \frac{dH_z}{d\xi} d\xi = \int_{\xi_n}^{\xi_{n+1}} \frac{a_0^2 \sin 2\xi}{2\delta_B} d\xi. \tag{4.55}$$

As we can see, the integrand in Eq.(4.55) is smaller than that in the expression (4.48) no matter what form of the magnetic field is. On the other hand, $d\delta_B/d\xi > d\delta/d\xi$ such that δ_B grows faster out of the nonadiabatic region, i.e., $\delta_B \tilde{<} 1$, than that for $A_B = 0$, which indicates that the contributing integral region in Eq. (4.55) is smaller than that in (4.48). As a result, we can conclude that the energy change in Eq. (4.55) is smaller than that in Eq. (4.48) and thus the stochastic acceleration is weakened with the presence of $A_B(z)$ when the laser polarized along the

magnetic field.

For the case where laser polarized across to the quasi-static magnetic field, the situation is more complex. This is because the energy variation also contains, apart from the integral in Eq. (4.55),

$$\Delta E_z^{(2)} = \int_{\xi_n}^{\xi_{n+1}} \frac{a_0 A_B \cos\xi}{2\delta_B} d\xi. \tag{4.56}$$

The enlarged electron momentum, $P_y = A_B + \tilde{A}_y$, due to A_B along the laser electric field makes it possible to gain more energy from the laser radiation, which, during one collision, is the combination of the integrals in Eq. (4.55) and (4.56). Assuming that the effect of the magnetic field is finite such that the electron still gets most acceleration in the vicinity of $\tilde{z}_{\max}$ and $\delta_B \lesssim 1$, then if A_B ($\tilde{z}_m$) is small such that the contribution to the electron energy variation from Eq. (4.56) is smaller than that from Eq. (4.55) and thus it is negligible, the stochasticity could be decreased like the case where the laser polarizes along the magnetic field. However, if the magnetic field is strong enough, i.e., $A_B(\tilde{z}_m) > a_0$, the electron energy change is then mainly determined by Eq. (4.56) and the stochastic motion could be enhanced. The study in Ref. [23] is an asymptotic limit of this case. The numerical simulations have been performed which agrees with these results.

4.2.3 Results of numerical simulations

We performed numerical simulations to integrate the Hamiltonian equations in Eq. (4.46) for different parameters of laser radiation and electric field. As shown in Eq. (4.54), the upper limit of the stochastic energy would be large for small electric field strength. Specifically, electric field coefficient satisfying $k_u \lesssim \min\{a_0, a_0^{2-p}\}$ could cause strong stochastic electron acceleration beyond the ponderomotive scaling. In the simulations we specify the static electric field as $U = k_u \tilde{z}^2/2$ and thus consider $k_u < \min\{a_0, a_0^{2-p}\} = \min\{a_0, 1\}$. Although smaller k_u can lead to larger stochastic electron energy, $k_u \sim 0.1$ would be used in the simulations for time saving

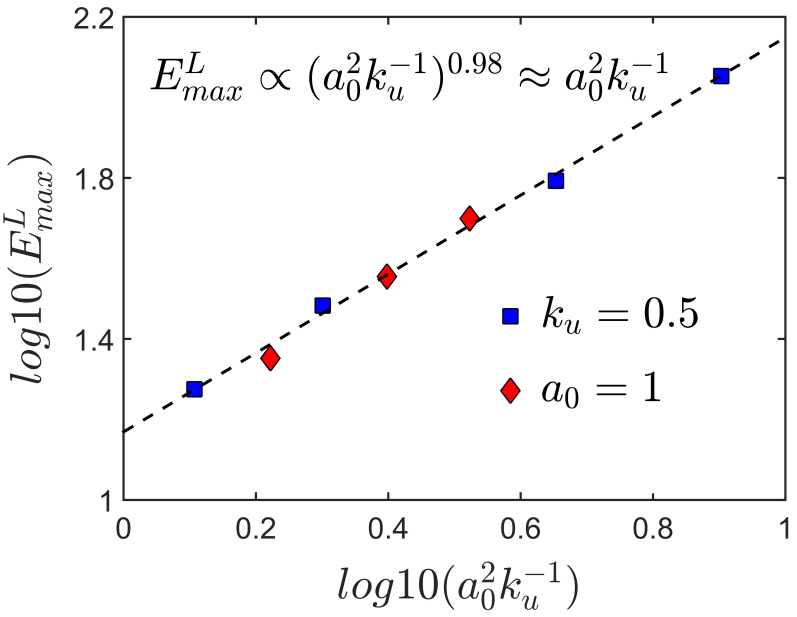

Figure 4.7: The maximum stochastic energy $E^L_{\max}$ versus $a_0^2 k_u^{-1}$ of electrons in the longitudinal electric field described by $U = k_u \tilde{z}^2/2$ in the logarithmic diagram and its fitting by a linear polynomial (the blue squares are for $k_u = 0.5$ and varying a_0, whereas the red diamonds are for $a_0 = 1$ and different k_u).

consideration, which is sufficient to check the results. Moreover, the laser polarization for $A_B(z) = 0$ is not important so we would take $\vec{\tilde{A}} = a_0 \sin(\xi)\vec{e}_x$.

The Poincaré mappings in the same way with section 4.1 will be used to exhibit the numerical results: it's on 2D energy E and laser phase $\Delta\xi$ ($0 < \Delta\xi < \pi$), where E_n and ξ_n are picked when electron passes through the nonadiabatic region $\tilde{z} = 0$ from the negative z. In Fig. 4.7 we have shown the maximum stochastic energy $E^L_{\max}$ versus $a_0^2 k_u^{-1}$ of electrons in the longitudinal electric field described by $U = k_u \tilde{z}^2/2$ in the logarithmic diagram and its fitting by a linear polynomial (the blue squares are for $k_u = 0.5$ and varying a_0 whereas the red diamonds are for $a_0 = 1$ and different k_u). As we can see, the numerical simulations agree with the analytic results in Eq. (4.54).

Fig. 4.8 shows the Poincaré mapping of electron for $a_0 = 1$ and $k_u = 0.5$ as an example. As we can see, it exhibits a series of stability islands not occupied by the electron trajectories.

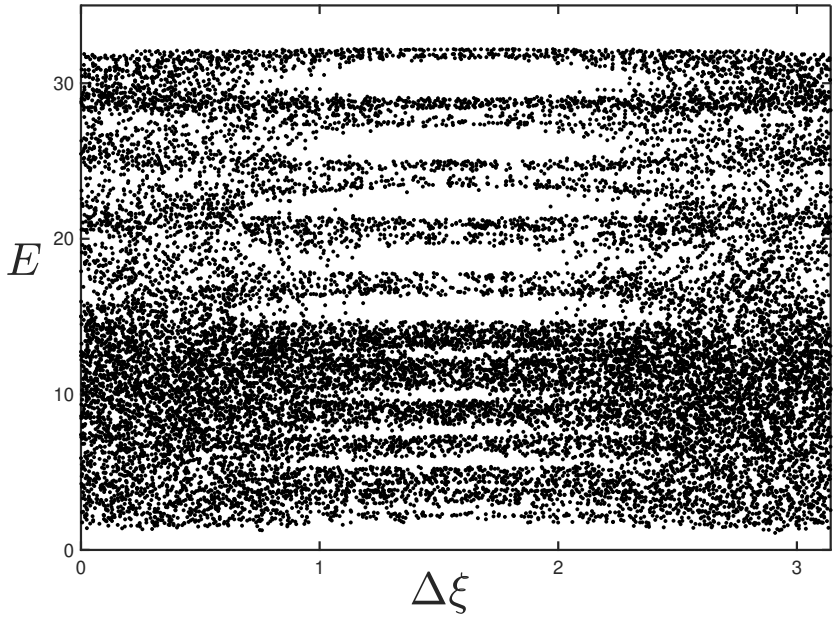

Figure 4.8: Poincaré mapping of electrons in the longitudinal electric field with $k_u = 0.5$ and $a_0 = 1$.

Their physics can be studied by examining the mapping in Eq. (4.52), where the stationary points in the phase space are determined by the solutions of

$$Q \sin \psi_0 = 0,\ \Pi_0^{1/3} = 2\pi N, \tag{4.57}$$

Therefore we have $\psi_0 = 0$ or $\psi_0 = \pi$ and $\Pi_0 = 8^3 k_u^{-3/2} E^{3/2} = (2\pi N)^3$. Again, the stability of these stationary points are determined by the eigenvalues of the Jacobian of the map, which requires that

$$|2 + 3^{-1} \Pi_0^{-2/3} Q \cos \psi_0| < 2. \tag{4.58}$$

Therefore the stationary points at $\psi_0 = 2n\pi$ (n is integer) is always unstable while for $\psi_0 = (2n+1)\pi$ the stability requires $\Pi_0^{-2/3} Q < 12$, which corresponds to

$$E > \Lambda a_0^2 / 2k_u. \tag{4.59}$$

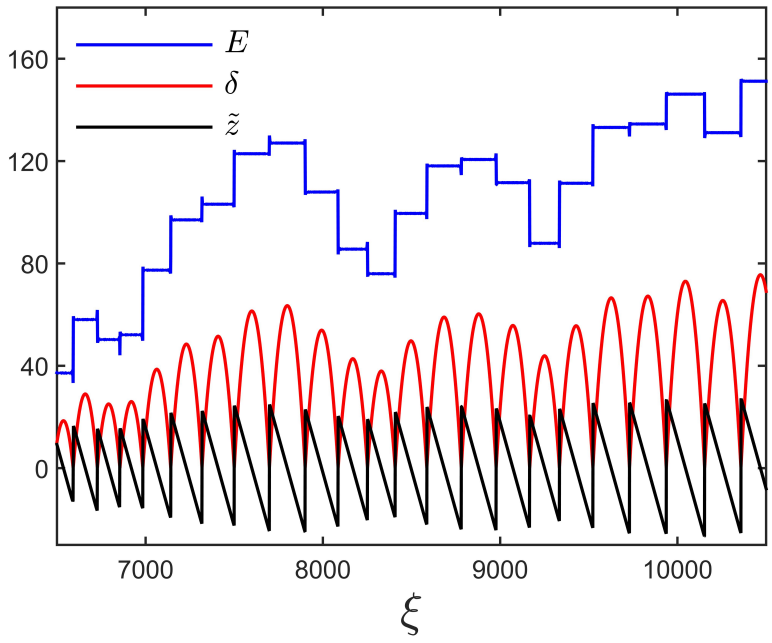

Figure 4.9: Electron motion for $a_0 = 5$ and $k_u = 0.1$. To make them readable, the canonical coordinates have been shrunk by some factors to illustrate their shapes.

It indicates that larger stability islands occurs at higher electron energy and $\psi_0 = (2n+1)\pi$ ($\Delta\xi = \pi/2$) as shown in Fig. 4.8.

In Fig. 4.9 we show the evolution of electron trajectories and energy. As one can see, it agrees with the analytic results, where the electron trajectories will exhibit a long tail distribution of the Fourier spectrum. The nonadiabatic interaction of electrons with the laser radiation occurs at a short time period near the local minimum of δ, where electrons can fly from $-\tilde{z}_{max}$ to $\tilde{z}_{max}$. As a result, the electron energy variation mainly comes from $\delta \ll 1$ and $\tilde{z} \approx \pm\tilde{z}_{\max}$. Moreover, we see that the electron motion in the longitudinal electric field as shown in Fig. 4.9 experiences relatively smaller oscillations in the adiabatic region compared with that in the transverse electric field as shown in Fig. 4.5. This is because the energy variation inversely depends on the dephasing rate, where, in the transverse case, the dephasing rate $\gamma - p_z = C_\perp - U$ is always smaller than $C_\perp$ (order of unity) such that even $|\theta| \sim 1$ region could cause variation of the electron energy, while, in the longitudinal case, the dephasing rate $\gamma - p_z = \delta$ can be much larger than unity (see Fig. 4.9)

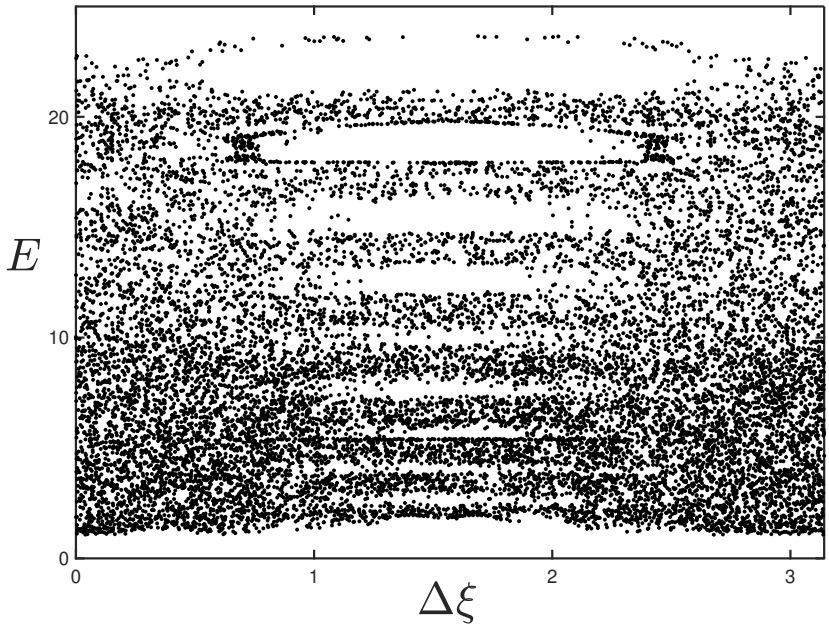

Figure 4.10: Poincaré mapping of electrons for the same parameters with Fig. 4.8 but $v_p = 1.01$.

such that the energy variation is much smaller.

Fig. 4.10 shows the numerical results for the same parameters with Fig. 4.8 but $v_p = 1.01$ to investigate the impact of the superluminal phase velocity. Compared with Fig. 4.8, it demonstrates that the superluminal phase velocity indeed weakens the stochastic acceleration, which agrees with the analyses. However, in contrast to the transverse electric field case, the impact of superluminal phase velocity on stochastic electron acceleration is relatively small. This agrees with the analyses, where the superluminal phase velocity significantly reduces the dephasing rate for electrons in the transverse field via $\gamma - P_z = C_\perp - U(y) + (v_p - 1)P_z$ and thus the electron interaction with the laser radiation, whereas in the longitudinal electric field case, it only introduces some modest oscillations in Eq. (4.48).

4.3 Electron in transverse electric and longitudinal magnetic fields

In this section, we will investigate the impact of a self-generated or externally applied longitudinal magnetic field on the electron dynamics studied in section 4.1. The problem of a free electron interacting with a laser propagating along a static homogeneous magnetic field has been treated before by several different authors [11, 96, 100, 101, 102, 103, 104]. It was shown that a matching condition between the electron gyro-frequency and the laser frequency can significantly facilitate the electron acceleration [11, 96]. Such matching condition usually requires a strong magnetic field (for example, for a laser pulse with wavelength $\lambda = 1\mu m$, the matching condition for an initially rest electron requires $10kT$ magnetic field), which implies that the potential for significant electron cyclotron resonance absorption is rather limited even though a pre-acceleration of electron or longitudinal electric field can relax the requirement [11]. However, the presence of the longitudinal magnetic field may significantly change the electron dynamics in the transverse electric field and thus should not be neglected. This will be studied in this section. Two cases will be considered: one is for a strong magnetic field such that the electron gyro-frequency in the magnetic field and laser frequency are approximately matched so that the electron dynamics will be dominated by the resonant acceleration due to the magnetic field, which will be modulated by the transverse electric field. The second case is for a weak magnetic field so that electrons will still undergo stochastic acceleration like in the transverse electric field only.

We assume that both the electrostatic potential, $U(y)$, and magnetic vector potential, $A_B(y)$, describing, respectively, the transverse electric and longitudinal magnetic fields, depend only on the coordinate y, while an arbitrarily polarized laser wave is denoted by the vector potential $\tilde{\vec{A}} = \tilde{A}_x(\xi)\vec{e}_x + \tilde{A}_y(\xi)\vec{e}_y$ with $\tilde{A}_x(\xi)$ and $\tilde{A}_y(\xi)$ being arbitrary functions of the variable

$\xi \equiv t - z/v_p$. As a result, the total QEM fields can be described by the vector potential

$$\vec{A} = \tilde{\vec{A}} - \vec{e}_y t \partial U(y)/\partial y + \vec{e}_x A_B(y), \tag{4.60}$$

where $\vec{E}_{stat.} \equiv \nabla U$ to denote an attractive potential well. Then, from Eqs. (4.2, 4.3), it is easy to show that there are two integrals of electron motion

$$\bar{P}_x \equiv P_x - \left(\tilde{A}_x + A_B\right),\ C_\perp \equiv \gamma - v_p P_z + U(y), \tag{4.61}$$

where $P_{x,z}$ are the (x,z)-components of electric momentum. Introducing the variable $\tilde{p}_y = P_y - \tilde{A}_y$, after some algebra similar to those in section 4.1, we obtain the Hamiltonian equations

$$\frac{d\tilde{p}_y}{d\xi} = -\frac{\partial H}{\partial y},\ \frac{dy}{d\xi} = \frac{\partial H}{\partial \tilde{p}_y}, \tag{4.62}$$

where

$$H(\tilde{p}_y, y, \xi) = \frac{v_p}{{v_p}^2 - 1}\left\{\sqrt{(U - C_\perp)^2 + ({v_p}^2 - 1)\,P_\perp^2} + v_p U - \frac{C_\perp}{v_p}\right\} \equiv \gamma + U = E, \tag{4.63}$$

and

$$P_\perp^2 = 1 + \left(\bar{P}_x + \tilde{A}_x + A_B\right)^2 + \left(\tilde{p}_y + \tilde{A}_y\right)^2. \tag{4.64}$$

For the luminal phase velocity $v_p \to 1$, the Hamiltonian in Eq. (4.63) becomes

$$H = \frac{1}{2}\left\{\frac{P_\perp^2}{C_\perp - U(y)} + U(y) + C_\perp\right\} = E = P_z + C_\perp, \tag{4.65}$$

As we can see, the longitudinal magnetic field doesn't affect the dephasing rate between the electron and the laser radiation. Therefore, the strongest interaction between the electron and the laser also occurs at local minimum of $\gamma - P_z = C_\perp - U(y) + (v_p - 1)P_z$. This demonstrates that

the location of the nonadiabatic interaction is determined by the quasi-static electric field, where the electron laser interaction is enhanced when U approaches $C_\perp$. Whereas the magnetic field has nothing to do with the determination of the nonadiabatic regions, provided that the gyro-motion of the electron in the magnetic field is isotropic in the transverse directions. Moreover, the superluminal phase velocity of laser radiation $v_p > 1$ will reduce the electron interaction with the laser radiation. Therefore, for simplicity, in the following, we consider the luminal case, $v_p = 1$, as well as $\bar{P}_x = 0$.

To specify static transverse electric and longitudinal magnetic fields, we take $U = \kappa y^2/2$ and $A_B = B_0 y$ where κ and B_0 are some constants (we take $\kappa > 0$ such that the electric field will force the electron towards the axis). This is equivalent to the setup of constant longitudinal magnetic field and electric field with linear dependence on the transverse coordinate. This choice of electric field is widely used in the ion channels, while the constant longitudinal magnetic field was used to study the resonantly matching acceleration (e.g., see Refs. [11, 97]). Taking into account the dephasing rate is positive, $\gamma - P_z = C_\perp - U(y) > 0$, such choice of electrostatic potential guarantees that $C_\perp > 0$. Moreover, we will use linearly polarized planar laser wave, i.e., either $\tilde{\vec{A}} = a_0 \sin(\xi)\vec{e}_y$ or $\tilde{\vec{A}} = a_0 \sin(\xi)\vec{e}_x$ where a_0 is the normalized amplitude of laser radiation.

We again consider first the electron trajectories neglecting an impact of the laser field, where the Hamiltonian in Eq. (4.65) is conserved. From Eq. (4.62) we find

$$y = \sqrt{2EC_\perp(\kappa E + B_0^2)^{-1}}\cos\theta,\ \tilde{p}_y = -\sqrt{2EC_\perp}\sin\theta, \tag{4.66}$$

where the angle θ is determined by

$$\frac{d\theta}{d\xi} = \frac{(\kappa E + B_0^2)^{3/2}}{(B_0^2 + \kappa E \sin^2\theta)C_\perp}. \tag{4.67}$$

Note that the unperturbed electron trajectory and thus θ is similar to that in Fig. 4.1 for $B_0 = 0$.

Integrating Eq. (4.67) one can find

$$\xi = \frac{C_\perp}{\left(\kappa E + B_0^2\right)^{3/2}} \left[B_0^2 \theta + \frac{2\theta - \sin(2\theta)}{4} \kappa E \right] + const.. \tag{4.68}$$

It follows that the period of unperturbed electron motion is $T = \xi(\theta = 2\pi) - \xi(\theta = 0)$ and thus the oscillating frequency, $\Omega = 2\pi/T$, reads

$$\Omega = \frac{\left(\kappa E + B_0^2\right)^{3/2}}{C_\perp} \left(B_0^2 + \frac{\kappa E}{2} \right)^{-1}, \tag{4.69}$$

which can also be obtained from $\Omega = \partial E/\partial I$, where $I = \oint \tilde{p}_y dy/2\pi = EC_\perp \left(\kappa E + B_0^2\right)^{-1/2}$ is the action of electron oscillation. However, an impact of laser wave on electron trajectory could be largely ignored, from Eq. (4.65), only for the energies $E > E_{pond} = a_0^2/2C_\perp$, where E_{pond} is considered as the ponderomotive energy scaling.

Recalling that according to our normalization convention, where the frequency Ω is normalized to the laser frequency, we conclude that there are two candidate mechanisms for efficient electron acceleration: One is the low harmonic resonance of the electron frequency Ω with the laser frequency [11, 97], $n\Omega = 1$ (where $n \tilde{>} 1$ is the integer number); while the second is the resonance broadening resulting in the overlapping of the resonances for $n \gg 1$ and thus causing stochastic electron heating. However, no matter which mechanism is active, the requirement of $\Omega \leq 1$ will limit the electron acceleration considering that at $\Omega > 1$, an impact of laser field becomes adiabatic. From Eq. (4.69) one can see that the inequality $\Omega > 1$ requires B_0, E or both of them are large. Especially, for

$$B_0 > C_\perp, \tag{4.70}$$

$\Omega > 1$ is true for all E, whereas for

$$E > E_{\max}^{abs} = C_{\perp}^2/4\kappa, \tag{4.71}$$

$\Omega > 1$ for all B_0. Therefore, $E_{\max}^{abs}$ could be considered as an absolute maximum energy that an electron can be gained via interaction with laser wave, and the small parameter $\varepsilon \equiv \sqrt{E_{pond}/E_{\max}^{abs}} = \sqrt{2}a_0\kappa^{1/2}C_{\perp}^{-3/2} < 1$ in Eq. (4.22) should be considered for electron being accelerated beyond the ponderomotive scaling.

From Eqs. (4.62, 4.65), the electron energy variations, $E(\xi) = \int^{\xi}(\partial H/\partial\xi)d\xi$, due to an impact of the laser radiation are

$$E_y(\xi) - E_y(\xi_{\max}) = \int_{\xi_{\max}}^{\xi} \frac{a_0(a_0\sin\xi + \tilde{p}_y)\cos\xi}{C_{\perp} - U(y)}d\xi, \tag{4.72}$$

and

$$E_x(\xi) - E_x(\xi_{\max}) = \int_{\xi_{\max}}^{\xi} \frac{a_0\left[a_0\sin\xi + A_B(y)\right]\cos\xi}{C_{\perp} - U(y)}d\xi, \tag{4.73}$$

for $\tilde{\vec{A}} = a_0\sin(\xi)\vec{e}_y$ and $\tilde{\vec{A}} = a_0\sin(\xi)\vec{e}_x$, respectively. In the following we will examine the electron dynamics in the aforementioned two regimes.

4.3.1 Low harmonics resonant acceleration

We first examine the electron dynamics for low-n resonance. If $\kappa = 0$, the resonant (matching) condition is given by $B_0 = C_{\perp}$, which, independent with electron energy, usually requires a strong longitudinal magnetic field for $C_{\perp} \sim 1$ (e.g., for laser wavelength of $\lambda = 1\mu m$, the matching condition is satisfied for $B_0 \sim 10kT$). Fortunately, the pre-acceleration of electron in the direction of laser propagating ($C_{\perp} < 1$) could relax this limitation [11]. However, in the presence of quasi-static electric field, the acceleration of electron will lead to the departure of

electron from the matching condition as seen from Eq. (4.69). If the electron is accelerated $\kappa E \gg B_0^2$, the further acceleration of the electron will be terminated. Therefore, to maximize the efficiency of electron acceleration, it is important that the frequency $\Omega = 1/n$ is dominated by the magnetic field and we will consider the case of $B_0^2 \gg \kappa E$ even for the possible maximum electron energy. As a result, we have $\Omega \approx B_0/C_\perp$, and thus the initial matching condition remains still great importance.

For the condition of $\Omega \sim 1$, the electron laser interaction could be effective along the whole electron orbit for $E > E_{pond}$ (the nonadibatic regions are not localized). Using the expansion of

$$e^{iz\sin\theta} = \sum_{m=-\infty}^{\infty} J_m(z) e^{im\theta}, \tag{4.74}$$

where $J_{-m}(z) = (-1)^m J_m(z)$ is the m-th Bessel function of the first kind [16], we obtain the energy variation in Eqs. (4.72, 4.73) as following:

$$\Delta E_y \approx \frac{\pi a_0 (EC_\perp)^{1/2}}{2^{1/2} B_0} \sum_m J_{m=(\Omega_B^{-1}\pm 1)/2}(\rho)\sin\xi_j + \frac{\pi a_0^2}{2B_0} \sum_m J_{m=\Omega_B^{-1}}(2\rho)\sin(2\xi_j), \tag{4.75}$$

$$\Delta E_x \approx \frac{\pi a_0 (EC_\perp)^{1/2}}{2^{1/2} B_0} \sum_m J_{m=(\Omega_B^{-1}\pm 1)/2}(\rho)\cos\xi_j + \frac{\pi a_0^2}{4B_0} \sum_m J_{m=\Omega_B^{-1}}(2\rho)\sin(2\xi_j), \tag{4.76}$$

where

$$\rho = (4\Omega_E)^{-1} \ll 1,\ \Omega_E = \frac{(\kappa E + B_0^2)^{3/2}}{C_\perp \kappa E} \gg 1,\ \Omega_B = \frac{(\kappa E + B_0^2)^{3/2}}{C_\perp B_0^2} \sim 1. \tag{4.77}$$

Considering the property of Bessel function as $\rho \to 0$, the efficient electron energy gain is only possible for $m = 0$ ($\Omega_B = 1$ and thus $C_\perp \approx B_0$ for considered $B_0^2 \gg \kappa E$), where the difference of the energy change due to the laser polarization has disappeared.

From Eqs. (4.75, 4.76) we see that $\Delta E \propto E^{1/2}$ and thus it will continuously increase to infinity if the transverse electric field disappears (the exact matching condition is true for all E). However, the presence of the transverse electric field, which induces a correction to the electron

frequency, $|\Delta\Omega| \approx \kappa E/B_0^2$, will set an upper limit to the resonant electron energy since after $m \simeq 1/|\Delta\Omega|$ circles of cyclotron motion the sign of the energy gain (due to $\sin\xi_j$ or $\cos\xi_j$) in Eqs. (4.75, 4.76) changes. Then the maximum of the electron energy for $\Omega_B = 1$ can be estimated as

$$E_{\max}^{\Omega_B=1} \approx \frac{\pi^2 a_0^2 C_\perp}{2^3 B_0^2} \times m^2, \tag{4.78}$$

Noticing that Ω depends on the electron energy, we can approximate m by using the averaged electron energy, $\bar{E} \approx E_{\max}^{\Omega_B=1}/2$, such that $m \approx B_0^2/2\kappa\bar{E}$. As a result, the maximum electron energy obtained from Eq. (4.78) reads

$$E_{\max}^{\Omega_B=1} \approx (2\pi)^{2/3} E_{\max}^{abs} \varepsilon^{2/3} = (2\pi)^{2/3} E_{pond} \varepsilon^{-4/3}, \tag{4.79}$$

It follows that, for the small parameter $\varepsilon \ll 1$, this resonant energy is smaller than $E_{\max}^{abs}$ but larger than the ponderomotive scaling.

To confirm the energy scaling in Eq. (4.79), we numerically integrate the Hamiltonian equations in Eqs. (4.62, 4.65), where the results are shown in Fig. 4.11. In the left, we show the logarithmic scaling of the maximum electron energy versus ε for different $B_0 = C_\perp$, a_0 and κ of initially rest electrons in the center of channel, i.e., $y = 0$ and $\tilde{p}_y = 0$, which is in great agreement with Eq. (4.79). In the middle, we show the impact of initial conditions on the evolution of electron energy, from which we see that the initial conditions have almost no effect on the energy gain but only shift the profile. The typical electron orbit in the phase space is sketched in the right figure.

4.3.2 High-n resonances and stochastic electron acceleration

In this section, we examine the case where $\Omega \ll 1$ (thus $\kappa E + B_0^2 \ll C_\perp^2$) and thus electron acceleration is possible via overlapping of high-n resonances (stochastic acceleration). One main characteristic of stochastic acceleration is that the Hamiltonian (electron energy) variation occurs

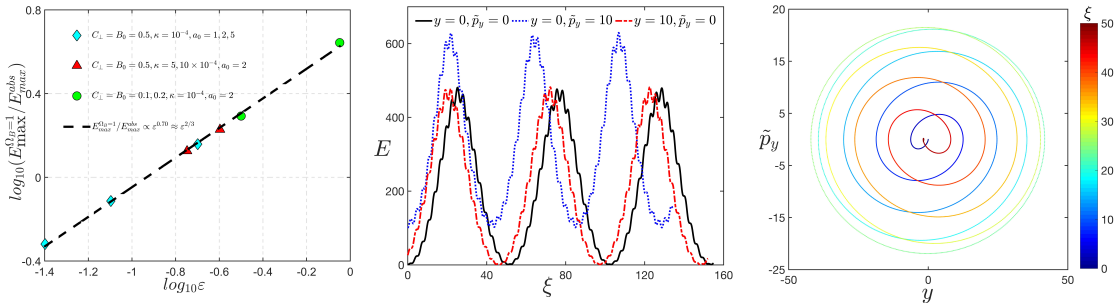

Figure 4.11: Left: Maximum electron energy scaling of low-n resonant acceleration with initial conditions $y = 0, \tilde{p}_y = 0$ and different parameters of $B_0 = C_\perp$, a_0, and κ; Middle: Evolution of E for $B_0 = C_\perp = 0.5$, $a_0 = 2$, $\kappa = 10^{-4}$ and different initial conditions $(y, \tilde{p}_y)$; Right: Schematic view of the electron trajectories for $B_0 = C_\perp = 0.5$, $a_0 = 2$, $\kappa = 10^{-4}$ and initial conditions $y = 0$, $\tilde{p}_y = 0$, where color bar shows the evolution of time.

only in a relatively short time compared with the electron oscillation period. From Eq. (4.65), such nonadiabatic interaction ("kick") takes place in the vicinity of $y = y_{min}$ and $y = y_{max}$. If we assume that the electron energy variation, ΔE, during single kick is small $|\Delta E| \ll E$ [23], the unperturbed electron trajectories in Eqs. (4.66, 4.67) can be applied to assess the electron energy change between two consecutive collisions in Eqs. (4.72, 4.73) yielding

$$\begin{aligned}\Delta E_y &= a_0\left(\frac{2EC_\perp}{\kappa E + B_0^2}\right)^{1/2}\sin\xi_j \int_{-\pi/2}^{\pi/2}\sin\theta\sin\left[\frac{\theta}{\Omega_B}+\frac{2\theta-\sin(2\theta)}{4\Omega_E}\right]d\theta \\ &+ \frac{a_0^2}{2(\kappa E+B_0^2)^{1/2}}\sin(2\xi_j)\int_{-\pi/2}^{\pi/2}\cos\left[\frac{2\theta}{\Omega_B}+\frac{2\theta-\sin(2\theta)}{2\Omega_E}\right]d\theta, \qquad (4.80)\end{aligned}$$

and

$$\begin{aligned}\Delta E_x &= a_0 B_0\frac{(2EC_\perp)^{1/2}}{\kappa E + B_0^2}\cos\xi_j \int_{-\pi/2}^{\pi/2}\cos\theta\cos\left[\frac{\theta}{\Omega_B}+\frac{2\theta-\sin(2\theta)}{4\Omega_E}\right]d\theta \\ &+ \frac{a_0^2}{2(\kappa E+B_0^2)^{1/2}}\sin(2\xi_j)\int_{-\pi/2}^{\pi/2}\cos\left[\frac{2\theta}{\Omega_B}+\frac{2\theta-\sin(2\theta)}{2\Omega_E}\right]d\theta, \qquad (4.81)\end{aligned}$$

where ξ_j is the "time" of previous "collision" .

In section 4.1, it was shown that the transverse electric filed itself leads to stochastic electron acceleration, depending on laser polarization, up to the energies

$$E^{y}_{\max}(B_0=0)\sim E^{abs}_{\max}\varepsilon^{6/7},\ E^{x}_{\max}(B_0=0)\sim E^{abs}_{\max}\varepsilon^{12/11}. \tag{4.82}$$

We note that for $\varepsilon \ll 1$ both of these energies are below $E^{abs}_{\max}$ and even smaller than $E^{\Omega_B=1}_{\max}$ in Eq. (4.79), but above the ponderomotive scaling. However, the presence of B_0 will change the electron dynamics.

Taking into account that $|\theta| \ll 1$ mostly contributes to the integrals in Eqs. (4.80, 4.81) under the condition of $\Omega \ll 1$, we can use Taylor expansion of the terms in the square brackets

$$\Omega_B^{-1}\theta+\Omega_E^{-1}\left[2\theta-\sin(2\theta)\right]/4\approx\Omega_B^{-1}\theta+\Omega_E^{-1}\theta^3/3, \tag{4.83}$$

and the integral limit can be extended to infinity. As a result, the integrals in Eqs. (4.80, 4.81) are degenerated to the Airy function $Ai(x)$ and its first derivative $Ai'(x)$, i.e.,

$$\Delta E_y\approx-2\pi a_0\left(\frac{2EC_\perp}{\kappa E+B_0^2}\right)^{1/2}\Omega_E^{2/3}\sin\xi_j Ai'(\eta)+\frac{2^{-1/3}\pi a_0^2\Omega_E^{1/3}}{\left(\kappa E+B_0^2\right)^{1/2}}\sin(2\xi_j)Ai\left(2^{2/3}\eta\right), \tag{4.84}$$

$$\Delta E_x=2\pi a_0 B_0\frac{\left(2EC_\perp\right)^{1/2}}{\kappa E+B_0^2}\Omega_E^{1/3}\cos\xi_j Ai(\eta)+\frac{2^{-1/3}\pi a_0^2\Omega_E^{1/3}}{\left(\kappa E+B_0^2\right)^{1/2}}\sin(2\xi_j)Ai\left(2^{2/3}\eta\right), \tag{4.85}$$

where $\eta\equiv\Omega_E^{1/3}\Omega_B^{-1}=B_0^2C_\perp^{2/3}(\kappa E)^{-4/3}/(1+B_0^2/\kappa E)$. We note that the results in Eqs. (4.84, 4.85) recover the results presented in section 4.1 for $B_0=0$. Considering the exponential decaying property of $Ai(x)$ and $Ai'(x)$ for $x>1$, we see that efficient electron energy gain occurs for $\eta\tilde{<}1$. Note that efficient stochastic acceleration requires the electron frequency strongly depending on electron energy and thus we consider the case of $B_0^2\ll\kappa E$ such that $\Omega\approx\Omega_E$.

We first consider the case where the laser radiation polarized in the y-direction. Ignoring

the differences induced by $Ai(\eta)$, $Ai'(\eta)$ and $Ai(2^{2/3}\eta)$ which are in the same order, the condition of $|\Delta E| \ll E$ and thus $E \gg E_{\max}^{abs}\varepsilon^{3/2} = E_{pond}\varepsilon^{-1/2}$ as seen from Eq. (4.84) guarantees that the first part on the right hand side (RHS) of Eq. (4.84) dominates and as a result, we obtain

$$\Delta E_y \approx -2^{7/3}\pi Ai'(\eta)\left(E_{\max}^{abs}\right)^{2/3}\varepsilon E^{1/3}\sin(\xi_j), \tag{4.86}$$

and $\eta \approx (B_0/C_\perp)^2(4E_{\max}^{abs}/E)^{4/3}$. The time interval between two consecutive kicks can be approximated by half the unperturbed electron period

$$\Delta\xi(E_{n+1}) \equiv \xi_{n+1} - \xi_n = \pi/\Omega(E_{n+1}) \approx \pi/\Omega_{E_{n+1}}, \tag{4.87}$$

for the condition $B_0^2 \ll \kappa E$. As a result, Eqs. (4.86, 4.87) can form a Chirikov-like mapping, from which the stochastic condition reads $K_y = |d\xi_{n+1}/d\xi_n - 1| = \left|d\Delta\xi/dE_{n+1}\cdot d\Delta E_y/d\xi_n\right| \tilde{>} 1$, where

$$K_y^B = k_y\left(E_{\max}^{abs}/E\right)^{7/6}\varepsilon > 1, \tag{4.88}$$

and $k_y = -2^{4/3}\pi^2 Ai'(\eta)$ is a numerical factor. It follows that the decaying of $Ai'(\eta)$ with the increase of B_0 will lead to a lower boundary for the stochastic electron energy to keep η small. The maximum energy is reduced from that without B_0 in Eq. (4.82) (e.g., see the blue filled region in Fig. 4.12, where the red curve corresponds to $K_y^B = 1$). If we ignore the numerical factor order of unity, then the stochastic electron motion approximately takes place in the energy region of $\left(B_0 C_\perp^{-1}\right)^{3/2} < E/4E_{\max}^{abs} < \varepsilon^{6/7}$ and, therefore, for $B_0 > B_{cri} \equiv C_\perp\varepsilon^{4/7}$ there is no room for stochasticity.

However, for the laser polarized in the x-direction, the first term on RHS of Eq. (4.85) is present due to the magnetic field. As a result, this part could slightly increase the energy gain during each kick and thus increase the maximum stochastic energy shown in Eq. (4.82) for $B_0 = 0$. One similar figure with Fig. 4.12 can be obtained for this case except that the approximately

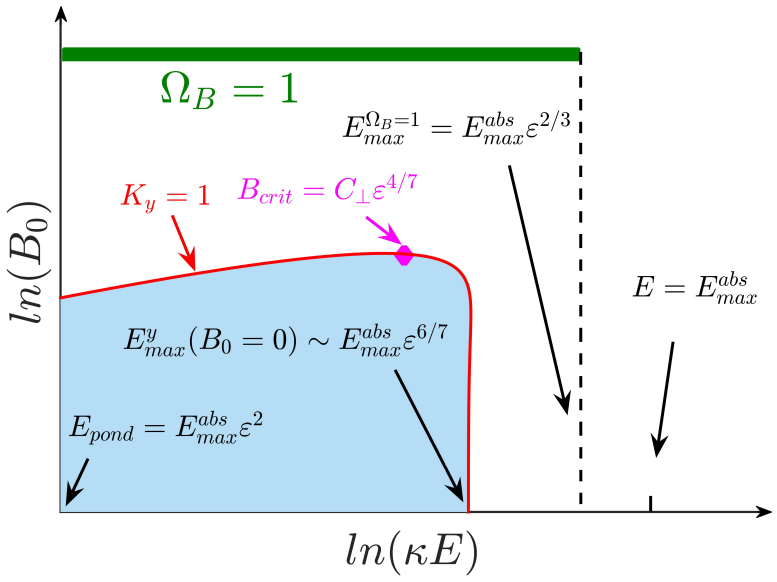

Figure 4.12: Schematic view of the electron acceleration via the overlapping of the resonances $n\Omega = 1$ for high-n (stochasticity in the blue filled region) for laser polarized along the static electric field and single low-n resonance of $\Omega_B = 1$ (green bar, where the width has no meaning, and it covers the energy $0 < E < E_{\max}^{\Omega_B=1}$) for both laser polarizations. The numerical factors order of unity for these maximum energies have been omitted.

vertical line along the maximum stochastic energy has a tiny curvature toward large E for proper B_0. For both cases, the maximum stochastic electron energies are smaller than that of the low-n resonant energy.

In order to check these analyses, we perform numerical simulations to solve the Hamiltonian equations and display the electron motion in the Poincaré mappings (E_n, ξ_n), where the quantities are picked from the center of the nonadiabatic regions as $\tilde{p}_y = 0$. Fig. 4.13 shows the results of electron in the laser wave polarized along the transverse electric for $a_0 = 1$, $\kappa = 10^{-5}$, $C_\perp = 1$ and longitudinal magnetic field with $B_0 = 0$ (left), $B_0 = 0.02$ (middle), and $B_0 = 0.04$ (right). From the middle figure we see that a lower stochastic energy boundary appears due to an impact of B_0, while the upper boundary remains almost unchanged compared with the case of $B_0 = 0$ in the left figure. However, for relatively large B_0 near the critical value, the upper boundary will be slightly decreased as shown in Fig. 4.12 and in the right plot of Fig. 4.13, where

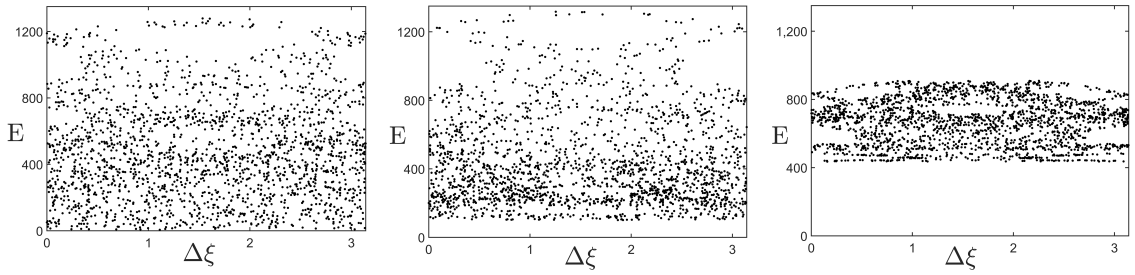

Figure 4.13: Poincaré mappings of electrons in the laser polarized along the transverse electric for $a_0 = 1$, $\kappa = 10^{-5}$, and $C_\perp = 1$, where $\Delta\xi \equiv \xi_n - m\pi$ and $m \equiv [\xi_n/\pi]$ is the largest integer that is smaller than ξ_n/π. Left: $B_0 = 0$; Middle: $B_0 = 0.02$; and Right: $B_0 = 0.04$.

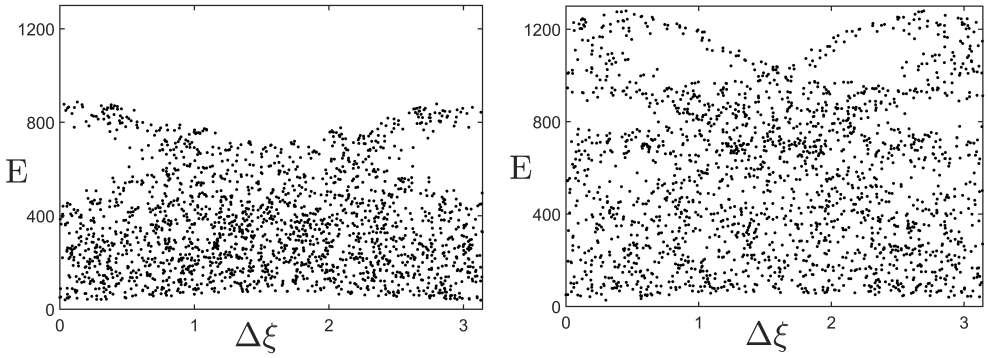

Figure 4.14: Poincaré mappings of electrons in the laser polarized across to the transverse electric for $a_0 = 8$, $\kappa = 10^{-4}$, $C_\perp = 1$, and $B_0 = 0$ (left) and $B_0 = 0.05$ (right).

the termination of the stochasticity occurs around the critical magnetic field of $B_{cri} \approx 0.04$ (in the simulations, we found that $B_0 = 0.04$ is just below the critical magnetic field and any small increase of B_0 will result in regular electron motion).

Shown in Fig. 4.14 are the results for the laser polarized along the x-direction with the parameters of $a_0 = 8$, $\kappa = 10^{-4}$, $B_0 = 0$ (left), and $B_0 = 0.05$ (right). We see a slight increase of the maximum stochastic energy for a proper B_0. For even stronger magnetic field, the electron Poincaré mappings are similar to those in Fig. 4.13. However, the difference between the stochastic electron motions due to the laser polarizations could be eliminated by adding relativistic momentum component of $\bar{P}_x \gg 1$.

4.4 Conclusion

The dynamics of electrons in the intense laser radiation and different configurations of QEM fields have been studied. For ultra-relativistic electrons, the laser radiation can be seen as a perturbation and thus the new Hamiltonian, which is the total electron energy, is time-independent without the perturbation. This property significantly simplifies the analysis of stochastic electron motion.

The Chirikov-like mappings are derived for electrons in all the cases, where the criterion for the onset of stochasticity is obtained. It is shown that for the linearly polarized laser radiation in the plane wave form, there exist upper limits of the electron energies gained from the stochastic acceleration, which will be increased by using large laser intensity but weak electric field strength.

We have found that the stochastic electron dynamics in the transverse electric field are quite different from those in the longitudinal one. In the first place, for the transverse case, the unperturbed electron oscillation frequency is increasing with the increase of the electron energy such that lower harmonics resonances are achieved for electron near the boundary of stability. It was shown that the maximum stochastic electron energy depends only on the ponderomotive scaling and a universal small parameter $\varepsilon = \sqrt{2}a_0\kappa_u^{1/2}C_\perp^{-2/3}$. The situation for electrons in the longitudinal electric field is different, where high harmonic resonances take place at large electron energy. Secondly, the roles played by the quasi-static electric field are different. The presence of the transverse electrostatic potential directly decreases the dephasing rate between the electron and laser radiation such that the strong electron laser interaction occurs when the electron climbs the potential well. However, the strong electron interaction with laser in the longitudinal electric field locates at the bottom of the electrostatic potential well and thus the longitudinal electric field seems to provide only the confinement which forces the electron to enter the nonadiabatic region multiple times. Moreover, the polarization of the laser is of great importance for electrons in the transverse electric field but not for those in the longitudinal electric field. In the Chirikov-like

mappings, the stability islands also behave differently as shown in Fig. 4.4 and 4.8.

The effects of transverse magnetic fields on the electron dynamics are discussed qualitatively. For electrons in the transverse electric field, $\kappa_u + \kappa_b$ plays the effective role of κ_u for the same dependence of $U(y)$ and $A_B(y)$. As a result, the quasi-static magnetic field can enhance, weaken, or terminate the stochastic electron motion depending on the sign and magnitude of κ_b. Whereas for electrons in the longitudinal electric field, the effect of the quasi-static magnetic field depends on the laser polarization direction, where the stochasticity of electron motion is always weakened by the magnetic field if the laser is polarized along the magnetic field, whereas, for laser polarized across to the magnetic field, the stochastic motion can also be enhanced for relatively large magnetic field.

However, in the presence of the longitudinal magnetic field, the electron dynamics in the transverse electric field are more complex. Two mechanisms of electron acceleration are examined, i.e., the stochastic acceleration when the magnetic field is weak, and the low-n resonant acceleration for a strong magnetic field. For both cases, the maximum electron energy can be well beyond the ponderomotive scaling for the small parameter ε. In the stochastic acceleration regime, the presence of a weak longitudinal magnetic field would slightly reduce the maximum stochastic energy for the electron in the laser polarized along the static electric field, whereas for the laser across to the electric field, it can also slightly increases the maximum energy. The magnetic field also sets a lower boundary of the stochastic electron energy such that the stochasticity will be terminated when the lower boundary meets the upper one (magnetic field exceeds a critical value $B_{crit} \sim C_\perp \varepsilon^{4/7}$). In the low-$n$ resonant acceleration regime, the efficient electron acceleration is only possible via the first harmonic resonance of $\Omega \approx \Omega_B \approx 1$. The maximum resonant energy, regardless of the laser polarization, is above the maximum stochastic energy.

Numerical simulations directly solving the Hamiltonian equations are performed, which confirmed all the analytic results. We should note that the stochastic acceleration requires high harmonic resonances, $\Omega \ll 1$. As a result, the electron motion in the QEM fields takes a few

laser periods to complete one oscillation so that the stochastic acceleration will lead to a slow electron energy growth. For large stochastic parameter $K \gg 1$, the electron acceleration in the energy space is characterized by a slower diffusion, where the averaged energy of an ensemble of electrons with different initial conditions has a powerful time dependence. The diffusive "kicks" of electron energy in the simulations indicate a highly stochastic motion of the electrons.

The work presented in this chapter is a reprint of the materials as they appear in *Stochastic electron heating in the laser and quasi-static electric and magnetic fields* in Physics of Plasmas 25, 123110, by Y. Zhang, S. Krasheninnikov, and A. Knyazev, 2018; and in *Electron dynamics in laser and quasi-static transverse electric and longitudinal magnetic fields* in Plasma Physics and Controlled Fusion 61, 074008, by Y. Zhang and S. Krasheninnikov, 2019. The dissertation author was the primary investigator and author of this paper.

Chapter 5

Summary

The main objective of this thesis is to understand the electron dynamics in the laser-plasma interactions, paying special attention to the stochastic electron acceleration in different configurations of laser pulses and quasi-static EM fields. This was conducted through analytical work and numerical solution methods. More specifically, the electron dynamics in counter-propagating laser beams, in laser radiation and periodic quasi-static EM fields, and in laser and different confining quasi-static EM fields are investigated.

The main idea is to find the proper canonical variables so that the new Hamiltonian describing the electron dynamics is time-independent in the absence of an appropriate perturbation. The perturbation and thus the new Hamiltonian, as well as the canonical variables, are different for different cases. For electrons in the counter-propagating lasers, the perturbation can be taken as the weaker laser wave so that the new Hamiltonian is the dephasing rate between the electron with the dominant laser. The same Hamiltonian is used for the electron in the laser and periodic quasi-static EM fields, where the latter can be treated as the perturbations. However, for electrons in the laser and confining quasi-static EM fields, the laser is chosen as a perturbative field for the relativistic electrons so that the Hamiltonian is the total electron energy (the sum of the kinetic energy and potential energy in the quasi-static electric field).

The new Hamiltonian method can significantly simplify the analysis of electron dynamics and thus help us clearly reveal the physics underlying the stochastic electron acceleration. In all the cases, the Chirikov-like mappings are derived, from which the conditions for the onset of stochastic motion are obtained. For electrons in the counter-propagating lasers and in the laser and periodic quasi-static EM fields, the stochastic conditions require the amplitudes of the perturbative fields to exceed some thresholds as functions of the normalized (dominant) laser amplitude. The stochastic acceleration occurs in a region in the Hamiltonian space, where the maximum electron energy usually corresponds to the lower boundary of the stochastic region. However, for electrons in the laser and confining quasi-static EM fields, the stochastic conditions set some upper limits of the electron energy, where, for the transverse electric field, such limit depends only on a universal parameter and the amplitude of the laser wave. The analyses show that the maximum electron energy gained from the stochastic motion can significantly exceed the ponderomotive scaling energy of the (dominant) laser. Moreover, in all the cases, the strongest impact of the perturbative field on the electron trajectories occurs at the small dephasing rate between the electron and the perturbative field, which is the denominator of the new Hamiltonian.

For electrons in the counter-propagating lasers, the relative polarization directions of the lasers are important, where the threshold for stochasticity (and the maximum energy) is smaller (larger) for the lasers being parallel polarized than that for the lasers being polarized orthogonally. The maximum electron kinetic energy can exceed the ponderomotive scaling when the dominant laser is relativistic (when the lasers have comparable wavelengths), where the lower boundary of the stochastic region in the Hamiltonian space and thus the maximum electron energy has a weak dependence on the amplitude of the perturbative laser above the threshold for stochasticity. It shows that the perturbative laser only stochastically changes the dephasing rate between the electron and the dominant laser (the new Hamiltonian) and thus enable net energy exchange. The periodic quasi-static EM fields play a similar role to that of a counter-propagating perturbative laser wave.

However, the confining quasi-static EM fields play a different role in the electron dynamics, where the fields confine the electron motion and thus offer an oscillating frequency to resonate with the laser frequency. Specifically, the transverse electrostatic potential can directly decrease the dephasing rate between electron and laser radiation such that the strong electron laser interaction occurs when the electron climbs the potential well, whereas the longitudinal electric field seems to provide only the confinement which forces the electron to enter the nonadiabatic region (the bottom of the electrostatic potential well) multiple times. Moreover, the polarization of the laser is of great importance for the electron in the transverse electric field, where the electron can obtain higher energy for the laser polarized along the electric field than that for the laser polarized across to the electric field.

The impacts of the superluminal phase velocity on the stochastic electron dynamics are qualitatively discussed, which can reduce the possible maximum electron energy. All these analytical results are confirmed by the numerical simulations, which directly solve the Hamiltonian equations.

Appendix A

Impacts of $\bar{P}_x$ and $\bar{P}_y$ on the stochastic condition in colliding lasers

Here we consider the impacts of $\bar{P}_x$ and $\bar{P}_y$ on the stochastic condition of electrons in colliding laser beams. Here we consider only the case of lasers with the same polarization direction. Including $\bar{P}_y \neq 0$, a similar result with Eq. (2.15) could be found

$$K_x \equiv \left| \frac{d\Delta\psi_n}{dH_{n+1}} \frac{d\Delta H_n}{d\psi_n} \right| = \frac{4\pi^2 a a_1 \left[2(1+\bar{P}_y^2)+a^2\right] \beta^2 |Ai'(\beta)|}{(1+\bar{P}_y^2)^2} \tilde{>} 1. \tag{A.1}$$

It follows that the presence of $\bar{P}_y$ only provides a factor less than unity and, therefore, will increase the threshold of a_1 ($K_x \approx 1$) for triggering stochastic motion, whereas it doesn't change the basic features of stochastic electron dynamics. This is because $\bar{P}_y$ simply increases the effective electron mass.

However, an impact of $\bar{P}_x$ on the stochastic condition is more complex providing that it not only changes the effective electron mass but also increases the energy exchange between electron and laser through the work done by the laser electric field in x-direction. Considering that the time interval from η_1 to η_2 is different from that from η_2 to next η_1 for $0 < |\bar{P}_x| < a$ (e.g., see Fig. 2.1), the method of Chirikov-like mapping to find the stochastic condition is not convenient, but we

could resort to the method of island overlapping. For this purpose, the unperturbed electron motion can be expressed by using the action-angle variables (I and θ):

$$I = -\frac{2\bar{P}^2 + a^2}{2H_0}\,, \text{and } \theta = \hat{\eta} - \frac{a^2 sin(2\hat{\eta})}{2(2\bar{P}^2 + a^2)} - \frac{4a\bar{P}_x\,[cos(\hat{\eta}) - 1]}{2\bar{P}^2 + a^2}, \tag{A.2}$$

where $\hat{\eta} = \eta - 2n\pi$ and the electron oscillating frequency in Eq. (2.9) can be written in terms of I as $\omega(I) = (2\bar{P}^2 + a^2)/2I^2$. Given that the electron motion is periodic with θ, we can expand the first order correction to H in Eq. (2.5) in Fourier series:

$$H_1 = 2a_1\,[asin(\eta) + \bar{P}_x]\,sin(k_1\xi)/\chi = \sum_{m,n} V_{mn}(I) e^{i(m\theta - nk_1\xi)} + c.c., \tag{A.3}$$

and $n = \pm 1$ as seen from Eq. (2.5). As a result, the resonance, corresponding to a constant phase of the perturbation, occurs at $\omega(I) = nk_1/m$.

The Fourier coefficients V_{mn} in Eq. (A.3) are given by

$$V_{mn} = \frac{k_2}{(2\pi)^2} \int_0^{2\pi/k_2} \int_0^{2\pi} H_1(I, \theta, \xi) e^{-i(m\theta - nk_2\xi)} d\theta d\xi. \tag{A.4}$$

After some algebra, we arrive at

$$|V_{mn}| = \frac{a}{2I} e^{-imC} \sum_{h=0,\pm 1} \left[ha + 2\delta_h^0 \bar{P}_x\right] C_{m-h}\left[\frac{ma^2}{2(2\bar{P}^2 + a^2)}, \frac{4ma\bar{P}_x}{2\bar{P}^2 + a^2}\right], \tag{A.5}$$

where

$$C_N(\alpha, \beta) = \sum_{q=-\infty}^{\infty} J_q(\alpha) J_{N-2q}(\beta) i^{N-2q}, \tag{A.6}$$

is the generalized Bessel function [62, 105], $C = 4a\bar{P}_x/(2\bar{P}^2 + a^2)$, and δ_i^j is the Kronecker symbols. Notice that similar result for V_{mn} was obtained in [62] by using multidimensional Hamiltonian methods.

The width of the island is approximated [4] as

$$\delta\omega = 4\left|2V_{mn}\frac{d\omega}{dI}\right|^{1/2}, \tag{A.7}$$

whereas the spacing between possibly overlapping resonances is

$$\Delta\omega = |\omega(I_{m'}) - \omega(I_m)| \approx \omega^2/k_1, \tag{A.8}$$

for $|m| \gg 1$. Then the stochastic condition reads

$$\bar{K}^2 = a_1\frac{16m^2}{(2\bar{P}^2+a^2)}\sum_{h=0,\pm1}\left[ha + 2\delta_h^0\bar{P}_x\right]C_{m-h}\left[\frac{ma^2}{2(2\bar{P}^2+a^2)}, \frac{4ma\bar{P}_x}{2\bar{P}^2+a^2}\right] > 1, \tag{A.9}$$

where $m \equiv k_1/\omega$ is the resonant harmonics, δ_i^j is the Kronecker symbols, and $C_N(\alpha,\beta)$ is the generalized Bessel function [62, 105]. Notice that similar results were obtained in [62, 60] by using multidimensional Hamiltonian methods. For $\bar{P}_x = 0$, one can show that $K_x \approx \bar{K}^2$.

Then, we can define $\bar{K}^2 \equiv a_1 g(m)$, where $g(m)$ shows how $\bar{K}^2$ varies with different m and thus H (e.g., see Fig. A.1). As a result, the threshold of stochastic instability requires $a_1 > (max\{g(m)\})^{-1}$. As we can see from Fig. A.1, for $|\bar{P}_x| \tilde{<} a$, the maximum value of $g(m)$ increases with the presence of $\bar{P}_x$ and thus the threshold value obtained in Eq. (2.18) for $\bar{P}_x = 0$ decreases. Whereas for $|\bar{P}_x| \gg a$, the peak of $g(m)$ decreases with increasing $|\bar{P}_x|$, which is eventually smaller than that for $\bar{P}_x = 0$ meaning that the effect of increasing the effective electron mass becomes dominant. Notice that there could be multiple stochastic peaks for $|\bar{P}_x| \tilde{<} a$ and from Eq. (A.9) the result is symmetric with respect to $\bar{P}_x = 0$. On the other hand, we notice that both the lower and upper stochastic boundaries in H ($g \sim 1/a_1$) shifts toward larger H. Therefore, the ratio of the maximum electron kinetic energy gained from stochasticity over the ponderomotive scaling, H_0/H^x_{min} for $k_1 \sim 1$, will decrease with the presence of $\bar{P}_x$.

To verify the results of our analytical considerations, we integrate Eqs. (2.3, 2.5) numer-

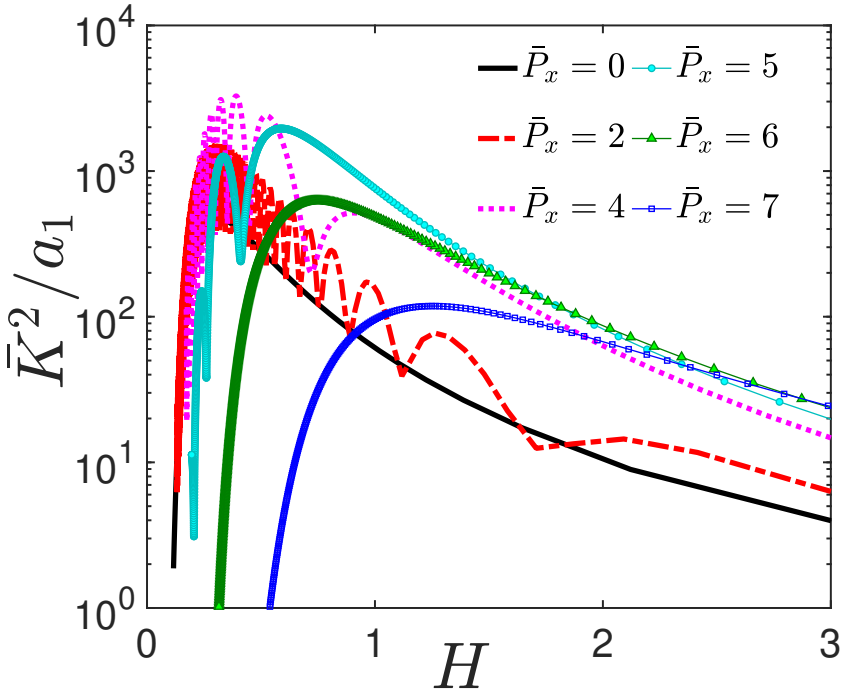

Figure A.1: Schematic view of $g\,[m(H)] = \bar{K}^2/a_1$ versus H for different $\bar{P}_x$, where $a = 5$, $k_1 = 1$, and $\bar{P}_y = 0$.

ically and present the results in the Poincaré maps of (H, ψ) or (γ, ψ), when $\eta = 2n\pi + \pi/2$, where χ and thus $\gamma = (\chi + H)/2$ reaches their maximum in one unperturbed electron period (here we use $\bar{P}_{x,y} \geq 0$). Notice that even though for $\bar{P}_x = 0$ the unperturbed period is $\Delta\eta = \pi$, we use $\Delta\eta = 2\pi$ instead in all the mappings considering the general case with $\bar{P}_x$).

Shown in Fig. A.2 are the results for counter-propagating lasers with same polarization directions, where the parameters are $a = 5$, $k_1 = 1$, and different $\bar{P}_{x,y}$ and a_1. As one can see, a stochastic "sea" is bounded by the KAM invariant [56] at H^x_{min} and H^x_{max}, which fully agree with Eqs. (2.20, 2.21) for $\bar{P}_x = \bar{P}_y = 0$. As seen from Figs. A.2(a) and A.2(b), the presence of $\bar{P}_y$ increases the lower boundary of the stochastic region and thus decreases the energy gain ratio. Comparing Fig. A.2(a) with Fig. A.2(c) where a_1 is different, we confirm that H^x_{min} has a weak dependence on a_1 being above the threshold value a^x_s. From Fig. A.2(c) and A.2(d), we see that both the lower and upper boundaries of the stochastic region become lager (while the corresponding maximum electron kinetic energy gain ratio becomes smaller) with the presence of

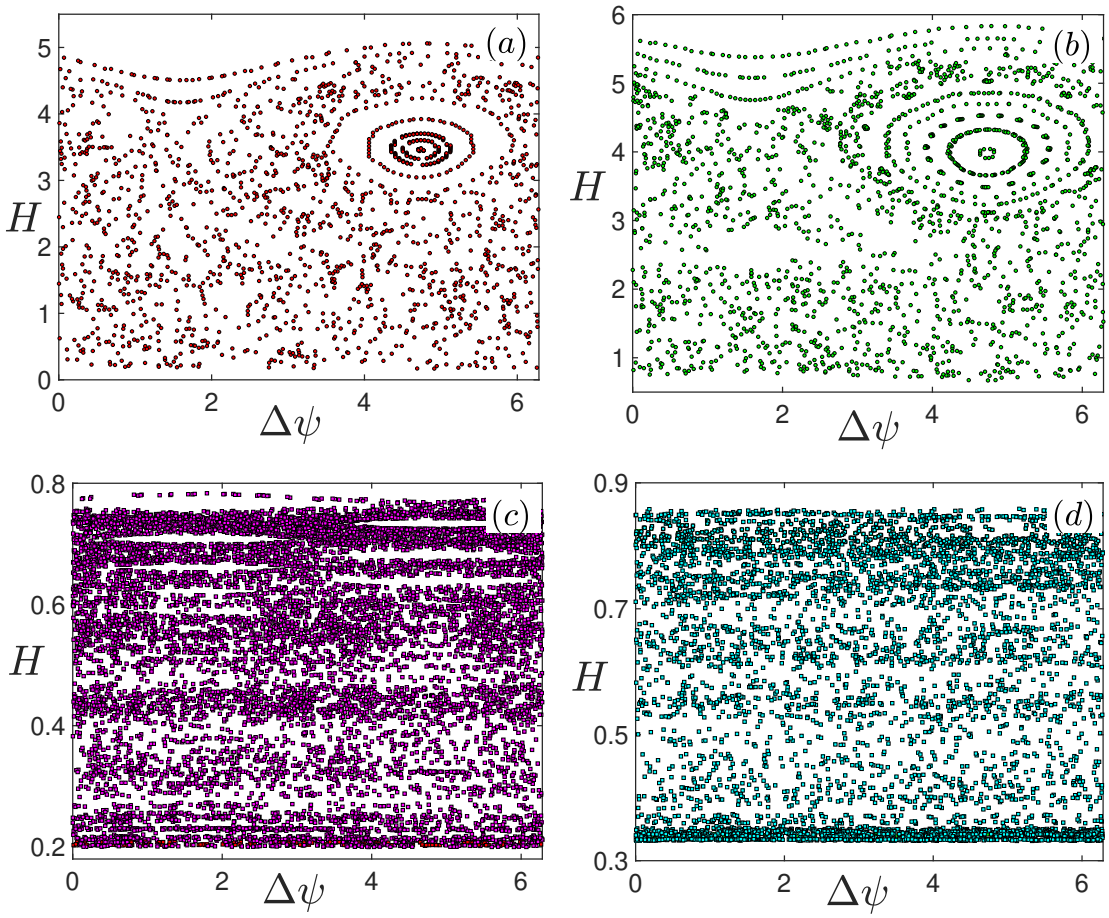

Figure A.2: Poincaré mappings of $(H,\ \psi)$ at $\eta = 2n\pi + \pi/2$ for $a = 5$, $\mathbf{A}_1 = a_1 sin(\tau)\mathbf{e}_x$ and different a_1, $\bar{P}_{x,y}$, where $\Delta\psi \equiv \psi - [\psi/2\pi] \times 2\pi$. (a) $a_1 = 0.2$, $\bar{P}_x = 0$ and $\bar{P}_y = 0$; (b) $a_1 = 0.2$, $\bar{P}_x = 0$ and $\bar{P}_y = 2$; (c) $a_1 = 0.005$, $\bar{P}_x = 0$ and $\bar{P}_y = 0$; (d) $a_1 = 0.005$, $\bar{P}_x = 5$ and $\bar{P}_y = 0$.

$|\bar{P}_x| > 0$, which agrees with the prediction from Fig. A.1.

Bibliography

[1] G. Mourou and D. Umstadter, "Development and applications of compact high-intensity lasers," *Physics of Fluids B: Plasma Physics*, vol. 4, no. 7, pp. 2315–2325, 1992.

[2] M. Rosenbluth and C. Liu, "Excitation of plasma waves by two laser beams," *Physical Review Letters*, vol. 29, no. 11, p. 701, 1972.

[3] T. Tajima and J. M. Dawson, "Laser electron accelerator," *Physical Review Letters*, vol. 43, no. 4, p. 267, 1979.

[4] A. B. Rechester and T. H. Stix, "Stochastic instability of a nonlinear oscillator," *Physical Review A*, vol. 19, no. 4, p. 1656, 1979.

[5] C. Menyuk, A. Drobot, K. Papadopoulos, and H. Karimabadi, "Stochastic electron acceleration in obliquely propagating electromagnetic waves," *Physical review letters*, vol. 58, no. 20, p. 2071, 1987.

[6] D. Bauer, P. Mulser, and W.-H. Steeb, "Relativistic ponderomotive force, uphill acceleration, and transition to chaos," *Physical review letters*, vol. 75, no. 25, p. 4622, 1995.

[7] S. P. Mangles, B. Walton, M. Tzoufras, Z. Najmudin, R. Clarke, A. E. Dangor, R. Evans, S. Fritzler, A. Gopal, C. Hernandez-Gomez, *et al.*, "Electron acceleration in cavitated channels formed by a petawatt laser in low-density plasma," *Physical Review Letters*, vol. 94, no. 24, p. 245001, 2005.

[8] M. Tanimoto, S. Kato, E. Miura, N. Saito, K. Koyama, and J. K. Koga, "Direct electron acceleration by stochastic laser fields in the presence of self-generated magnetic fields," *Physical Review E*, vol. 68, no. 2, p. 026401, 2003.

[9] J. Angus and S. Krasheninnikov, "Energy gain of free electron in pulsed electromagnetic plane wave with constant external magnetic fields," *Physics of Plasmas*, vol. 16, no. 11, p. 113103, 2009.

[10] A. V. Arefiev, V. N. Khudik, and M. Schollmeier, "Enhancement of laser-driven electron acceleration in an ion channel," *Physics of Plasmas*, vol. 21, no. 3, p. 033104, 2014.

[11] A. Arefiev, A. Robinson, and V. Khudik, "Novel aspects of direct laser acceleration of relativistic electrons," *Journal of Plasma Physics*, vol. 81, no. 4, 2015.

[12] A. V. Arefiev, V. N. Khudik, A. P. L. Robinson, G. Shvets, L. Willingale, and M. Schollmeier, "Beyond the ponderomotive limit: Direct laser acceleration of relativistic electrons in sub-critical plasmas," *Physics of Plasmas*, vol. 23, no. 5, p. 056704, 2016.

[13] V. N. Khudik, X. Zhang, T. Wang, and G. Shvets, "Far-field constant-gradient laser accelerator of electrons in an ion channel," *Physics of Plasmas*, vol. 25, no. 8, p. 083101, 2018.

[14] A. Pukhov and J. Meyer-ter Vehn, "Laser wake field acceleration: the highly non-linear broken-wave regime," *Applied Physics B*, vol. 74, no. 4-5, pp. 355–361, 2002.

[15] B. Paradkar, M. Wei, T. Yabuuchi, R. Stephens, M. Haines, S. Krasheninnikov, and F. Beg, "Numerical modeling of fast electron generation in the presence of preformed plasma in laser-matter interaction at relativistic intensities," *Physical Review E*, vol. 83, no. 4, p. 046401, 2011.

[16] L. D. Landau and E. M. Lifshitz, *The Classical Theory of Fields, V. 2, Course of Theoretical Physics*. Elsevier, 2009.

[17] E. Esarey, C. Schroeder, and W. Leemans, "Physics of laser-driven plasma-based electron accelerators," *Reviews of modern physics*, vol. 81, no. 3, p. 1229, 2009.

[18] G. Tsakiris, C. Gahn, and V. Tripathi, "Laser induced electron acceleration in the presence of static electric and magnetic fields in a plasma," *Physics of Plasmas*, vol. 7, no. 7, pp. 3017–3030, 2000.

[19] D. Forslund, J. Kindel, W. Mori, C. Joshi, and J. Dawson, "Two-dimensional simulations of single-frequency and beat-wave laser-plasma heating," *Physical review letters*, vol. 54, no. 6, p. 558, 1985.

[20] C. Gahn, G. Tsakiris, A. Pukhov, J. Meyer-ter Vehn, G. Pretzler, P. Thirolf, D. Habs, and K. Witte, "Multi-mev electron beam generation by direct laser acceleration in high-density plasma channels," *Physical Review Letters*, vol. 83, no. 23, p. 4772, 1999.

[21] A. Pukhov, Z.-M. Sheng, and J. Meyer-ter Vehn, "Particle acceleration in relativistic laser channels," *Physics of Plasmas*, vol. 6, no. 7, pp. 2847–2854, 1999.

[22] A. V. Arefiev, B. N. Breizman, M. Schollmeier, and V. N. Khudik, "Parametric amplification of laser-driven electron acceleration in underdense plasma," *Physical review letters*, vol. 108, no. 14, p. 145004, 2012.

[23] G. Zaslavskii, M. Y. Natenzon, B. Petrovichev, R. Sagdeev, and A. Chernikov, "Stochastic acceleration of relativistic particles in a magnetic field," *Sov. Phys. JETP*, vol. 66, pp. 496–503, 1987.

[24] J. Mendonca and F. Doveil, "Stochasticity in plasmas with electromagnetic waves," *Journal of Plasma Physics*, vol. 28, no. 3, pp. 485–493, 1982.

[25] B. Paradkar, S. Krasheninnikov, and F. Beg, "Mechanism of heating of pre-formed plasma electrons in relativistic laser-matter interaction," *Physics of Plasmas*, vol. 19, no. 6, p. 060703, 2012.

[26] S. Krasheninnikov, "On stochastic heating of electrons by intense laser radiation in the presence of electrostatic potential well," *Physics of Plasmas*, vol. 21, no. 10, p. 104510, 2014.

[27] Y. Zhang and S. Krasheninnikov, "Electron heating in the laser and static electric and magnetic fields," *Physics of Plasmas*, vol. 25, no. 1, p. 013120, 2018.

[28] Y. Zhang and S. Krasheninnikov, "Electron dynamics in the laser and quasi-static electric and magnetic fields," *Physics Letters A*, vol. 382, no. 27, pp. 1801–1806, 2018.

[29] V. Khudik, A. Arefiev, X. Zhang, and G. Shvets, "Universal scalings for laser acceleration of electrons in ion channels," *Physics of Plasmas*, vol. 23, no. 10, p. 103108, 2016.

[30] W. Kruer, *The physics of laser plasma interactions*. CRC Press, 2018.

[31] S. Wilks, W. Kruer, M. Tabak, and A. Langdon, "Absorption of ultra-intense laser pulses," *Physical review letters*, vol. 69, no. 9, p. 1383, 1992.

[32] A. Kemp and L. Divol, "Interaction physics of multipicosecond petawatt laser pulses with overdense plasma," *Physical review letters*, vol. 109, no. 19, p. 195005, 2012.

[33] S. Kneip, C. McGuffey, S. Nagel, C. Palmer, C. Bellei, J. Schreiber, C. Huntington, F. Dollar, T. Matsuoka, V. Chvykov, *et al.*, "Comparative study of betatron radiation from laser-wakefield and direct-laser accelerated bunches of relativistic electrons," in *Harnessing Relativistic Plasma Waves as Novel Radiation Sources from Terahertz to X-Rays and Beyond*, vol. 7359, p. 73590T, International Society for Optics and Photonics, 2009.

[34] B. Walton, S. Mangles, Z. Najmudin, M. Tatarakis, M. Wei, A. Gopal, C. Marle, A. Dangor, K. Krushelnick, S. Fritzler, *et al.*, "Measurements of forward scattered laser radiation from intense sub-ps laser interactions with underdense plasmas," *Physics of plasmas*, vol. 13, no. 11, p. 113103, 2006.

[35] K. Wharton, C. Boley, A. Komashko, A. Rubenchik, J. Zweiback, J. Crane, G. Hays, T. Cowan, and T. Ditmire, "Effects of nonionizing prepulses in high-intensity laser-solid interactions," *Physical Review E*, vol. 64, no. 2, p. 025401, 2001.

[36] T. Yabuuchi, B. Paradkar, M. Wei, J. King, F. Beg, R. Stephens, N. Nakanii, M. Hatakeyama, H. Habara, K. Mima, *et al.*, "Transport study of intense-laser-produced fast electrons in solid targets with a preplasma created by a long pulse laser," *Physics of Plasmas*, vol. 17, no. 6, p. 060704, 2010.

[37] A. MacPhee, L. Divol, A. Kemp, K. Akli, F. Beg, C. Chen, H. Chen, D. Hey, R. Fedosejevs, R. Freeman, *et al.*, "Limitation on prepulse level for cone-guided fast-ignition inertial confinement fusion," *Physical review letters*, vol. 104, no. 5, p. 055002, 2010.

[38] S. Baton, M. Koenig, J. Fuchs, A. Benuzzi-Mounaix, P. Guillou, B. Loupias, T. Vinci, L. Gremillet, C. Rousseaux, M. Drouin, *et al.*, "Inhibition of fast electron energy deposition due to preplasma filling of cone-attached targets," *Physics of Plasmas*, vol. 15, no. 4, p. 042706, 2008.

[39] L. Van Woerkom, K. Akli, T. Bartal, F. Beg, S. Chawla, C. Chen, E. Chowdhury, R. Freeman, D. Hey, M. Key, *et al.*, "Fast electron generation in cones with ultraintense laser pulses," *Physics of Plasmas*, vol. 15, no. 5, p. 056304, 2008.

[40] R. Wagner, S.-Y. Chen, A. Maksimchuk, and D. Umstadter, "Electron acceleration by a laser wakefield in a relativistically self-guided channel," *Physical Review Letters*, vol. 78, no. 16, p. 3125, 1997.

[41] M. Santala, Z. Najmudin, E. Clark, M. Tatarakis, K. Krushelnick, A. Dangor, V. Malka, J. Faure, R. Allott, and R. Clarke, "Observation of a hot high-current electron beam from a self-modulated laser wakefield accelerator," *Physical review letters*, vol. 86, no. 7, p. 1227, 2001.

[42] C. Geddes, C. Toth, J. Van Tilborg, E. Esarey, C. Schroeder, D. Bruhwiler, C. Nieter, J. Cary, and W. Leemans, "High-quality electron beams from a laser wakefield accelerator using plasma-channel guiding," *Nature*, vol. 431, no. 7008, p. 538, 2004.

[43] L. Willingale, A. Thomas, P. Nilson, H. Chen, J. Cobble, R. Craxton, A. Maksimchuk, P. Norreys, T. Sangster, R. Scott, *et al.*, "Surface waves and electron acceleration from high-power, kilojoule-class laser interactions with underdense plasma," *New Journal of Physics*, vol. 15, no. 2, p. 025023, 2013.

[44] Y. Zhang and S. Krasheninnikov, "Electron dynamics in laser and quasi-static transverse electric and longitudinal magnetic fields," *Plasma Physics and Controlled Fusion*, vol. 61, no. 7, p. 074008, 2019.

[45] A. Bourdier, D. Patin, and E. Lefebvre, "Stochastic heating in ultra high intensity laser-plasma interaction," *Physica D: Nonlinear Phenomena*, vol. 206, no. 1-2, pp. 1–31, 2005.

[46] J. Mendonca, "Threshold for electron heating by two electromagnetic waves," *Physical Review A*, vol. 28, no. 6, p. 3592, 1983.

[47] Z.-M. Sheng, K. Mima, Y. Sentoku, M. Jovanović, T. Taguchi, J. Zhang, and J. Meyer-ter Vehn, "Stochastic heating and acceleration of electrons in colliding laser fields in plasma," *Physical review letters*, vol. 88, no. 5, p. 055004, 2002.

[48] J. Meyer-ter Vehn and Z. M. Sheng, "On electron acceleration by intense laser pulses in the presence of a stochastic field," *Physics of Plasmas*, vol. 6, no. 3, pp. 641–644, 1999.

[49] V. L. Ginzburg, "The propagation of electromagnetic waves in plasmas," *International Series of Monographs in Electromagnetic Waves, Oxford: Pergamon, 1970, 2nd rev. and enl. ed.*, 1970.

[50] F. Brunel, "Not-so-resonant, resonant absorption," *Physical Review Letters*, vol. 59, no. 1, p. 52, 1987.

[51] E. S. Weibel, "Anomalous skin effect in a plasma," *The Physics of Fluids*, vol. 10, no. 4, pp. 741–748, 1967.

[52] P. Catto and R. M. More, "Sheath inverse bremsstrahlung in laser produced plasmas," *Physics of Fluids*, vol. 20, p. 704, 1977.

[53] W. Kruer and K. Estabrook, "J× b heating by very intense laser light," *The Physics of fluids*, vol. 28, no. 1, pp. 430–432, 1985.

[54] J. Shaw, F. Tsung, N. Vafaei-Najafabadi, K. Marsh, N. Lemos, W. Mori, and C. Joshi, "Role of direct laser acceleration in energy gained by electrons in a laser wakefield accelerator with ionization injection," *Plasma physics and controlled fusion*, vol. 56, no. 8, p. 084006, 2014.

[55] X. Zhang, V. N. Khudik, and G. Shvets, "Synergistic laser-wakefield and direct-laser acceleration in the plasma-bubble regime," *Physical review letters*, vol. 114, no. 18, p. 184801, 2015.

[56] R. Z. Sagdeev, D. Usikov, and G. M. Zaslavskii, *Nonlinear physics: from the pendulum to turbulence and chaos*. Harwood Academic, 1990.

[57] A. J. Lichtenberg and M. A. Lieberman, *Regular and stochastic motion*, vol. 38. Springer Science & Business Media, 2013.

[58] B. V. Chirikov, "A universal instability of many-dimensional oscillator systems," *Physics reports*, vol. 52, no. 5, pp. 263–379, 1979.

[59] D. K. Umberger and J. D. Farmer, "Fat fractals on the energy surface," *Physical review letters*, vol. 55, no. 7, p. 661, 1985.

[60] S. G. Bochkarev, E. d'Humières, V. T. Tikhonchuk, P. Korneev, and V. Y. Bychenkov, "Stochastic electron heating in an interference field of several laser pulses of a picosecond duration," *Plasma Physics and Controlled Fusion*, vol. 61, p. 025015, 2018.

[61] G. Zaslavskii and N. Filonenko, "Stochastic instability of trapped particles and conditions of applicability of the quasi-linear approximation," *Soviet Journal of Experimental and Theoretical Physics*, vol. 27, p. 851, 1968.

[62] J.-M. Rax, "Compton harmonic resonances, stochastic instabilities, quasilinear diffusion, and collisionless damping with ultra-high-intensity laser waves," *Physics of Fluids B*, vol. 4, no. 12, pp. 3962–3972, 1992.

[63] Z.-M. Sheng, K. Mima, J. Zhang, and J. Meyer-ter Vehn, "Efficient acceleration of electrons with counterpropagating intense laser pulses in vacuum and underdense plasma," *Physical Review E*, vol. 69, no. 1, p. 016407, 2004.

[64] H. Avetissian, H. Jivanian, and R. Petrossian, ""reflection" and catching of charged particles by a plane electromagnetic wave in an undulator," *Physics Letters A*, vol. 66, no. 3, pp. 161–163, 1978.

[65] R. B. Palmer, "Interaction of relativistic particles and free electromagnetic waves in the presence of a static helical magnet," *Journal of Applied Physics*, vol. 43, no. 7, pp. 3014–3023, 1972.

[66] H. Avetissian and K. V. Sedrakian, "Nonlinear interaction of charged particles with strong laser pulses in a magnetic undulator," *Physical Review Special Topics-Accelerators and Beams*, vol. 13, no. 8, p. 081301, 2010.

[67] I. Andriyash, R. Lehe, A. Lifschitz, C. Thaury, J.-M. Rax, K. Krushelnick, and V. Malka, "An ultracompact x-ray source based on a laser-plasma undulator," *Nature communications*, vol. 5, p. 4736, 2014.

[68] H. Mehdian and A. Raghavi, "Dispersion relation and growth rate for a high gain ion-channel fel with a helical wiggler pump," *Plasma Physics and Controlled Fusion*, vol. 49, no. 1, p. 69, 2006.

[69] J. Rajput, N. Kant, H. Singh, and V. Nanda, "Resonant third harmonic generation of a short pulse laser in plasma by applying a wiggler magnetic field," *Optics Communications*, vol. 282, no. 23, pp. 4614–4617, 2009.

[70] R. Fedele, G. Miano, and V. Vaccaro, "The plasma undulator," *Physica Scripta*, vol. 30, pp. 192–197, 1990.

[71] S. Bochkarev, A. Brantov, V. Y. Bychenkov, D. Torshin, V. Kovalev, G. Baidin, and V. Lykov, "Stochastic electron acceleration in plasma waves driven by a high-power subpicosecond laser pulse," *Plasma Physics Reports*, vol. 40, no. 3, pp. 202–214, 2014.

[72] M. Lobok, A. Brantov, D. Gozhev, and V. Y. Bychenkov, "Optimization of electron acceleration by short laser pulses from low-density targets," *Plasma Physics and Controlled Fusion*, vol. 60, no. 8, p. 084010, 2018.

[73] G. Shvets, N. Fisch, A. Pukhov, and J. Meyer-ter Vehn, "Superradiant amplification of an ultrashort laser pulse in a plasma by a counterpropagating pump," *Physical review letters*, vol. 81, no. 22, p. 4879, 1998.

[74] G. Shvets, N. J. Fisch, A. Pukhov, and J. Meyer-ter Vehn, "Generation of periodic accelerating structures in plasma by colliding laser pulses," *Physical Review E*, vol. 60, no. 2, p. 2218, 1999.

[75] Y. Sentoku, V. Y. Bychenkov, K. Flippo, A. Maksimchuk, K. Mima, G. Mourou, Z. Sheng, and D. Umstadter, "High-energy ion generation in interaction. of short laser pulse with high-density plasma," *Applied Physics B*, vol. 74, no. 3, pp. 207–215, 2002.

[76] L. Chopineau, A. Leblanc, G. Blaclard, A. Denoeud, M. Thévenet, J. Vay, G. Bonnaud, P. Martin, H. Vincenti, and F. Quéré, "Identification of coupling mechanisms between ultraintense laser light and dense plasmas," *Physical Review X*, vol. 9, no. 1, p. 011050, 2019.

[77] Y. Zhang and S. Krasheninnikov, "Novel approach to stochastic acceleration of electrons in colliding laser fields," *Physics of Plasmas*, vol. 26, no. 5, p. 050702, 2019.

[78] Y. Zhang and S. Krasheninnikov, "Electron dynamics in counter-propagating laser waves," *arXiv preprint arXiv:1907.05539*, 2019.

[79] L. D. Landau and E. Lifschic, *Course of theoretical physics. vol. 1: Mechanics*. Oxford, 1978.

[80] I. S. Gradshteyn and I. M. Ryzhik, *Table of integrals, series, and products*. Academic press, 2014.

[81] Y. Zhang and S. Krasheninnikov, "Stochastic electron acceleration in relativistic laser pulse and stationary periodic electric and magnetic fields," *Physics of Plasmas*, vol. 26, no. 11, p. 113112, 2019.

[82] T. Katsouleas and J. Dawson, "Unlimited electron acceleration in laser-driven plasma waves," *Physical Review Letters*, vol. 51, no. 5, p. 392, 1983.

[83] T. Esirkepov, M. Borghesi, S. Bulanov, G. Mourou, and T. Tajima, "Highly efficient relativistic-ion generation in the laser-piston regime," *Physical review letters*, vol. 92, no. 17, p. 175003, 2004.

[84] B. Pollock, C. Clayton, J. Ralph, F. Albert, A. Davidson, L. Divol, C. Filip, S. Glenzer, K. Herpoldt, W. Lu, *et al.*, "Demonstration of a narrow energy spread, 0.5 gev electron beam from a two-stage laser wakefield accelerator," *Physical review letters*, vol. 107, no. 4, p. 045001, 2011.

[85] P. Mulser, D. Bauer, and H. Ruhl, "Collisionless laser-energy conversion by anharmonic resonance," *Physical review letters*, vol. 101, no. 22, p. 225002, 2008.

[86] A. Robinson, A. Arefiev, and D. Neely, "Generating "superponderomotive" electrons due to a non-wake-field interaction between a laser pulse and a longitudinal electric field," *Physical review letters*, vol. 111, no. 6, p. 065002, 2013.

[87] S. Luan, W. Yu, F. Li, D. Wu, Z. Sheng, M. Yu, and J. Zhang, "Laser propagation in dense magnetized plasma," *Physical Review E*, vol. 94, no. 5, p. 053207, 2016.

[88] D. Wu, S. Luan, J. Wang, W. Yu, J. Gong, L. Cao, C. Zheng, and X. He, "The controllable electron-heating by external magnetic fields at relativistic laser-solid interactions in the presence of large scale pre-plasmas," *Plasma Physics and Controlled Fusion*, vol. 59, no. 6, p. 065004, 2017.

[89] D. Wu, S. Krasheninnikov, S. Luan, and W. Yu, "Identifying the source of super-high energetic electrons in the presence of pre-plasma in laser–matter interaction at relativistic intensities," *Nuclear Fusion*, vol. 57, no. 1, p. 016007, 2016.

[90] G. R. Smith and A. N. Kaufman, "Stochastic acceleration by a single wave in a magnetic field," *Physical Review Letters*, vol. 34, no. 26, p. 1613, 1975.

[91] C. McKinstrie and E. Startsev, "Dephasing time of an electron accelerated by a laser pulse," *Physical Review E*, vol. 56, no. 2, p. 2130, 1997.

[92] K. Tanaka, R. Kodama, H. Fujita, M. Heya, N. Izumi, Y. Kato, Y. Kitagawa, K. Mima, N. Miyanaga, T. Norimatsu, *et al.*, "Studies of ultra-intense laser plasma interactions for fast ignition," *Physics of Plasmas*, vol. 7, no. 5, pp. 2014–2022, 2000.

[93] J. Peebles, M. Wei, A. Arefiev, C. McGuffey, R. Stephens, W. Theobald, D. Haberberger, L. Jarrott, A. Link, H. Chen, *et al.*, "Investigation of laser pulse length and pre-plasma scale length impact on hot electron generation on omega-ep," *New Journal of Physics*, vol. 19, no. 2, p. 023008, 2017.

[94] J. E. Moore, "Nonlinear radiation pressure and stochasticity in ultraintense laser fields," *Physical Review E*, vol. 59, no. 2, p. 2281, 1999.

[95] Z. Sheng and J. Meyer-ter Vehn, "Inverse faraday effect and propagation of circularly polarized intense laser beams in plasmas," *Physical Review E*, vol. 54, no. 2, p. 1833, 1996.

[96] H. Liu, X. He, and S. Chen, "Resonance acceleration of electrons in combined strong magnetic fields and intense laser fields," *Physical Review E*, vol. 69, no. 6, p. 066409, 2004.

[97] B. Liu, H. Wang, J. Liu, L. Fu, Y. Xu, X. Yan, and X. He, "Generating overcritical dense relativistic electron beams via self-matching resonance acceleration," *Physical review letters*, vol. 110, no. 4, p. 045002, 2013.

[98] A. Kemp, Y. Sentoku, and M. Tabak, "Hot-electron energy coupling in ultraintense laser-matter interaction," *Physical Review E*, vol. 79, no. 6, p. 066406, 2009.

[99] M. Sherlock, "Universal scaling of the electron distribution function in one-dimensional simulations of relativistic laser-plasma interactions," *Physics of Plasmas*, vol. 16, no. 10, p. 103101, 2009.

[100] C. S. Roberts and S. Buchsbaum, "Motion of a charged particle in a constant magnetic field and a transverse electromagnetic wave propagating along the field," *Physical Review*, vol. 135, no. 2A, p. A381, 1964.

[101] A. Bourdier and S. Gond, "Dynamics of a charged particle in a circularly polarized traveling electromagnetic wave," *Physical Review E*, vol. 62, no. 3, p. 4189, 2000.

[102] A. Bourdier and S. Gond, "Dynamics of a charged particle in a linearly polarized traveling electromagnetic wave," *Physical Review E*, vol. 63, no. 3, p. 036609, 2001.

[103] R. Ondarza-Rovira, "Relativistic motion of a charged particle driven by an elliptically polarized electromagnetic wave propagating along a static magnetic field," *IEEE transactions on plasma science*, vol. 29, no. 6, pp. 903–906, 2001.

[104] R. Ondarza and F. Gomez, "Exact solution of the relativistic equation of motion of a charged particle driven by an elliptically polarized electromagnetic shaped pulse propagating along a static and homogeneous magnetic field," *IEEE transactions on plasma science*, vol. 32, no. 2, pp. 808–812, 2004.

[105] A. Nikishov and V. I. Ritus, "Quantum processes in the field of a plane electromagnetic wave and in a constant field. i," *Sov. Phys. JETP*, vol. 19, p. 529, 1964.